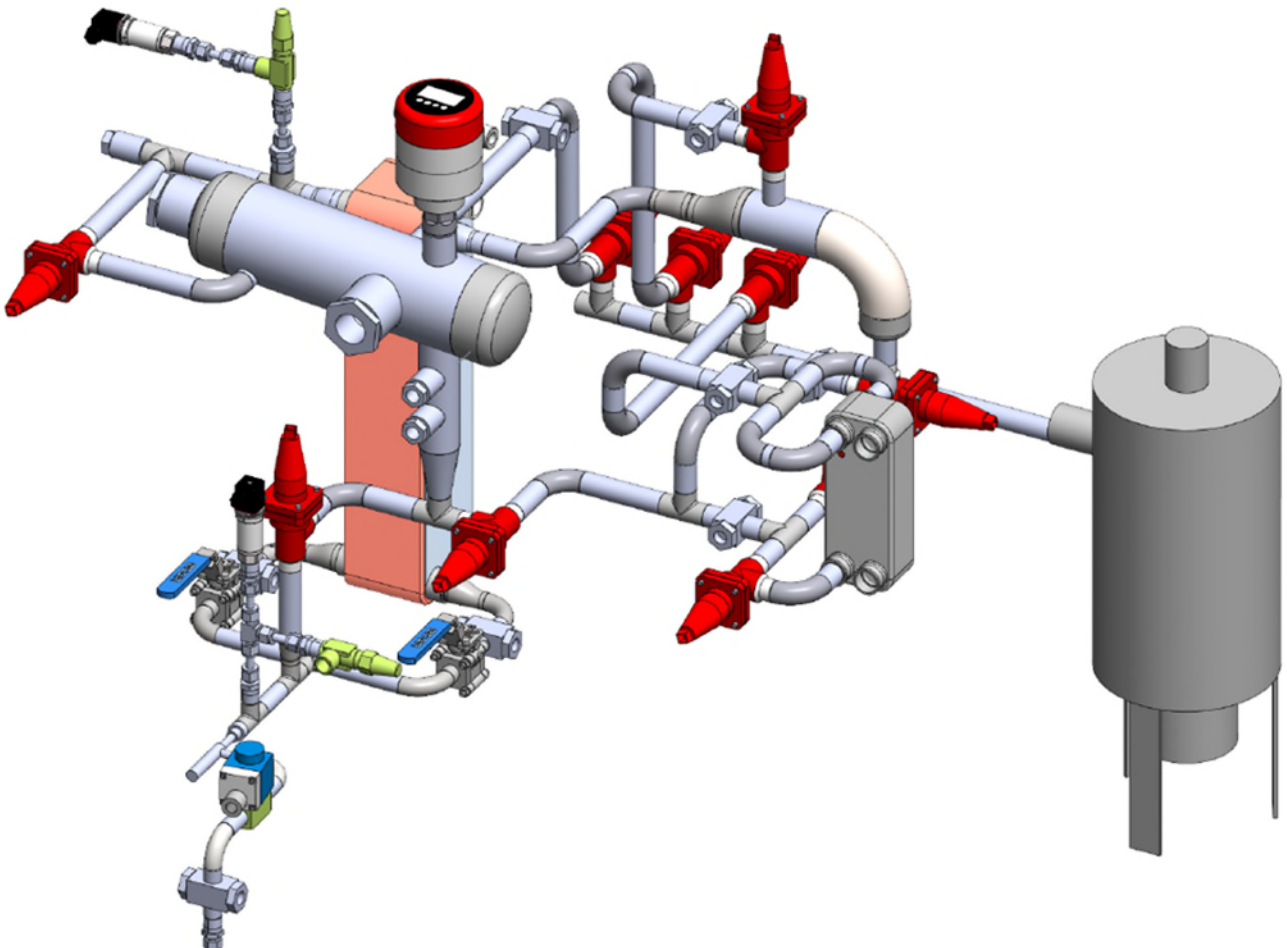




DANISH
TECHNOLOGICAL
INSTITUTE

Compact Energy Efficient Low Charge Ammonia Refrigeration Units (CLAUS)

- Final report



Title:

Compact Energy Efficient Low Charge Ammonia Refrigeration Units (CLAUS).

Prepared for:

EUDP, project no. 64018-0100.

Prepared by:

Danish Technological Institute
Gregersensvej 2, DK-2630 Taastrup
Refrigeration and Heat Pump Technology

Technical University of Denmark
Niels Koppels Allé, Bygning 403, DK-2800 Kongens Lyngby
Department of Mechanical Engineering

Project consortium:

Danfoss
Sondex
danARCTICA
Høje Taastrup District Heating Company
Technical University of Denmark
Danish Technological Institute (project leader)

May 2022

Authors:

Danish Technological Institute:
Jóhannes Kristófersson
Claus Madsen
Lars Olsen

Technical University of Denmark:
Brian Elmegaard
Wiebke B. Markussen
Valentin Salgado Fuentes

Table of Contents

1. Preface	5
1.1. Project details	6
1.2. Summary	6
1.3. Project objectives	8
1.4. Project implementation	14
1.5. Project results, dissemination, and utilization of results	15
1.6. Utilization of project results	22
1.7. Project conclusion and perspective	23
2. Research about compact ammonia chiller systems	24
3. Preliminary design of ammonia chiller and heat pump	26
3.1. Methods	26
3.1.1. Operating cycles	26
3.1.2. Possible configurations	26
3.2. Results	28
4. Experimental validation	31
4.1. Methods	31
4.1.1. Experimental setups	31
4.1.2. Testing procedure performed on the first experimental setup	32
4.1.3. Testing procedure performed on the second experimental setup	32
4.1.4. Validation of correlations for heat transfer coefficient and pressure drop	33
4.2. Results	34
5. Final design and control approach	37
5.1. Method	37
5.1.1. Compressor	37
5.1.2. Plate heat exchangers	37
5.1.3. Dynamic model	37
5.1.4. Analysis of chiller and heat pump operation	38
5.2. Results	39
5.2.1. Refrigerant charge	41
5.2.2. Dynamic model and chiller and heat pump operation	42
6. Research conclusions	46
7. Testing of concept	48

7.1.	Test setup	48
7.2.	Description of tests.....	51
7.2.1.	Results from Test 1 (15/2-2022)	52
7.2.2.	Results from Test 2 (15/2-2022)	58
7.2.3.	Results from Test 3 (22/2-2022)	65
7.2.4.	Results from Test 4 (4/3-2022)	73
7.2.5.	Results from Test 5.....	79
7.3.	Conclusions	83
8.	References	85
	Appendix 1 – List of dissemination activities	88

1. Preface

This report is the final report of the study: “**Compact Energy Efficient Low Charge Ammonia Refrigeration Units (CLAUS)**”. The objective of the project is to develop a novel energy efficient chiller and heat pump unit using the most efficient refrigerant found today, i.e., ammonia, in the capacity range from 20 to 200 kW. In this capacity range, the number of installations is large and the market potential extensive. At present, the existing refrigeration units in the market mainly use the environmental problematic CFC or HFC refrigerants. These refrigeration units use superheat controlled direct expansion to control the refrigerant feed to the evaporators which requires large superheating (10 to 12 K) and results in poor efficiency. One of the goals of the project is to develop a unit without or with very low suction superheat with an extremely low refrigerant charge.

This research project is financially supported by the Danish Energy Agency’s EUDP programme (Energy Technology Development and Demonstration). Project number: 64018-0100.

The project is carried out in cooperation with Technical University of Denmark and the following industrial partners: Danfoss, Sondex, danARCTICA and Høje Taastrup District Heating Company.

The following persons have participated in the project:

- Flemming Larsen, DanARCTICA
- Jan Larsen, DanARCTICA
- Filip S. Nielsen, DanARCTICA
- Niels P. Vestergaard, Danfoss
- Thomas Lund, Sondex
- Uffe Schleiss, Høje Taastrup District Heating Company (Høje Taastrup Fjernvarme)
- Brian Elmegaard, Technical University of Denmark
- Wiebke Brix Markussen, Technical University of Denmark
- Valentin Salgado Fuentes, Technical University of Denmark
- Erasmus Rothuizen, Technical University of Denmark
- Jóhannes Kristófersson, Danish Technological Institute
- Claus Madsen, Danish Technological Institute
- Lars Olsen, Danish Technological Institute.

The project team would like to thank the EUPD programme (Danish Energy Agency) for supporting the project with valuable inspiration.

1.1. Project details

Project title	Compact Energy Efficient Low Charge Ammonia Refrigeration Units (CLAUS)
Project identification	EUDP 2018, Project no.: 64018-0100
Name of the programme which has funded the project	Energiteknologisk Udviklings- og Demonstrationsprogram (EUDP)
Project managing company/institution	Danish Technological Institute, Gregersensvej 1, DK-2630 Taastrup
Project partners	Danfoss Sondex danARCTICA Høje Taastrup District Heating Company Technical University of Denmark
CVR (central business register)	56976116
Date for submission	23. May 2022

1.2. Summary

English version

The objective of the project was to develop a novel energy efficient chiller and heat pump unit using the most efficient refrigerant found today, i.e., ammonia, in the capacity range from 20 to 200 kW. In this capacity range, the number of installations is large and the market potential extensive. Ammonia has a long and successful history in industrial refrigeration systems but is not really used in ammonia-based systems of much lower capacity than approximately 200 kW. The original focus of the project was to develop a chiller/heat pump according to:

- Medium cooling capacity range, i.e., from 20 to 200 kW.
- Using the natural refrigerant ammonia.
- Compact unit – lower price – lower charge.
- Low charge under 10 kg, i.e., a specific charge of 0,05 kg/kW.
- Similar price as HFC units.
- Without or with very low suction superheat.
- Chiller energy savings of 23,5 % in full load and 31,5 % in part load.

- Heat pump energy savings of 28,5 % in full load and 33,5 % in part load.
- Encapsulate the charge inside the unit in case of leakage.
- Reduce heat loss.
- Increase oil separation.
- Optimized total control of the unit for optimum COP at all times.

The original plan was to develop the chiller/heat pump unit based on a Combi unit for chiller applications from danARCTICA.

The first step in the project was to develop and build a small test rig. An extensive data acquisition system was installed. This unit was built to test the different ideas that was devised before integrating them into the final unit to be installed at Høje Taastrup District Heating. The extensive tests on the small unit showed considerable challenges on the cold side of the unit. The original design was modified in order to solve the issues, and further tests were conducted.

The combi concept was developed for the final unit, i.e., combined chiller/heat pump, and prices were collected from suppliers. The final price for the unit turned out to be too high, and it was danARCTICA's evaluation that the unit would not be competitive in the market. Because of this and because of the challenges on the cold side, it was, in agreement with the project participants, decided to change the focus in the project to deal with the cold side and try to solve the issues there. Also, the EUDP Secretariat was continuously kept up to date on the adjustments of the focus in the project.

Because of the challenges on the cold side and because of the price issues on the combi heat pump design, the final unit to be installed at Høje Taastrup District Heating Company was not built, and the resources in the project were directed to solve the issues on the cold side. Thereby, some of the original focus areas in the project were not solved.

Danish version

Formålet med projektet var at udvikle en ny energieffektiv chiller- og varmepumpeenhed med anvendelse af det mest effektive kølemiddel, der findes i dag, dvs. ammoniak, i et kapacitetsområde fra 20 til 200 kW kølekapacitet. I dette kapacitetsområde er antallet af installationer stort, og det samme er markedspotentialet. Ammoniak har en lang og vellykket historie i industrielle kølesystemer, men findes stort set ikke i ammoniakbaserede systemer med lavere kølekapacitet end ca. 200 kW. Projektets oprindelige fokus var at udvikle en chiller/varmepumpe i henhold til:

- Et mellemområde med en kølekapacitet på 20-200 kW.
- Bruge det naturlige kølemiddel ammoniak.
- Kompakt unit – lavere pris – lavere fyldning.
- Lav fyldning på under 10 kg, dvs. en specifik fyldning på under 0,05 kg/kW.
- Lignende pris som for HFC-units.

- Uden eller med meget lav sugegasoverhedning.
- Energibesparelse for chillere/varmepumper på henholdsvis 23,5 % og 28,5 % i fuld last samt på 31,5 % og 33,5 % i dellast.
- Indkapsling af fyldning i enheden i tilfælde af lækage.
- Reduceret varmetab.
- Forøgelse af olie separationen.
- Optimeret kontrol af enheden for løbende at opnå en optimal COP.

Den oprindelige plan var at udvikle chiller-/varmepumpenheden baseret på en kombi-enhed til chiller-applikationer fra danARCTICA.

Det første skridt i projektet var at udvikle og bygge en lille testrig. Et omfattende dataopsamlingsystem blev installeret. Enheden blev bygget for at teste de forskellige ideer, der blev udtænkt, inden de blev integreret i den endelige enhed, der skulle installeres ved Høje Taastrup Fjernvarme. De omfattende test på den lille enhed viste dog betydelige udfordringer på den kolde side af enheden. Det originale design blev derfor justeret til at løse problemerne, og yderligere test blev udført.

Kombi-konceptet blev udviklet til den endelige enhed, dvs. kombineret køler/varmepumpe, og priser blev indsamlet fra leverandører. Den endelige pris for enheden viste sig at være for høj, og det var danARCTICAs vurdering, at enheden ikke ville være konkurrencedygtig på markedet. På grund af dette og på grund af udfordringerne på den kolde side blev det – i fuld overensstemmelse med projektdeltagerne – besluttet at ændre fokus i projektet for i stedet at håndtere den kolde side og forsøge at løse problemerne der. Ligeledes blev EUDP-sekretariatet løbende holdt orienteret om justeringerne af projektets fokus.

Grundet udfordringerne på den kolde side og prisproblemerne på kombi-varmepumpedesignet blev den endelige enhed, der skulle installeres ved Høje Taastrup Fjernvarme, ikke bygget, og ressourcerne i projektet blev rettet mod at løse problemerne på den kolde side. Derved blev nogle af de oprindelige fokusområder i projektet ikke løst.

1.3. Project objectives

The focus of the project was to develop compact energy efficient low charge ammonia refrigeration units (CLAUS) for both chiller and heat pump applications based on a patent from danARCTICA called 'combi unit'. In the combi unit, all of the high-pressure side of the heat pump is integrated into one vessel with the intent to reduce the cost of the unit.

The final unit should be installed in a field test at Høje Taastrup District Heating where it was intended to produce both cold energy for the district cold distribution network and utilize that energy through the heat pump into the district heating network.

Chiller unit

A chiller is a refrigeration unit used to cool water and it is normally built on its own frame. It has an evaporator on the suction side to cool the water and a condenser on the condensing side to reject the heat from the refrigeration unit to the environment. It is extensively used in, e.g., air conditioning systems for cooling purposes, to produce ice water for food industry, and for various other applications. In the project, a compact energy efficient low charge ammonia chiller in the medium capacity range (20-200 kW cooling capacity) was the target.

In the medium capacity range, a state-of-the-art chiller unit today is a unit that uses synthetic refrigerants, mostly R134a. The price of R134a has increased by 40 % in the beginning of 2018 because of quota restrictions which puts pressure on producers to find solutions with alternative refrigerants. R134a is being phased out and will be banned in the EU in 2022. The chillers use direct expansion to control the refrigerant flow to the evaporator. It uses plate heat exchangers as evaporators, and the compressor is semi hermetic. Typically, it uses plate heat exchangers on the condensing side when the condenser is water-cooled or fin and tube heat exchangers if it is air-cooled.

The typical chiller units on the market in the medium sized range have a relatively poor efficiency. The reason is that they use synthetic refrigerants which have lower efficiency compared to ammonia and that they use direct expansion to control the refrigerant flow to the evaporators.

Direct expansion uses the suction superheat to control the refrigerant flow. The suction superheat is typically in the range from 10 to 12 K. The high suction superheat required leads to low suction temperatures for the compressors that again results in large energy usage. The aim of the project is to develop low price chillers without or with very low suction superheat. For each degree the suction temperature is increased for chiller applications, calculations show that savings in power consumption, and thereby the increase in COP, for the same capacity of the compressors are around 4 %.

In Figure 1, the traditional refrigeration system with direct expansion is shown on the figure to the left. The cooling of the water corresponds to a traditional chiller, e.g., air conditioning systems with 7/12 °C water cooling. It is the suction superheat for the direct expansion valve that controls the heat exchanger for a traditional system. The pinch point of the heat exchanger is in the outlet. By using 2 K pinch point between the refrigerant and the inlet water and 10 K as suction superheat for the expansion valve, the required suction temperature is 0 °C in full load condition. For the part load situation (the dash lines), the water return temperature in this case is 10 °C. In this case, the suction temperature needs to be lowered to -2 °C to be able to maintain the 10 K suction superheat required for the expansion valve. Here, the efficiency of the refrigeration system drops by 8 % compared to full load. Additionally, the control system of the evaporator needs to ensure no freezing up in the heat exchanger at part load.

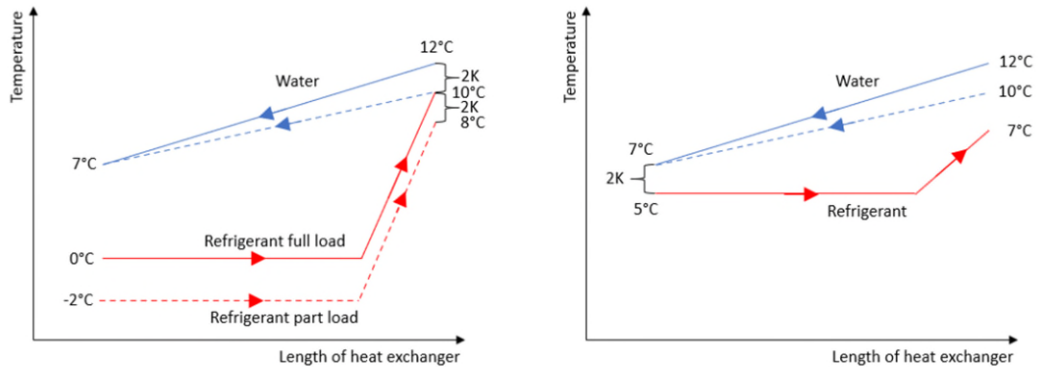


Figure 1: Evaporator on a chiller for full load and part load. To the left the traditional chiller. To the right the new CLAUS Principle.

The solution considered in the project has no or a very low superheat from 0 K to 2 K. Here, the evaporator’s pinch point has moved to the inlet (Figure 1 right) for the 12/7 °C temperature profile. In this way, the suction temperature can be raised to 5 °C and it is independent of part load conditions.

The efficiency increase caused by the suction superheat between a traditional chiller running on 0 °C suction temperature and the new concept running on 5 °C is for full load 20 %. In part load, where the suction temperature is down to -2 °C, the efficiency increases to 28 %.

By comparing the ammonia refrigerant with the traditional R134a which is the preferred refrigerant in chiller units, and by using the same conditions and capacity, the energy saving from the use of ammonia instead of synthetic refrigerant alone is around 3.5 %. The comparison is made by using an ideal refrigeration cycle and just changing the type of refrigerant. The expected combined effect of the higher suction temperature and the more energy efficient refrigerant on the energy savings is therefore estimated to be 23.5 % for full load and 31.5 % for part load compared to conventional chiller units. The increase in COP is the same.

danARCTICA has made a calculation of the return of investment (ROI) for the smallest industrial chiller unit of 200 kW using ammonia and compared it to HC (Hydrocarbons) and HFC chillers. The results can be seen in Table 1.

Table 1: Return of investment (ROI) for ammonia 200 kW chiller compared to other refrigerants. The water temperature on the cold side is 12/7 °C and on the warm side it is 37/42 °C.

Chiller type	EER	Energy consumption reference	Price reference	ROI [Years]
Ammonia	4.5	1	1	-
HC	3.6	1.25	0.88	0.7
HFC	3.2	1.4	0.58	1.5

The table shows that even with traditionally built ammonia chillers which are about 70 % more expensive than the HFC chillers, the ROI is just 1.5 years. By looking at new ways of building a cheaper, more energy efficient unit for the medium sized range from 20 to 200 kW cooling capacity, the ROI can be expected to be considerably lower. The table also shows that industrial ammonia chillers are more energy efficient than chillers using hydrocarbons (HC). This also holds for the medium range sized chillers.

Heat pump unit

A heat pump unit is a refrigeration unit that utilizes available low energy heat to produce valuable high energy heat that can be used for various heating purposes. For the capacity range in focus in the project these are, e.g., used for multi-family houses, for the service sector and for some industrial applications. For the low-capacity range up to 20 kW cooling capacity, a lot of heat pump producers are found, but for the capacity range addressed in the project, few products are known to exist. The preferred refrigerant for the low temperature heat pumps (up to 60 °C water temperature) is mostly R410A, and for higher temperatures it is R407C. And since the GWP is respectively 1725 and 1774, producers are starting to shift to R32 as a more future safe refrigerant even though it is slightly flammable. The R32 has a GWP of 677 and is thereby a short-term solution since the required GWP limit in the future will probably be lower than 150. The price of R410A and R407C has increased by 30 % in the beginning of 2018 because of quota restrictions and this puts extra pressure on finding solutions with alternative refrigerants. For the higher temperature heat pumps, there are not a lot of alternatives, but some of the new HFOs could be candidates, e.g., R1234ze, and some producers are turning to build units which run on transcritical R32. To meet the demand for the medium capacity range, which is the focus of the project, producers often apply a solution where more units of lower capacity are connected in parallel to supply the necessary capacity which gives more expensive and less efficient solutions. The project addresses the missing capacity link for heat pumps in the range between the commercial (0 to 20 kW) and up to the industrial heat pumps (200 to 10000 kW).

For the heat pumps found in the market, the preferred refrigerant is R410A. This refrigerant has a critical point at 72.8 °C which limits the available water temperature from the heat pump. The new refrigerant R32 that is a substitute for the R410A has a critical point of 78.1 °C which allows a slightly higher water temperature from the heat pump but still far lower than the water temperature available with ammonia with a

critical point of 132.3 °C, and where it is easy to reach 80 °C for normal available components. The new HFO, R1234ze, has its critical point at 109.4 °C. The solution in focus in this project will bridge the gap in capacity and can be used for higher temperature heat pumps as well.

To make a comparison to ammonia, we use R410A as the reference case for the heat pump. The heat pump warms water from 40 °C to 60 °C by cooling water from 12 °C down to 7 °C. The condition is the same on the evaporator side as for the chiller. To be able to reach 60 °C water temperature, the condensation temperature is considered to be 65 °C and the suction temperature the same as before for the chiller. For each degree the suction temperature is increased for heat pump applications using R410A, calculations show that the savings in power consumption, and thereby the increase in COP, are around 2.5 %, assuming the same capacity for the compressors.

By using the same prerequisites as for the chiller, the savings on the evaporator side based on raised suction temperature when running in full load is 12.5 %. In part load, the savings increase to 17.5 %.

By comparing the ammonia refrigerant with R410A and by using the same conditions and capacity and assuming subcooling of the refrigerant after the condenser to 50 °C, the energy saving from the use of ammonia instead of the synthetic refrigerant alone is around 16 %. The comparison is made by using an ideal refrigeration cycle and just by exchanging the refrigerant. In addition, there will be other benefits as, e.g., better efficiency of refrigeration compressors using ammonia.

The expected combined effect of the higher suction temperature and a more energy efficient refrigerant is therefore estimated to be 28.5 % for full load and 33.5 % for part load compared to a case where the heat pump would use R410A. The increase in COP is the same.

Low charge, compact

The objective of a low charge of ammonia for small units is to reduce the installation costs because of fewer safety actions and to increase the safety for small systems. In the standard for refrigeration systems EN-378-1, Appendix C, there is a limit of 10 kg refrigerant for ammonia systems placed in human occupied spaces. By complying with these limits, most of the administrative burden related to using ammonia is released which reduces the cost of the systems and increases their competitiveness to synthetic refrigerant systems. In the project, the aim is unit with a charge below the 10 kg limit, i.e., with a specific charge of 0.05 kg/kW for 200kW unit.

Since ammonia has a very distinct odor it can create a panic situation if exposed to persons not familiar with the smell of ammonia. To eliminate this risk, it is important to enclose the unit and ensure that no ammonia is released out of the casing in case of leakage. This could be done by ventilating the casing in case of release, but this requires refrigerant sensors and a ventilation system. Another way is to contain the ammonia inside the cabinet by absorbing it in case of a release. Reduction of the charge is an

important part in reducing the cost penalty related to this. How to accomplish this has not been addressed in the project.

To reduce the unit charge and increase the unit efficiency, the evaporator has been designed with that in mind in cooperation with Sondex. To increase the unit efficiency, the suction superheat is reduced or eliminated. The control of the refrigerant to the evaporator is designed in cooperation with Danfoss.

One of the project partners, danARCTICA, has developed and patented a very smart, compact and price efficient solution for the condensing side of a chiller, see Figure 2. The concept was developed for larger sized (above 200 kW cooling capacity) chiller applications, and it combines the oil separator, condenser, oil cooler, liquid and oil receiver in one hermetic sealed unit.

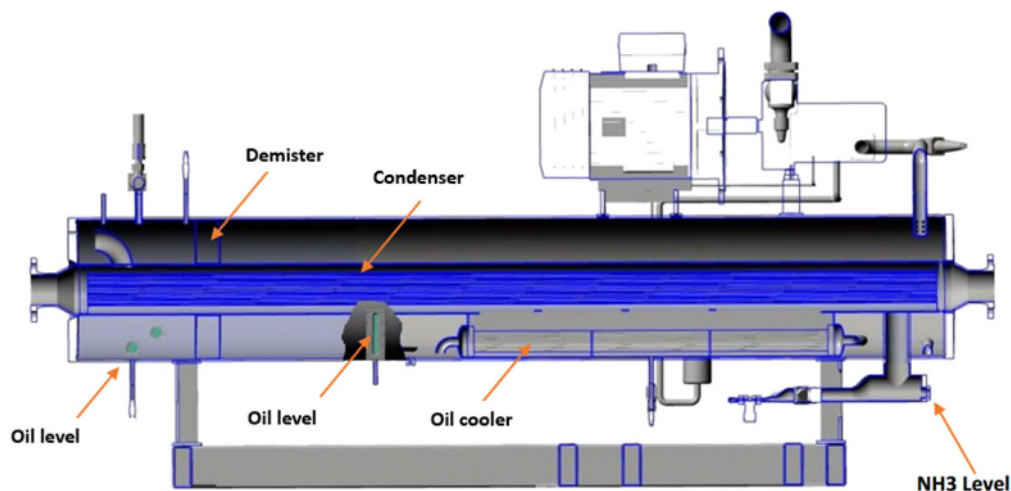


Figure 2: Combi chiller concept from danARCTICA.

This system is very promising and will increase the compactness of the system and lower the cost for chiller applications. There have been some technical challenges and a need for further development to make the system applicable to the market. Their concept has been further developed in the project, and a final design is developed, and construction drawings are made.

One of the features of the combi concept from danARCTICA is the integration of components inside a common shell. This means that there is just one pressure vessel, i.e., the oil separator shell. All other components inside the shell do not need to be designed as a separate pressure vessel which was expected to decrease the price considerably.

Another feature of the combi design is that the surface of the unit is small which reduces the heat loss from the unit and thereby increases the total efficiency of the unit.

The oil separation of the combi design is also a clever feature since the condenser is placed in the middle of the oil separator and acts as a desuperheater. In this way, the hot discharge gas from the compressor is cooled down in the oil separator leading to a better oil separation. In a normal oil separator, the oil in the discharge gas exists both as oil liquid droplets separated in the oil separator by gravity and as aerosol which flows with the gas through the oil separator and further to the refrigeration system. The aerosol part is highly dependent on the temperature of the discharge gas and is therefore especially important for heat pumps. By building a dedicated desuperheater into the oil separator, the discharge gas cooling can be extended. This will increase the oil separation and at the same time utilize the high valuable heat from the discharge gas to lower the condensing pressure and thereby increase the efficiency of the heat pump unit.

One of the disadvantages of ammonia compared to the other refrigerants is the high cost of the units. This is because conventional units using HFC and HC refrigerants use soldered copper piping. To reduce the price and make ammonia units more competitive, a new way of assembling the pipes needs to be used. New systems to assemble pipes for refrigeration systems are promising and have briefly been investigated in the project to reduce the piping cost. By using this assembling method, the pipes can be bent and formed to eliminate some of the joints and thereby reduce costs as well as the number of potential leakage points. Additionally, the compactness of the combi concept will also reduce the unit price and thereby increase the competitive advantage of the units.

A present possibility for solving the missing capacity range (20 to 200 kW) is to install several lower capacity heat pumps coupled in parallel to reach the requested total capacity. The benefit of using one unit instead is the utilization of the heat exchanger area. For the unit in scope in this project, the heat transfer area in heat exchangers stays the same for part load, while stopping one or more units will reduce the available area in part load for traditional units. The one-unit solution leads to a higher suction temperature and to a lower condensing temperature which results in a higher efficiency of the unit developed in the project.

1.4. Project implementation

The project has been divided into six work packages with corresponding milestones, where each contains several tasks. The work packages are:

WP00 – Project management and administration

WP01 – Knowledge gathering

WP02 – Design of chiller/heat pump unit

WP03 – Verification of chiller/heat pump unit at DTI

WP04 – Performance test of units at selected users

WP05 – Dissemination of knowledge.

Work package 00 runs throughout the project period and contains the administration and management of the project.

In WP01, the knowledge found in the scientific community was gathered by DTI and DTU as a basis for the following development.

In WP02, a design of a small 30 kW test unit was done as well as the design of the final unit for the field test. The research part of DTI and DTU was done in this work package.

In WP03, the various ideas concerning the control of the evaporator, control of the unit, and the low charge issues were tested. The small unit of 30 kW was built and equipped with data acquisition equipment. Several tests were conducted, and the initial tests showed some issues on the evaporator side. The test setup was modified to try to solve these issues, and further test were conducted. The results from the test were used to analyze the control issues and to verify the simulations done in the research part.

In WP04, the prices for the unit for the field tests developed in WP02 were found. It turned out that the prices for the developed combi unit was considerably more expensive than expected which ruined the competitiveness of the developed solution. This along with some unsolved issues on the evaporator side lead to a decision of dropping the final unit and following field tests at Høje Taastrup District Heating and concentrate the resources in the project on solving the issues concerning the evaporator side.

WP05 was running in parallel with the other work packages and here the results of the project were disseminated.

The project experienced different difficulties. First, the two main technical employees from danARCTICA connected to the project resigned. To keep the project going, the technical design in the project and the drawings which were intended to be done by danARCTICA were solved by DTI. Another important factor was the corona pandemic which hit danARCTICA hard and was the main reason for the delay of the project by six months. Delays have also occurred due to changes of staff at the project participants.

One of the major obstacles was that the cost of the "large unit" with the proposed design showed to be far more expensive than expected together with control difficulties on the evaporator side. This resulted in a change of the project plan. Therefore, the work was continued with the small unit to come closer to a solution for the evaporator side, instead of shifting to the final unit.

Even though it was not possible to follow the original plan, it was still possible to obtain valuable results which will be of great importance when the concept of compact designs with small amounts of ammonia will be implemented in new development projects.

1.5. Project results, dissemination, and utilization of results

The outcome of the project has been a verified simulation model and measurements to better understand the challenges with controlling the evaporators in ammonia systems without or with very low superheat. The measurements are described in more detail in

chapter 7. As the superheat is reduced, more liquid will occur in the evaporator and that liquid has to be handled. In larger ammonia systems, this issue has been dealt with by including a large surge drum to separate the liquid droplets out of the gas before entering the compressor. This increases the cost of the systems and requires large charges. To solve this, the project has investigated how to run with very low superheat and lead the droplets out of the evaporator through a plate heat exchanger to be evaporated by the energy in the liquid refrigerant flowing to the expansion valve. To separate the liquid out of the gas, two types of separators have been designed, built, and tested. One highly efficient separator shown in Figure 3 and a low-cost liquid separator consisting of only piping material shown in Figure 5. The low-cost separator is not considered as a vessel but just as part of the piping system and thereby need no safety valves.

For the highly efficient liquid separator in Figure 3, the mixture of liquid and gas from the evaporator flows into the separator as shown in the figure. It goes through a bent to provide the first measure of separation. Then the gas and liquid flow along the vessel side before entering the bottom of the vessel. There, the gas is diverted 180° and flows to the top of the vessel on its way to the exit pipe. The exit pipe has a number of holes in the outlet pipe in the direction diverted to the center of the vessel to once again divert the gas flow before exiting the vessel.

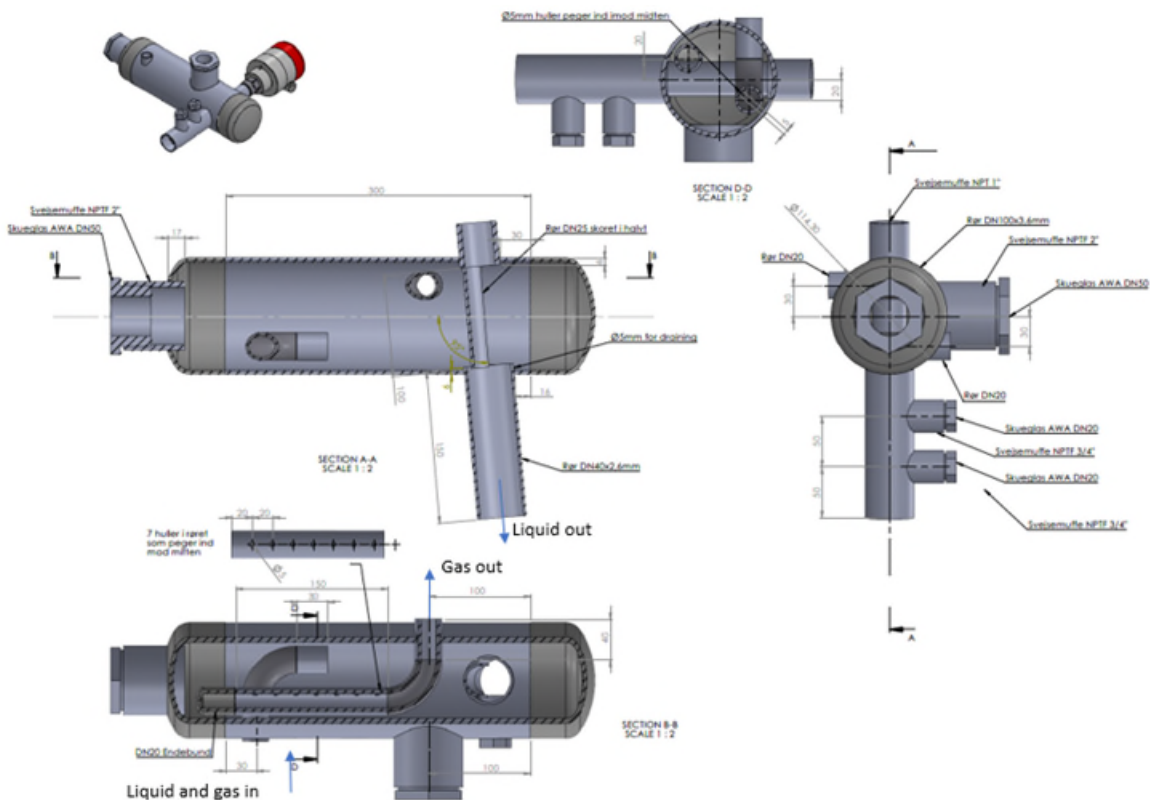


Figure 3: Highly efficient liquid separator.

A particle simulation was done in CFD which showed that for particles of size 0.05 mm the separator was able to separate them from the gas. This means that particles larger than 0.05 mm would be separated. For 0.01 mm particle size, a small number of particles exited the separator. The normal particle reference of 0.1 mm which is used for designing liquid separators in ammonia systems is well met.

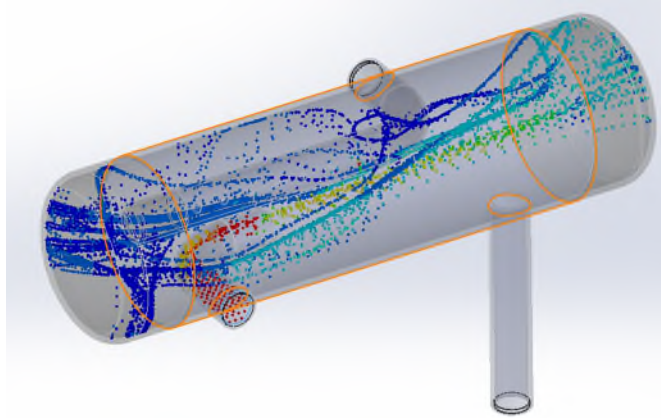


Figure 4: Particle simulation with particles of 0.05 mm diameter.

The simple liquid separator shown in Figure 5 consists of piping material, i.e., some concentric reductions, a pipe, and a bent. The gas and the liquid from the evaporator flow into the straight pipe which has a gradually increasing size. This reduces the gas speed to enhance the separation. Before exiting the separator through the pipe in the top, the gas will hit the bent and is redirected to enhance the liquid droplets to be separated.

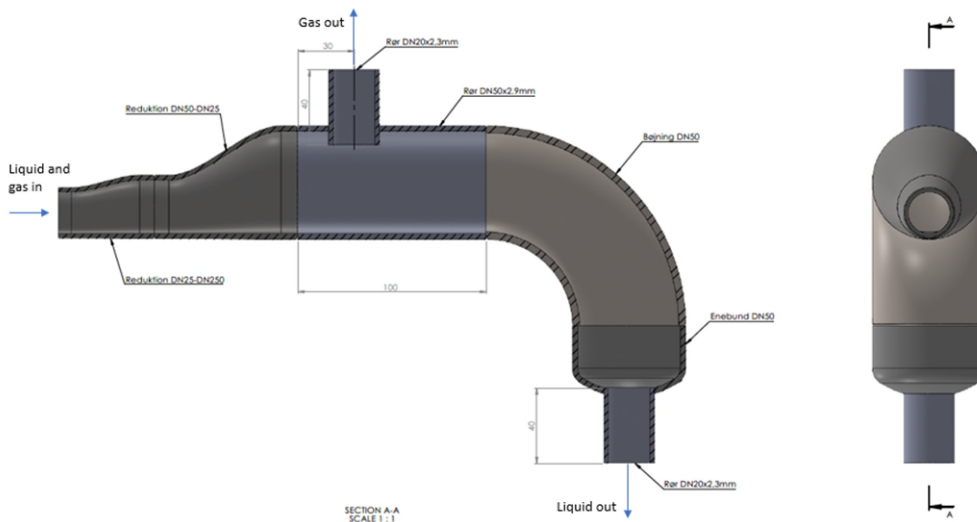


Figure 5: Simple liquid separator.

For the simple liquid separator, the CFD particle analysis showed that for the 0.05 mm, a small number of liquid droplets left the separator together with the gas. The limit of 0.1 mm was though met.

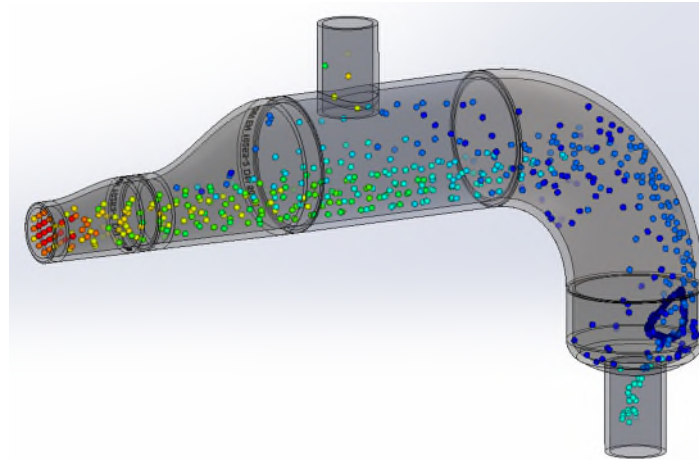


Figure 6: Particle simulation with particles of 0.05 mm diameter.

One outcome of the project is a test setup (see Figure 7) and measurements on the evaporator side of the chiller and heat pump that give an indication of the challenges in the control of evaporators for ammonia when the superheat has to be very low or zero.

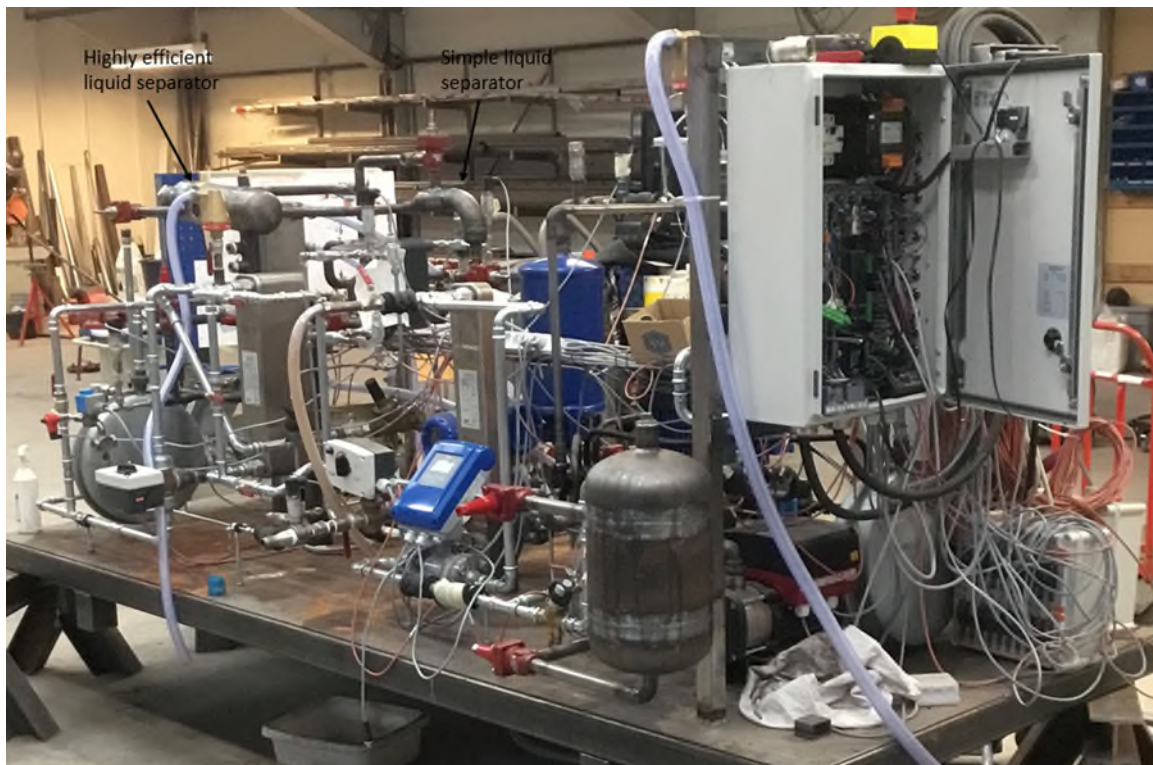


Figure 7: Test rig in the project.

The project has also produced a chiller and heat pump design based on the patented combi concept, see Figure 8. Because of the price issues, this design must be reevaluated to reduce the price to increase the competitiveness of the product before testing and marketing is initiated.

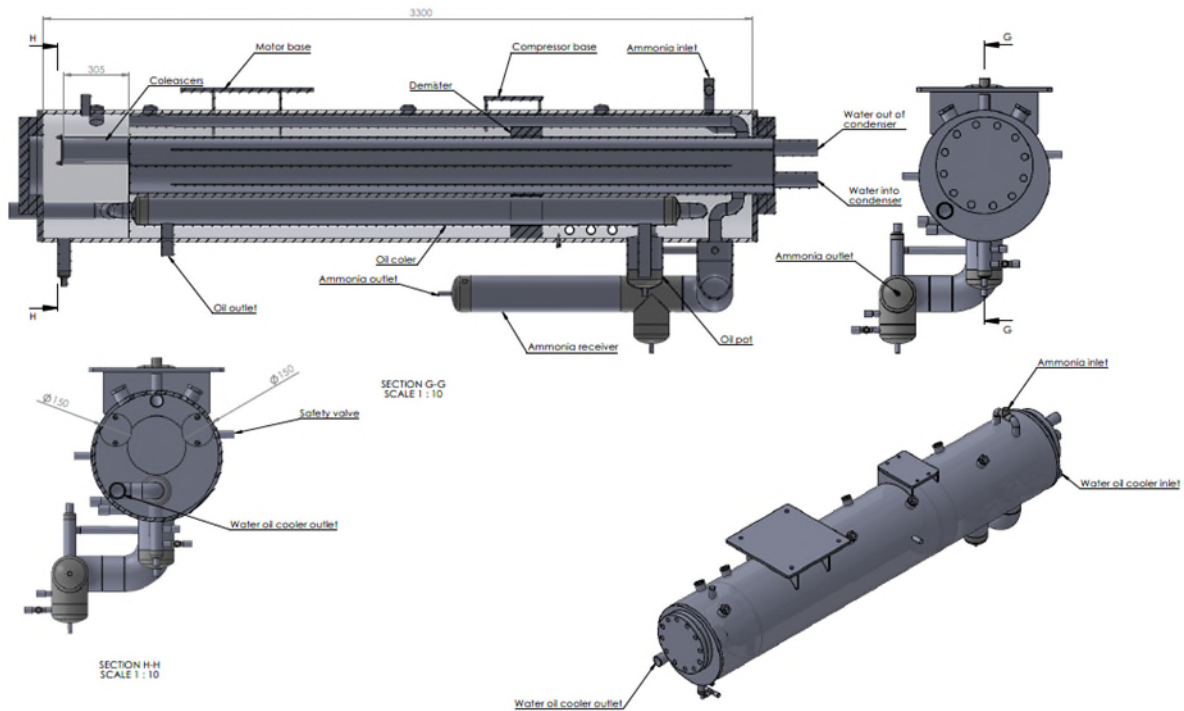


Figure 8: The new combi design for heat pumps.

In this design, the high-pressure side is encapsulated into the shell of the oil separator. The oil separator is a three-stage separator with a gravity separation to start with. Then there is a demister to assemble the small oil droplets to larger ones to be separated from the gas in the section behind the demister. Then, at last, there is a coalescing filter that separates the smallest droplets. The oil flows to the bottom of the vessel and is sucked into the oil cooler from the oil pot. The desuperheater, condenser, and subcooler are all built into the middle section of the unit. The middle section is not insulated so the water running through cools down the discharge gas on its way through the oil separator and is thereby increasing the oil separation.

In Figure 9, the flow of the discharge gas through the oil separator is shown. The discharge gas from the compressor comes into the oil separator in the top of the shell and is divided in two streams to distribute it through the oil separator space. The flow through the separator follows the red arrows and flows through the demister and at last through the coalescing filters before entering a pipe (the green arrows) that leads the gas to the inlet of the desuperheater.

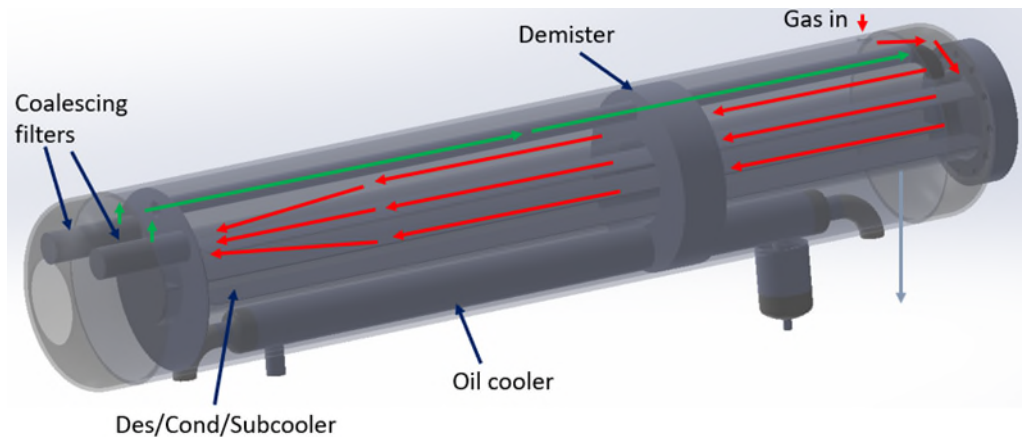


Figure 9: The discharge gas flow through the oil separator.

The contribution from the research from DTU and DTI in the project has provided some knowledge to better understand the evaporator control of the chiller and heat pump units. DTI is a leading knowledge institution within industrial refrigeration and has gained increased competences and experience in relation to ammonia applications. Through this project, DTI has acquired the latest knowledge on the subject both from the academic research and from performance verification based on laboratory tests. DTI can utilize this knowledge to advise companies in obtaining energy savings on their refrigeration systems and distribute the knowledge through courses and hosting theme days for the industry.

A complete design of the final unit has been done, and the elaborated P&I diagram of the design is shown in Figure 10.

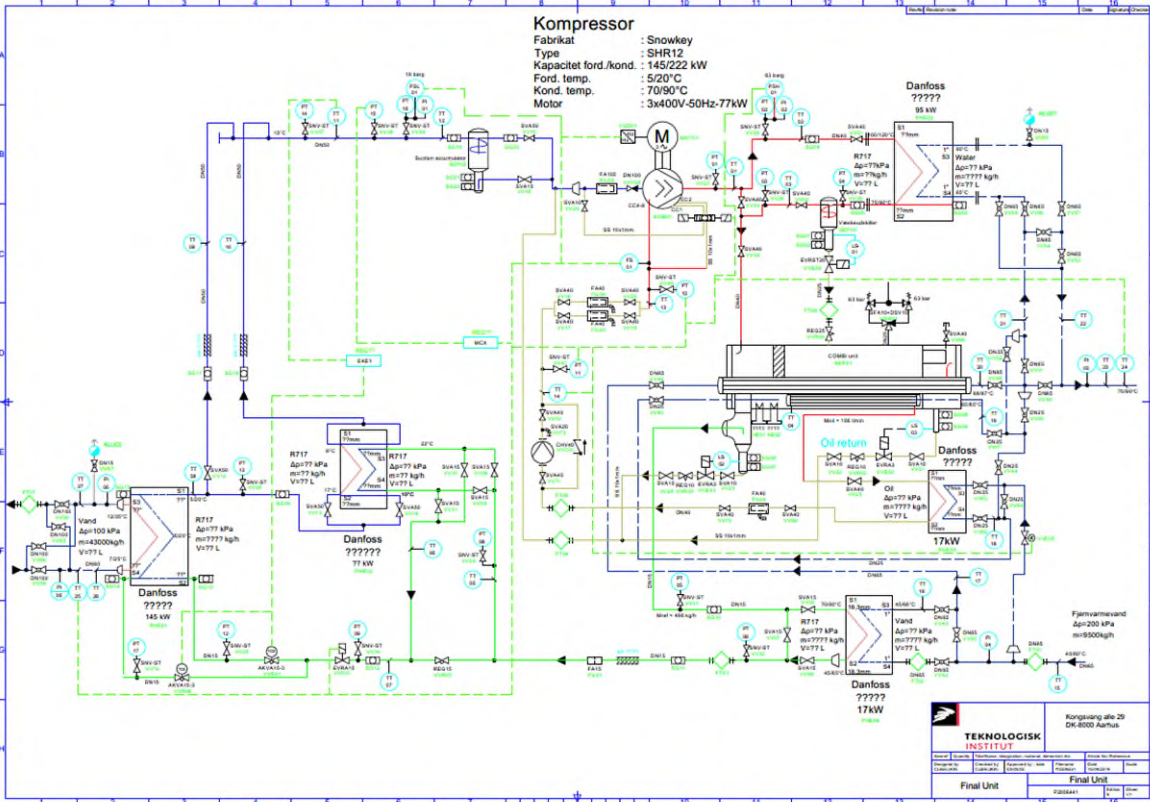


Figure 10: P&I diagram for the final unit design.

The control issues on the evaporator side must still be solved before the final design is done. The price of the combi unit must be reduced to increase the competitiveness of the unit.

In Figure 11, a rough 3D drawing of the final unit is shown.

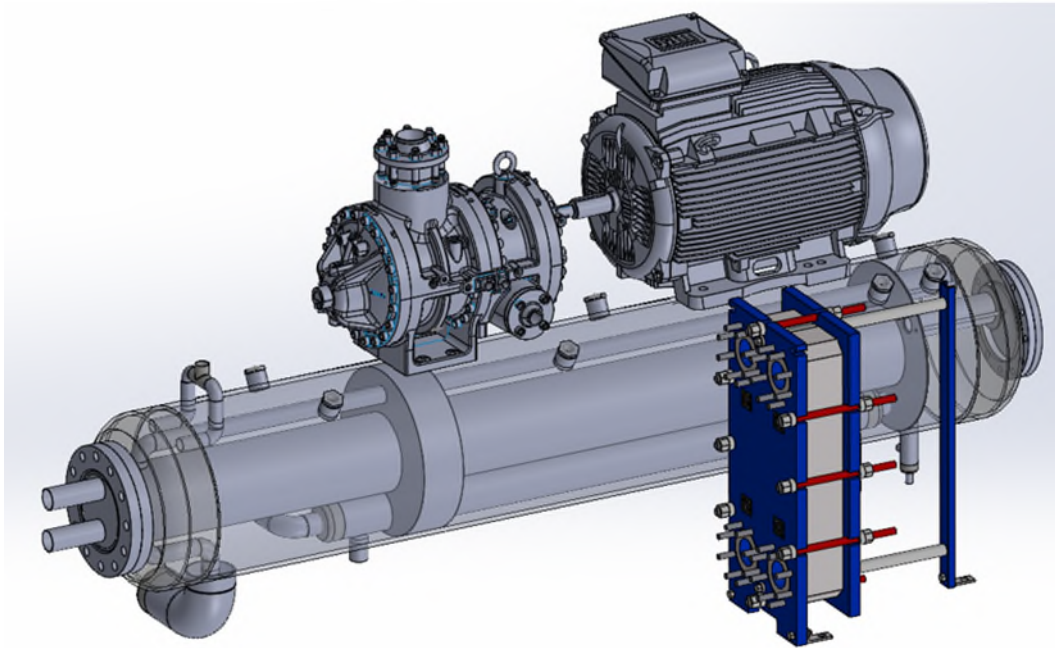


Figure 11: A 3D drawing of the final unit.

This objective has been achieved by carrying out research based on optimization by simulations and testing.

The result is an improved overall performance of the CLAUS concept compared to traditional system designs.

The results of the project can be used for control of all ammonia evaporators for both chillers and heat pumps.

The dissemination of the project results has been done by publishing papers on the subject and discussing the results on theme days and on the participating companies' home pages.

See list of dissemination activities in Appendix 1.

1.6. Utilization of project results

The results obtained in the project have increased the understanding of the challenges to overcome when applying a minimum of superheat for the evaporators to maximize the efficiency of the chillers and heat pumps. The results from tests have indicated the necessary equipment to accomplish this. This will have to be further developed before it can be applied in commercial products on the market.

The benefits of using the CLAUS concept are, first of all, an increased efficiency of both heat pumps and chillers by using ammonia as the refrigerant. The application of the concept by using a compact solution will have many benefits such as a reduced ammonia charge, lower cost, lower heat loss, and finally an increased efficiency. The technology,

when fully developed, will also increase the flexibility by being able to operate also in part load with a high efficiency.

The result of all the benefits is that the concept will be able to achieve a favorable economy, when fully developed, compared to traditional units. Due to the gained benefits observed in the project, the project participants, involved companies, and other stakeholders will be able to adapt the CLAUS concept in their planned development of heat pump and chiller units.

Another result from the project regarding using the patented combi solution as an efficient and price competitive solution to heat pumps is that in order to realize the developed concept, the price of the combi technology must be reduced. This can be done by finding another producer that can give better prices or developing the concept by optimizing the production processes.

1.7. Project conclusion and perspective

The original plan of the project to develop a market ready, low charge highly efficient combined chiller and heat pump unit for the 20 to 200 kW capacity range with ammonia as refrigerant has not been realized. The reason is unexpected challenges on the evaporator control that has required a lot of effort and a reconfiguration of the test setup. Another factor has been the corona pandemic that has given the participating companies a number of challenges.

The project has though brought the technology closer to the goal by indicating the challenges on the evaporator side and pointing at a possible solution with a new sensor technology for the expansion valve that has been briefly tested in the project.

Another part of the project, concerning the use of the patented combi unit principle to heat pumps, has been designed, but showed to be too expensive to be competitive. In this case, a product development to decrease the price is needed.

The project has shown that to reduce the charge and increase the efficiency, a solution that can run the evaporator close to non-superheat conditions is needed.

Models of the unit have been made and verified and these will be valuable for future developments.

2. Research about compact ammonia chiller systems

The research part of the project has been based on the PhD project by Valentin Salgado Fuentes, which was supervised by Brian Elmegaard, Wiebke Brix Markussen, and Erasmus Rothuizen. It included a comprehensive literature review related to ammonia chiller and heat pumps. The current work presents a concept that could be a suitable option to supply medium capacity cooling and heating applications. The purpose of the CLAUS project was to install a combined chiller and heat pump unit in the headquarters of Rockwool International A/S located in Hedehusene, Høje-Taastrup Municipality. The company in charge of allocating the unit, Høje Taastrup Fjernvarme a.m.b.a. (HTF), established that the primary purpose of the unit should be to provide space cooling for the office buildings and should be able to increase the heating capacity of the already existing heat pump of 488 kW. Figure 12 shows the standard rating conditions of a water-to-water chiller for process cooling according to European standards EN 14511-2_2018 (European Committee for Standardization, 2018). In the case of the evaporator, HTF has reported that other cooling systems installed in the municipality have supply temperatures of 6 °C to 10 °C and return temperatures of 10 °C to 16 °C.

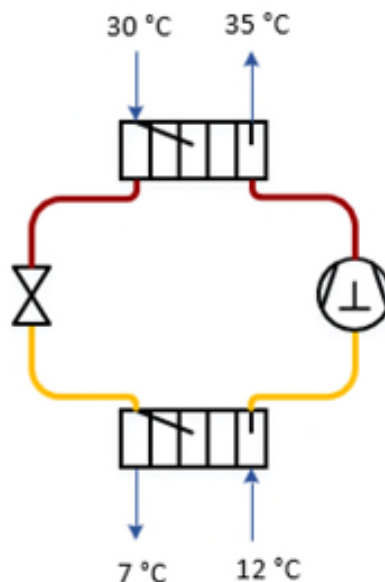


Figure 12: Standard operating temperatures of a chiller according to EU regulations.

The district heating network operated by HTF has three supply water temperature categories. The first category, named "Traditional district heating Temperature", is at 85 °C, produced by combined heat and power plants. The second category, named "Heat pump temperature", is at 70 °C, and it is produced by the heat pumps installed some years ago. The first and second categories have a return temperature restriction that HTF has imposed on the users. Thus, the customers must cool down the district heating water to a return temperature of 43 °C or below. Otherwise, they must pay an additional fee. The third category and most recent one is the "Low-temperature district heating LTDH", and it has a supply temperature of 55 °C and a return temperature of 30 °C. HTF plans

to replace the outdated traditional district heating installations with new and energy saving district heating systems such as the last two categories. Hence, the development of the heating section of the combined unit should supply those temperature setpoints. Based on the operating conditions mentioned above, two different design conditions for combined chiller and heat pump units are presented in Figure 13. Figure 13a shows the design conditions for a standard chiller combined with the second district heating temperatures and Figure 13b with the third category of district heating temperatures.

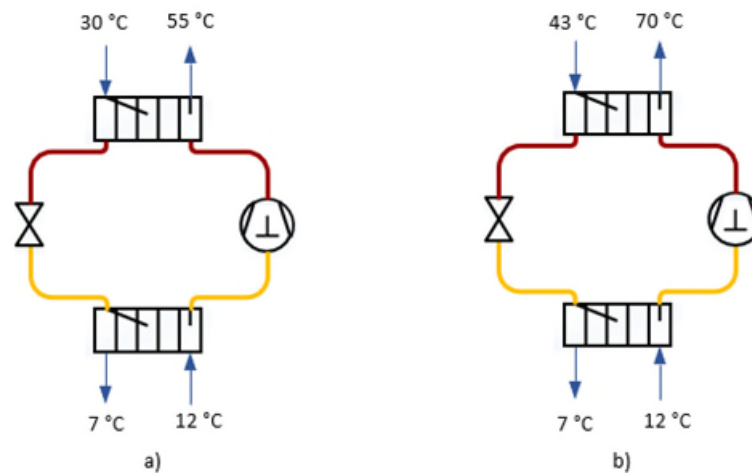


Figure 13: Design conditions of chiller and heat pump unit to supply cooling according to EU regulations and heating based on the requirements of HTF.

The capacity of the unit was determined based on the cooling needs of Rockwool, and HTF established that the new combined unit should have 200 kW of cooling capacity. The operating conditions of the unit to be analysed in the current project or, as it will be referred to in further documents, "modes" will be:

- Chiller and Heat Pump CHHP mode for both cooling and heating to the district heating grid.
- Chiller CH mode producing cooling, while the heating is not being used.
- Heat Pump HP mode producing heating, while the cooling is not used.

The research hypothesis is that a suitable chiller and heat pump unit design will be supported and improved employing advanced numerical models. With the work that will be presented in this research project, it will be possible to:

- Define the most suitable design for an efficient ammonia chiller and heat pump, considering different components and configurations.
- Determine the distribution of the refrigerant within the components of the system.
- Understand the dynamic response of these systems under different operating conditions and how the performance and charge distribution will be affected.

3. Preliminary design of ammonia chiller and heat pump

This chapter describes the procedure to perform a preliminary ammonia chiller and heat pump design.

3.1. Methods

3.1.1. Operating cycles

The system is intended to work as CH, HP or CHHP mode. However, the operating conditions of the chiller and heat pump presented in Figure 13 were used as design conditions. The rating test conditions for process chillers of the European standard EN 14511:2018 (European Committee for Standardization, 2018) were used as an inspiration to define the design conditions of the evaporator. In the condenser case, the same standard does not establish design conditions for the condenser of heat pumps. However, for chiller applications, it was established that a temperature difference of 5 K between condensation temperature and water outlet temperature should be used on condensers. Thus, this temperature difference will be used as a design condition for the condenser of the proposed chiller and heat pump. Table 2 presents the design conditions for the two concepts of chiller and heat pump.

Table 2: Design conditions of the two concepts of chiller and heat pump.

Temperature/Operation Mode	Chiller-Heat Pump 1	Chiller-Heat Pump 2
Evaporation [°C]	0	0
Inlet/outlet water in evaporator [°C]	12/07	12/07
Condensation [°C]	60	75
Inlet/outlet water in condenser [°C]	30/55	43/70

3.1.2. Possible configurations

Three configurations presented in Figure 14 were analysed to quantify the difference in performance and refrigerant charge. First Figure 14a, which was named HPR, shows a direct expansion (DX) configuration with the addition of a high-pressure receiver to store the excess of refrigerant needed by the cooling and heating mode. Second, Figure 14b, which was named CSC, shows a DX configuration with a subcooler to improve operational reliability and COP. Finally, Figure 14c, which was named LPR, shows a DX configuration with a low-pressure receiver which was analysed using the latest propane residential heat pumps in the market as an inspiration. The analysis of these three systems required additional operating conditions to be defined. Proper superheating at the evaporator outlet for the first and second systems should be assessed to guarantee stable operation. For the second and third systems, adequate subcooling at the condenser outlet should also be defined. Therefore, a superheating and subcooling analysis took place. The coefficient of performance, COP, was used to assess the proper superheating and subcooling for the system. From the design conditions presented in Table 2, the inlet water temperature into the evaporator was used to limit the amount of

superheating. In the same way, the inlet water temperature into the condenser was used to limit the amount of subcooling into the system.

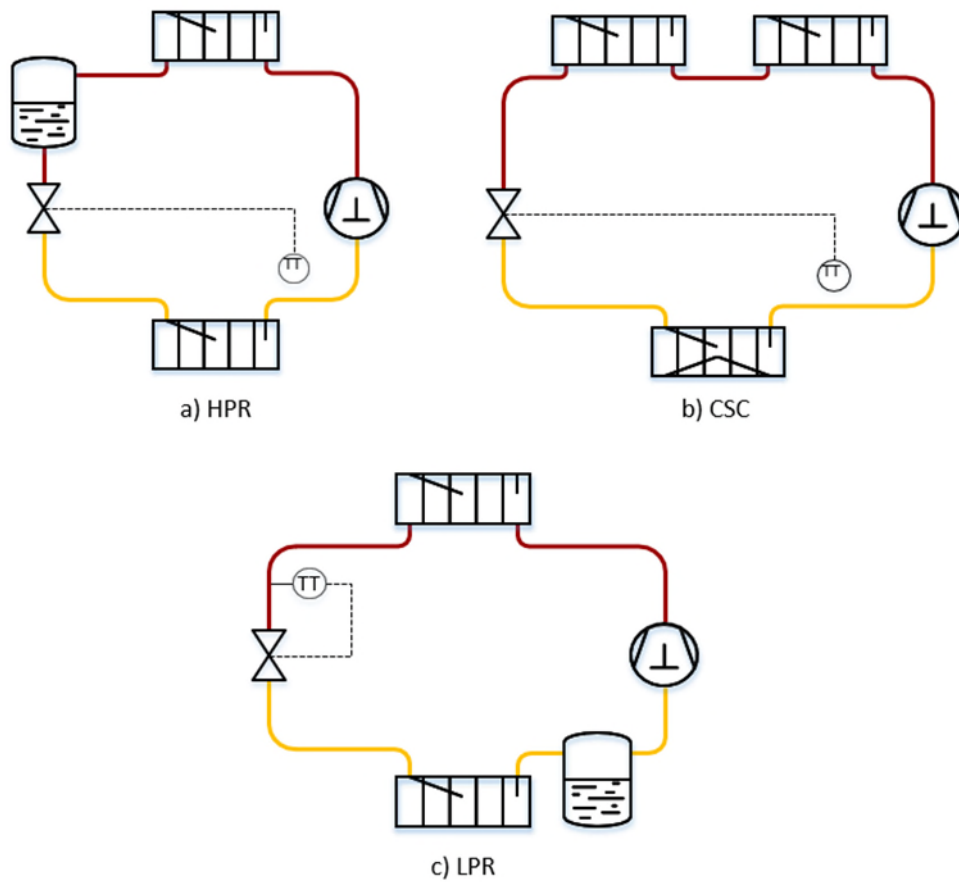


Figure 14: Possible configurations.

The three main components in the system (compressor, valve, and heat exchangers) were selected based on the market availability of equipment for ammonia systems. For the design, steady state models of the components were developed, including 1D-discretized heat exchanger models for the evaporator and the condenser. The available correlations for heat transfer and pressure drop were analysed for the present application.

3.2. Results

Figure 15 and Figure 16 show the operating cycle of the two concepts considering an ideal adiabatic compression process and without superheating or subcooling. The first concept has a COP of 3.5, and the second concept has a COP of 2.6.

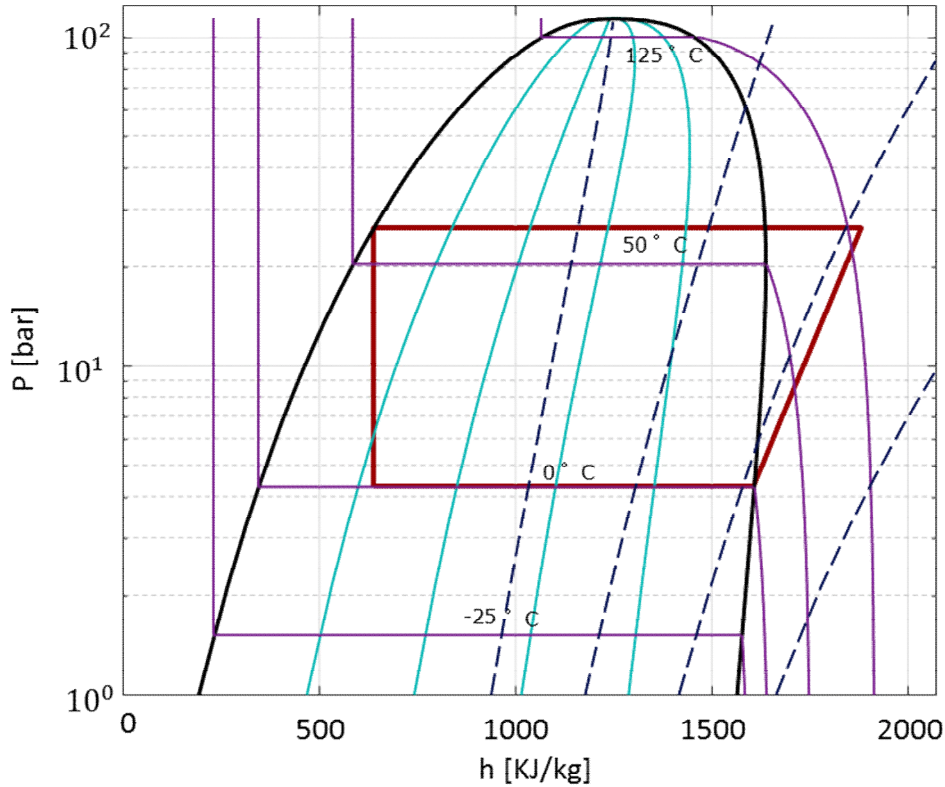


Figure 15: Vapour compression cycles of the first chiller-heat pump concept.

The superheating and subcooling analysis performed on the two concepts is presented in Figure 17a and

Figure 17b. In the case of ammonia, increasing the superheating decreases the COP, which is opposite to what usually happens with the common HFCs where increasing superheat increases the COP. An increment on the subcooling also increases the COP; thus, the current system should have as low superheating as possible and high subcooling. Nonetheless, due to the high latent heat of ammonia, the energy required for evaporation is higher than a standard HFC refrigerant, and even at lower values of superheating, there might still be a presence of liquid ammonia. Hence, manufacturers of ammonia systems recommend superheating values above 7 K, or the system might be complicated to control.

Table 3 presents the superheating, subcooling, and COP of the two concepts when using the three configurations presented in Figure 14. For the design of the chiller and heat pump unit, superheating of 10 K and a subcooling of 25 K were selected. In the HPR configuration, no subcooling can be expected due to the presence of the receiver after the condenser. In the same way, no superheating can be expected in the LPR configuration.

The screening process excluded the unsuitable correlations for calculating the local heat transfer coefficient of ammonia. The screening of the void fraction models performed with the conditions proposed for the evaporator and the condenser showed that some correlations are not suitable for the current application depending on the saturation temperatures and mass flow rates tested on the system.

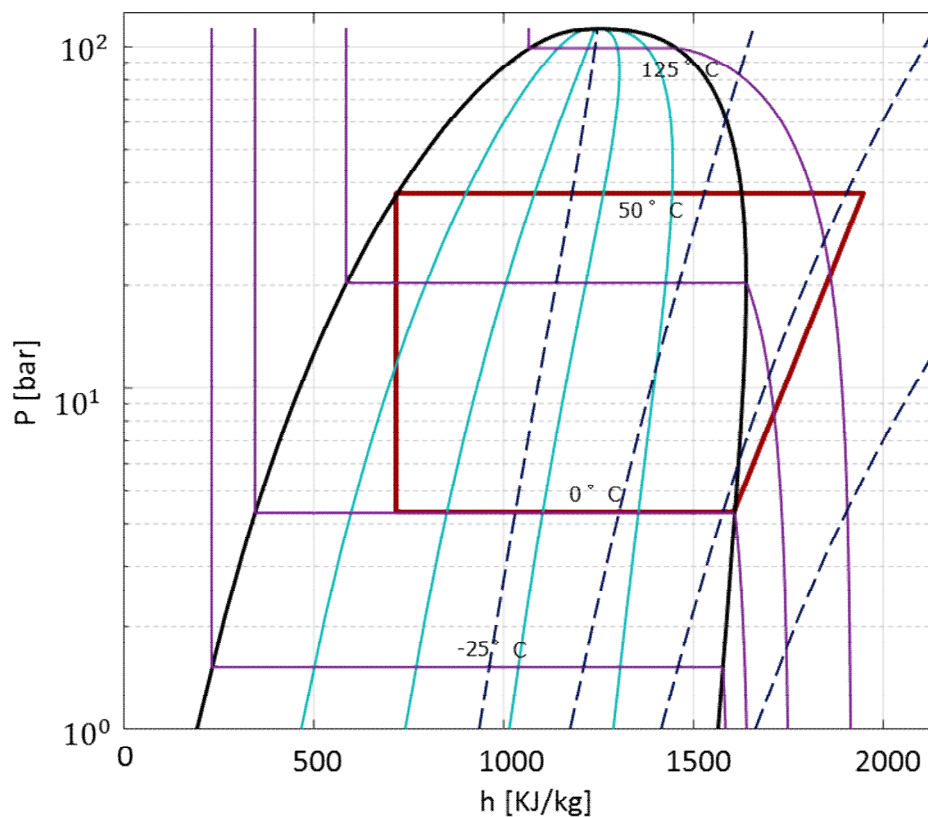


Figure 16: Vapour compression cycles of the second chiller-heat pump concept.

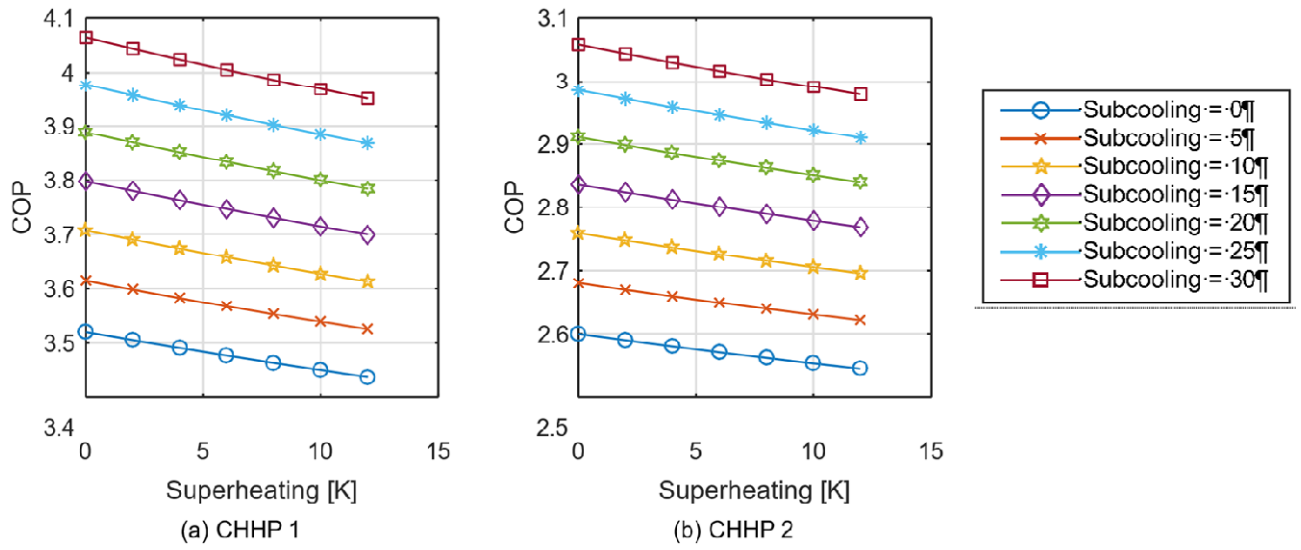


Figure 17: COP as a function of superheating for multiple values of subcooling.

Table 3: Superheating, subcooling, and COP of the chiller and heat pump concepts.

Configuration	CHHP 1			CHHP 2		
	HPR	CSC	LPR	HPR	CSC	LPR
Superheating [K]	10	10	0	10	10	0
Subcooling [K]	0	25	25	0	25	25
COP	3.45	3.88	3.97	2.55	2.92	2.98

4. Experimental validation

This chapter describes the validation of the numerical models developed for the heat exchangers in the previous chapter.

4.1. Methods

4.1.1. Experimental setups

The first experimental setup from where experimental data was obtained was like the first proposed system configuration presented in Figure 14a. The analysed system presented in Figure 18 was a 29 kW at 1240 RPM (43 Hz) water-to-water ammonia chiller with a direct expansion evaporator. The system had plate heat exchangers as evaporator and condenser. A Frigopol variable speed reciprocating compressor drives the unit. The compressor had a nominal swept volume of 35 m³/h at 1450 RPM (50 Hz) and was charged with 2.7 L of synthetic oil grade ISO 68. The oil was separated from the ammonia with a 7 L oil separator located in the discharge line of the compressor. In the suction line of the compressor, there was a liquid separator of 15 L capacity. The system also had a high-pressure receiver of 0.45 L capacity installed between the condenser and evaporator that stores refrigerant charge when varying boundary conditions and release it when needed.

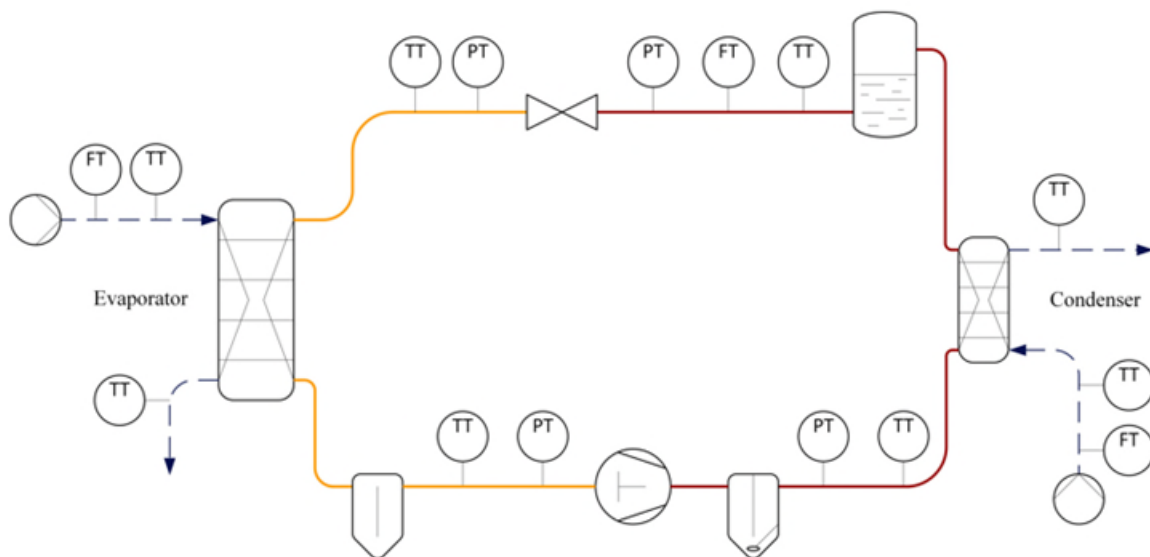


Figure 18: PI Diagram of the first configuration of the test rig.

The second experimental setup was like the proposed system configuration presented in Figure 14b. The system components are the same as the first system configuration. The only difference is that the high-pressure receiver was replaced by a subcooler which is also a plate heat exchanger. The specifications of the plate heat exchangers used as condenser, evaporator, and subcooler in both configurations are presented in Table 4.

Table 4: Plate heat exchanger specifications.

Geometry	Unit	Evaporator	Condenser	Subcooler
Volume	L	1.9	0.21	0.42
Heat transfer area	m ²	2.24	0.45	0.5
Width	mm	124	90	90
Length	mm	478	279	182
Number of plates	-	40	24	30
Corrugation depth	mm	2	1	2
Enlargement Factor	°	1.14	1.14	1.14
Corrugation pitch	mm	8	4	8
Hydraulic Diameter	mm	3.5	1.8	3.5
Chevron angle	°	30	35	35

4.1.2. Testing procedure performed on the first experimental setup

The testing procedure collected data of the heat exchangers when working at multiple mass flow rates and heat loads but maintaining water temperatures constant in both the evaporator and condenser. Table 5 presents the desired fixed operating conditions used during the data acquisition procedure. Aside from the nominal operating frequency of 1240 RPM (43 Hz), the testing procedure was performed at the part load operating frequencies of 40 Hz, 35 Hz, 30 Hz, and 25 Hz. Finally, the total amount of refrigerant charge inside the first experimental setup was 1.73 kg.

Table 5: Test conditions of the chiller.

Condenser			Evaporator			
P _{con}	T _{water_inlet}	T _{water_outlet}	P _{ev}	T _{water_inlet}	T _{water_outlet}	Superheat
[bar]	[°C]	[°C]	[bar]	[°C]	[°C]	[K]
15	16	40	5.9	20	10	10

4.1.3. Testing procedure performed on the second experimental setup

The testing procedure collected data of the heat exchangers when the compressor of the system was working at the same operating frequency of 40 Hz. However, two different refrigerant charges, 1.88 and 2.02 kg, were used to analyse the effects of different refrigerant charges in the system. To perform the test, the operating conditions in the evaporator, presented in Table 6, maintained the same evaporating pressure and inlet and outlet water temperature. Nevertheless, the superheating was an unknown of the testing procedure. In the case of the condenser and subcooler, the operating conditions presented in Table 6 wanted to maintain constant inlet and outlet water temperatures. However, the condensation pressure will change due to the variation in charge thus; different water temperatures and subcooling were expected.

Table 6: Second testing conditions of the chiller.

Subcooler-Condenser		Evaporator		
$T_{\text{water_inlet_Subcooler}}$	$T_{\text{water_outlet_Condenser}}$	P_{evp}	$T_{\text{water_inlet}}$	$T_{\text{water_outlet}}$
[°C]	[°C]	[bar]	[°C]	[°C]
15	40	5.9	20	10

4.1.4. Validation of correlations for heat transfer coefficient and pressure drop

In chapter 3, it was explained that to calculate the heat flow rate on the heat exchangers, heat transfer coefficient correlations for water and ammonia are needed. Figure 19 shows the procedure followed to validate the evaporator model. The cases, that were not discarded in the screening process, were used to generate different combinations of heat transfer correlations to calculate the overall heat transfer coefficient. Thus, 2940 simulations were performed to identify suitable heat transfer coefficient correlations to calculate the heat flow rate between water and ammonia. 105 simulations were done to estimate the pressure drop per successful combination of heat transfer coefficient correlations.

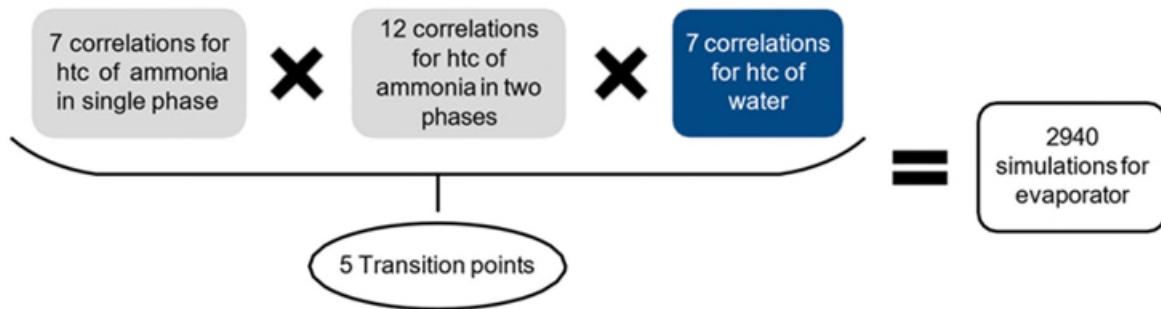


Figure 19: Validation of correlations to calculate heat transfer coefficient in the evaporator.

For the condenser, 2352 simulations were performed to identify suitable heat transfer coefficient correlations to calculate the heat flow rate between ammonia and water. For the condenser, 98 simulations were done to estimate the pressure drop per successful combination of heat transfer coefficient correlations. The procedure yielded a set of correlations that can be used to model heat flow rate and pressure drop in ammonia evaporators and condensers with a minimum error compared to experimental data. The presented procedure was also used to perform the simulations of the second experimental setup. The mass calculation was challenged to estimate the unaccounted mass term. (Shen et al., 2006) first introduced this term to account for the multiple factors that cause inaccuracies in refrigerant charge prediction, such as liquid volumes, refrigerant dissolved in the oil, or inaccurate void fraction models. The unaccounted mass term was calculated, and the veracity of the result was assessed based on two facts. The first fact was the maximum amount of liquid ammonia that the receiver can hold. The second was the reported maximum amount of refrigerant that can be dissolved in the lubricant oil. Based on the previous facts, the mass estimation of the evaporator and condenser was

considered acceptable if it was fulfilled for the first experimental setup. Hence, if the unaccounted mass term is below the maximum amount of liquid refrigerant that the receiver can hold plus the maximum value of refrigerant dissolved in the oil ($\approx 30\%$), it can be assumed that the estimation is within possible values. For the second experimental setup that has no liquid receiver, the mass estimation of the evaporator, condenser, and subcooler was considered acceptable in cases where only the maximum value of refrigerant dissolved in the oil ($\approx 30\%$) is considered.

4.2. Results

The mass flow rate of refrigerant and water was obtained from the testing procedure in chapter 3.1.2. The first experimental setup was used to calculate the refrigerant mass flux through the evaporator and condenser at different operating frequencies, as presented in Table 7. Moreover, the pressure drop of each heat exchanger is reported.

Table 7: Ammonia mass flow rate, mass flux, and pressure drop through the evaporator and condenser.

Frequency [Hz]	\dot{m}_A [kg/s]	$G_{A_{ev}}$ [kg/s·m ²]	Δp_{ev} [bar]	$G_{A_{con}}$ [kg/s·m ²]	Δp_{con} [bar]
25	0.0149	3.4	0.23	17.3	0.33
30	0.0182	4.2	0.38	21.1	0.44
35	0.0215	4.9	0.54	24.9	0.47
40	0.0246	5.6	0.72	28.5	0.49
43	0.0259	5.9	0.82	30.0	0.51

Table 8 shows the results at different operating conditions and the propagated uncertainty of the calculation. The chiller simulations at different operating frequencies were performed.

Table 8: Water mass flow rate and heat flow rate through the evaporator and condenser.

Frequency [Hz]	$\dot{m}_{W_{ev}}$ [kg/s]	Q_{ev} [kW]	Uncertainty [%]	$\dot{m}_{W_{con}}$ [kg/s]	Q_{con} [kW]	Uncertainty [%]
25	0.3882	16.7	4.0	0.2020	19.1	2.8
30	0.4800	20.3	3.9	0.2248	23.4	2.7
35	0.5711	23.9	3.9	0.2706	27.7	2.7
40	0.6615	27.1	3.9	0.3064	32.3	2.7
43	0.7057	28.7	3.9	0.3215	34.1	2.8

Table 9 presents the combination of correlations for the heat transfer coefficients in the condenser. In this case, (Longo & Gasparella, 2007) for ammonia in single-phase and water yielded the best results for all the frequencies analysed. Regarding the two-phase region, (Zhang et al., 2019) performed better at the lower frequencies, but above 35 Hz; the correlation of (Arman & Rabas, 1995) presented the most accurate results.

Table 9: Combination of heat transfer coefficient correlations during condensation.

Frequency	Superheated region	Condensation region	Water	Q'con	Q' model	Deviation
[Hz]				[kW]	[kW]	[%]
25	(Longo & Gasparella, 2007)	(Zhang et al, 2019)	(Longo & Gasparella, 2007)	19.1	18.2	-4.8
30	(Longo & Gasparella, 2007)	(Zhang et al, 2019)	(Longo & Gasparella, 2007)	23.4	22.6	-3.6
35	(Longo & Gasparella, 2007)	(Arman & Rabas, 1995)	(Longo & Gasparella, 2007)	27.7	27.2	-1.9
40	(Longo & Gasparella, 2007)	(Arman & Rabas, 1995)	(Longo & Gasparella, 2007)	32.3	31.4	-2.7
43	(Longo & Gasparella, 2007)	(Arman & Rabas, 1995)	(Longo & Gasparella, 2007)	34.1	34.4	0.7

For the discretized 1-D model of the condenser, Figure 20a and Figure 20b present the local heat transfer coefficient and pressure drop calculation.

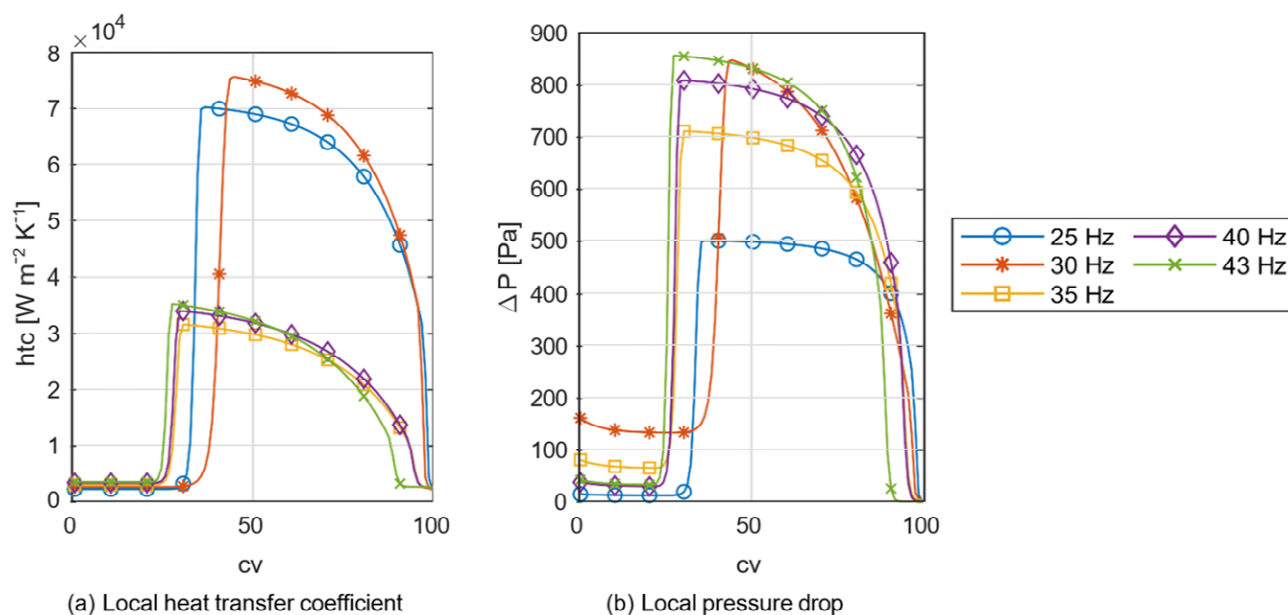


Figure 20: Local heat transfer coefficients and pressure drop in 1-D discretized model of condenser.

For the second experimental setup, a similar analysis was completed. One of the results of this is the refrigerant mass estimation shown in Table 10. The maximum ammonia dissolved in the oil is 0.5633 kg for the first experimental setup and 0.6059 kg for the second experimental setup.

Table 10: Mass estimation of the second experimental setup.

Frequency [Hz]	Components [kg]	Condenser [kg]	Subcooler [kg]	Evaporator [kg]	Unaccounted [kg]
1	0.2490	0.0240	0.1840	0.6290	0.7910
2	0.2560	0.0240	0.1940	0.6550	0.8910

5. Final design and control approach

This chapter presents the final design of the chiller and heat pump unit concepts. Furthermore, a dynamic model of the concepts and the implementation of the control approach is also presented.

5.1. Method

In chapter 3, it was determined that the LPR configuration could be the best configuration to develop the chiller and heat pump unit. Therefore, a design of the LPR configuration was developed for the two proposed concepts to compare the difference in component size, performance, and refrigerant charge.

5.1.1. Compressor

The compressor used was from Bitzer (BITZER, 2021). The polynomials provided by Bitzer are based on the AHRI rating standards (Aute et al., 2015). The discharge temperature was controlled by oil cooling.

5.1.2. Plate heat exchangers

Plate heat exchangers were used to guarantee the compactness of the system, and the models presented in chapter 3 were used to design the geometry of the plate heat exchangers for the current concepts. Specifications from plate heat exchanger manufacturers that can provide heat exchangers for the current system, such as SWEP (SWEP, 2021), were used to define the limits on the geometrical parameters for the analysed heat exchanger cases. The optimisation procedure of the geometry of the heat exchanger was performed using the distribution of CasADi (Andersson et al., 2019) for MATLAB (MATLAB, 2021). In this case, the non-linear programming solver IPOPT (Wächter, 2002) was used to perform the geometrical optimisation. The development of a chiller and heat pump unit requires a complex control approach. Thus, a closed loop control system must be developed. However, whether a closed control loop is stable can only be answered in a dynamic simulation. This chapter will present the development of the dynamic models and will also analyse the dynamic operation of the chiller and heat pump unit.

5.1.3. Dynamic model

Dynamic models of the chiller and heat pump concepts designed in the previous chapter were implemented in the object-oriented modelling language Modelica (Modelica, 2022) through the simulation software Dymola (Dempsey, 2006). Moreover, the Model library for thermal components and systems TIL (Richter, 2008) was used. A PI controller was used to control the valve. Thus, subcooling became the control variable for the valve. In this way, it was possible to mimic the operation of the electronic expansion valve. A second PI controller was used to control the compressor speed by measuring cold water supply temperature as the second control variable of the system. The hot water supply temperature was the third control variable that helped to control the speed of the

circulation pump through a third PI controller. The complete control diagram of the system can be seen in Figure 21, where each control component is connected to the sensor that measures its respective control variable.

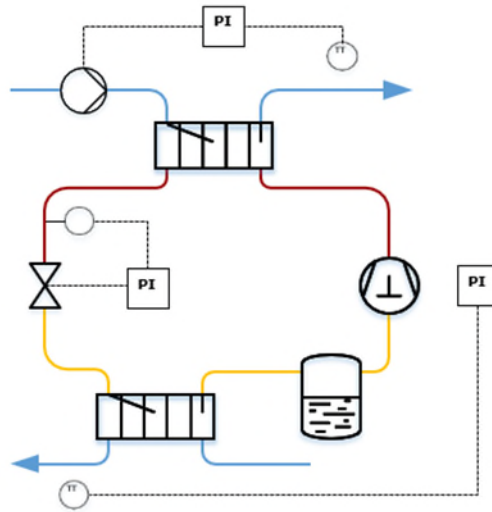


Figure 21: Control diagram of the chiller and heat pump.

The AMIGO method was used to calculate the parameters in the PI controllers of the chiller and heat pump. The AMIGO method required a step response method in which the pump and compressor were submitted to a ± 1 Hz step response, and the valve was submitted to a ± 0.001 m³/h of K_v value change.

5.1.4. Analysis of chiller and heat pump operation

The operation of the chiller and heat pump concepts with the implemented control approach must be assessed. Since three operating modes have been proposed, chiller operation (CH), heat pump operation (HP), and chiller/heat pump (CHHP), it was imperative to analyse the transition between the different modes. As an example, Figure 22 represents the change in the temperature setpoint of the condenser in the first chiller and heat pump concept; thus, the system tended to shift from CHHP to CH mode.

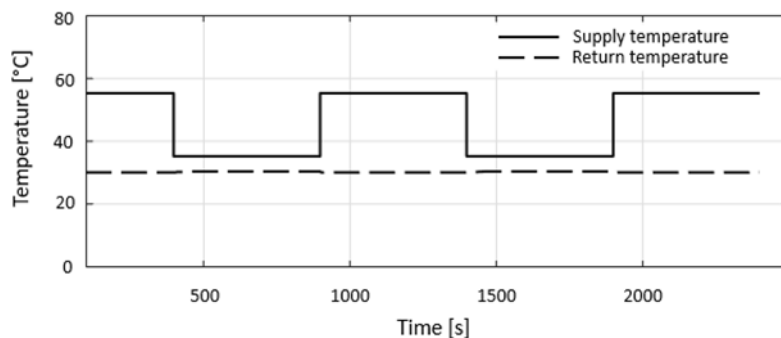


Figure 22: Temperature change from CHHP mode to CH mode in concept 1.

5.2. Results

Table 11 compiles the main characteristics of the compressor when working at design conditions. The efficiencies of the Bitzer compressor are higher than the efficiencies of the GEA compressor, which is an expected value since the second concept that used the GEA has a higher pressure ratio at the design condition. Thus, lower efficiencies can be expected.

Table 11: Specifications of compressors at design conditions.

	Bitzer	GEA
Displacement [m^3/h]	266	393
Minimum Speed [RPM]	1450	1500
Nominal Speed [RPM]	3500	3550
Maximum Speed [RPM]	4000	3600
Isentropic Efficiency [-]	0.58	0.49
Volumetric Efficiency [-]	0.84	0.58

The parameter study generated several possible geometrical configurations of plate heat exchangers that can be used on the chiller and heat pump concepts. Figure 23a shows the refrigerant mass as a function of the length and pressure drops, which are the three outputs of the parameter study plotted in a two-dimensional plane. The performed parameter study had several inputs; thus, a multidimensional set of possible solutions was obtained. Therefore, the mass of the refrigerant inside the condenser is represented as a function of the parameter study inputs to represent better the influence of each parameter on the refrigerant charge and pressure drop. The mass is plotted as a function of the pressure depth and pressure drop in Figure 23b. The figures show that using a length below 300 mm or a pressure depth of 1 mm only produces solutions with significantly lower refrigerant charge values. However, higher pressure drops, whereas using higher values of length or pressure depth yields a more spread set of possible solutions.

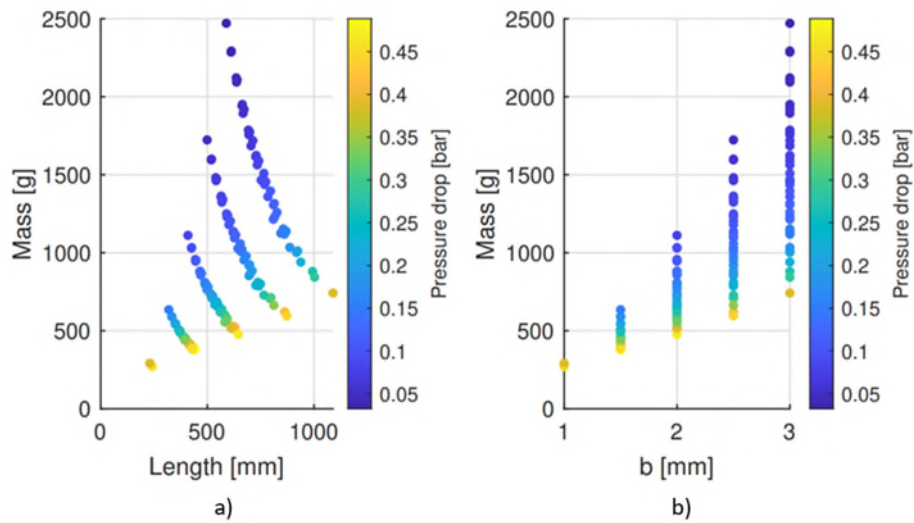


Figure 23: a) Mass as a function of length and pressure drop. b) Mass as a function of pressure depth b and pressure drop.

Figure 24a shows the mass of refrigerant as a function of the width and pressure drop, and Figure 24b shows the mass of refrigerant as a function of the number of channels and pressure drop.

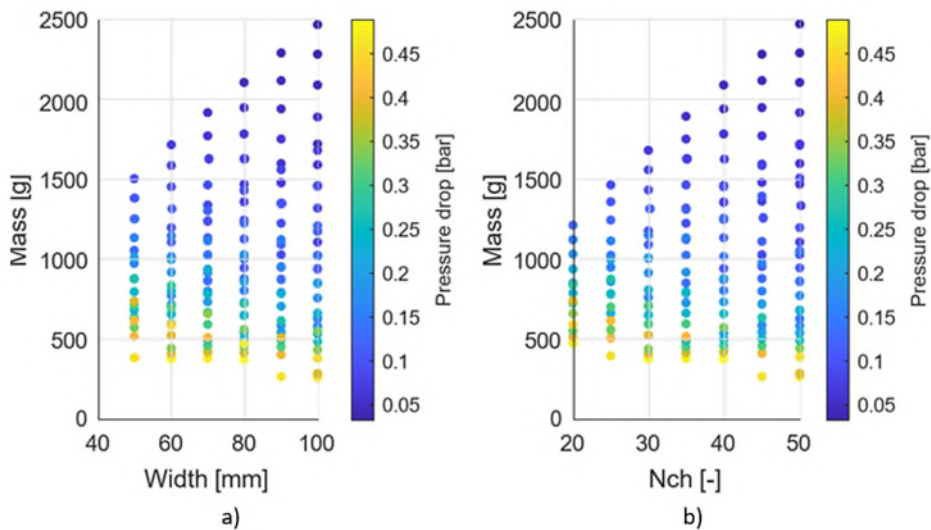


Figure 24: a) Mass as a function of width and pressure drop. b) Mass as a function of number of channels and pressure drop.

The point with the lower mass shown in Figure 23a and b also correspond to the point of higher width and number of channels. Besides, it can be seen that for the presented ranges of width and number of channels, there are plenty of possible geometrical configurations that can be designed. The geometrical optimisation performed on the evaporator and condenser yielded the geometries used to design the chiller and heat pump concepts. Table 12 compiles the geometrical specifications of the designed condenser and evaporator for the first concept, and Table 13 compiles the specifications for

the second concept. The application of actual compressor specifications and polynomials defines the mass flow of the system. Thus, different heat flow rates in both evaporator and condenser are calculated under the desired operating conditions. In practice, when regulating the system to supply the desired 200 kW, a change in evaporation and condensation temperature occurs.

Table 12: Plate heat exchanger specifications of first concept.

Geometry	Unit	Evaporator	Condenser
Heat transfer area	m ²	6.72	2.14
Width	mm	140	100
Length	mm	420	188
Number of plates	-	102	102
Corrugation depth	mm	3	1
Enlargement Factor	-	1.14	1.14
Corrugation pitch	mm	12	4
Hydraulic Diameter	mm	5	2
Chevron angle	°	30	60
Heat Transfer	kW	236.15	258.3
Pressure Drop	bar	0.40	0.37

Table 13: Plate heat exchanger specifications of second concept.

Geometry	Unit	Evaporator	Condenser
Heat transfer area	m ²	6.37	1.84
Width	mm	140	100
Length	mm	499	179
Number of plates	-	82	92
Corrugation depth	mm	3.5	1
Enlargement Factor	-	1.14	1.14
Corrugation pitch	mm	14	4
Hydraulic Diameter	mm	6	2
Chevron angle	°	30	60
Heat Transfer	kW	223	253.6
Pressure Drop	bar	0.35	0.31

5.2.1. Refrigerant charge

The refrigerant mass inside the system for both concepts has been calculated and presented in Table 14. The volume of the receiver was calculated as 1.8 L for the first concept and as 2 L for the second concept. The charge calculated inside the compressor can be considered negligible in further analysis since it is much smaller than the other components. The specific charge is usually used to measure the effectiveness between the cooling load and the amount of refrigerant used by the system. In this case, the first concept has a specific charge of 4.83 [g/kW] and the second one of 5.72 [g/kW].

Table 14: Mass estimation and receiver volume of the concepts.

	Compressor [g]	Condenser [g]	Evaporator [g]	Receiver [g]	Oil [g]	Total [g]
Concept 1	13.6	208.0	701.7	113.7	103.7	1140.7
Concept 2	25.3	183.0	826.5	126.2	116.1	1277.1

5.2.2. Dynamic model and chiller and heat pump operation

Table 15 shows a comparison of the refrigerant charge calculated by the TIL models using the homogeneous model and the modified VLE cell with the void fraction model of Kanizawa implemented. As can be seen from the table, the homogenous model drastically underpredicts the refrigerant charge, especially on the evaporator.

Table 15: Comparison of refrigerant charge estimation for Concept 1 and Concept 2.

		Homogeneous	Kanizawa
Concept 1	Evaporator	85.8	1035
	Condenser	168.7	225.3
Concept 2	Evaporator	90.8	1121.0
	Condenser	88.0	141.3

The calculated control parameters with the AMIGO method are presented in Table 16. It was impossible to achieve a stable operation in both concepts when shifting from CHHP to CH mode.

Table 16: PI controller parameters.

	Pump	EEV	Compressor
K	1	0.7	0.5
Ti	2	7	2

Figure 25 presents the inlet and outlet temperatures of the condenser in the first concept during the shifting between the operation mode. It can be seen that the system successfully shifted from 55 °C to 35 °C in supply temperature.

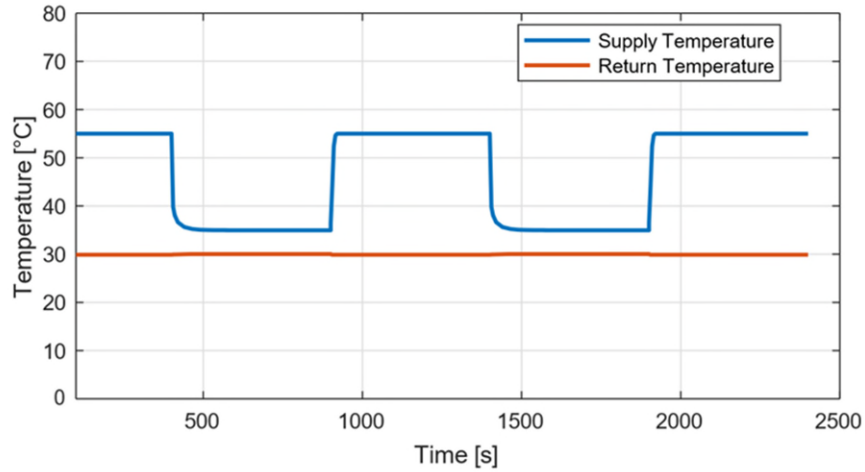


Figure 25: Condenser temperatures in the first concept.

Figure 26 presents the refrigerant charge inside the evaporator, condenser, and receiver.

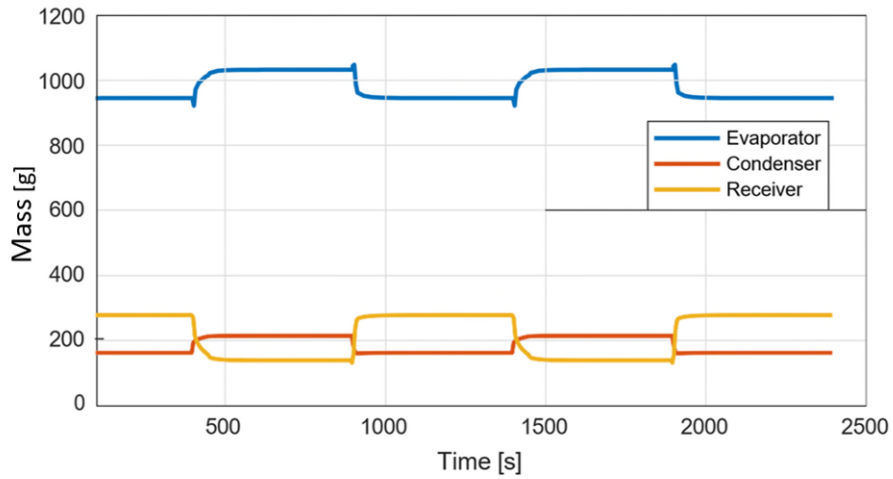


Figure 26: Refrigerant charge distribution in the first concept.

Figure 27 presents the inlet and outlet temperatures of the condenser in the second concept during the shifting between the operation mode. It can be seen that the system successfully shifted from 70 °C to 35 °C in supply temperature and from 43 °C to 30 °C in return temperature.

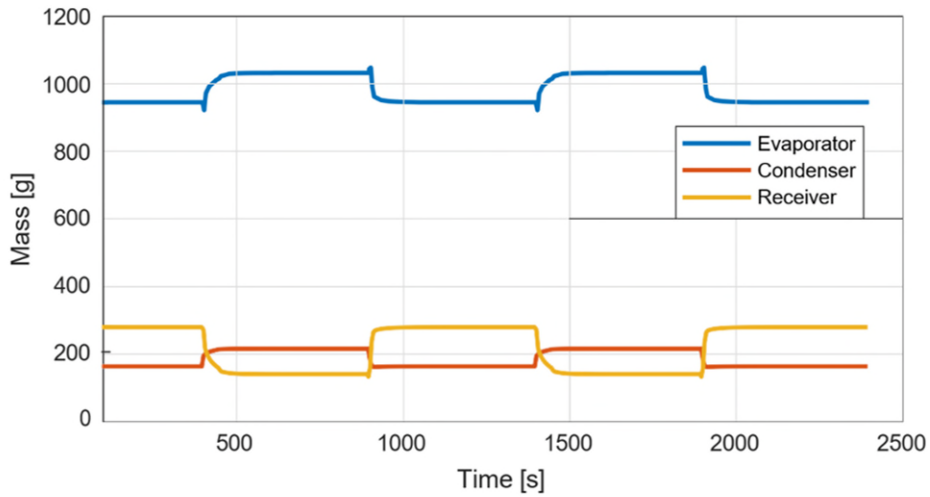


Figure 27: Condenser temperatures in the second concept.

Figure 28 presents the refrigerant charge inside the evaporator, condenser, and receiver.

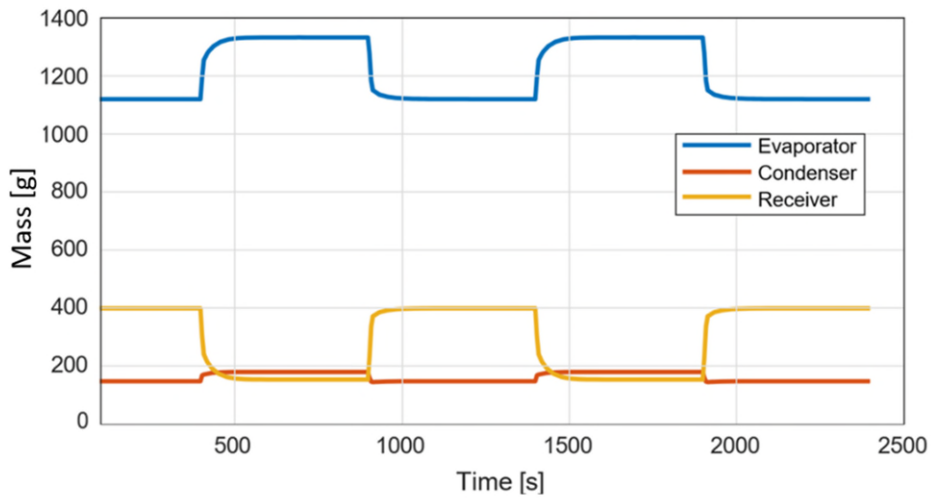


Figure 28: Refrigerant charge distribution in the second concept.

Figure 29 presents the inlet and outlet temperatures of the evaporator in the second concept during the shifting between the operation mode. The system successfully shifted from 7 °C to 34 °C in supply temperature and from 12 °C to 39 °C in return temperature.

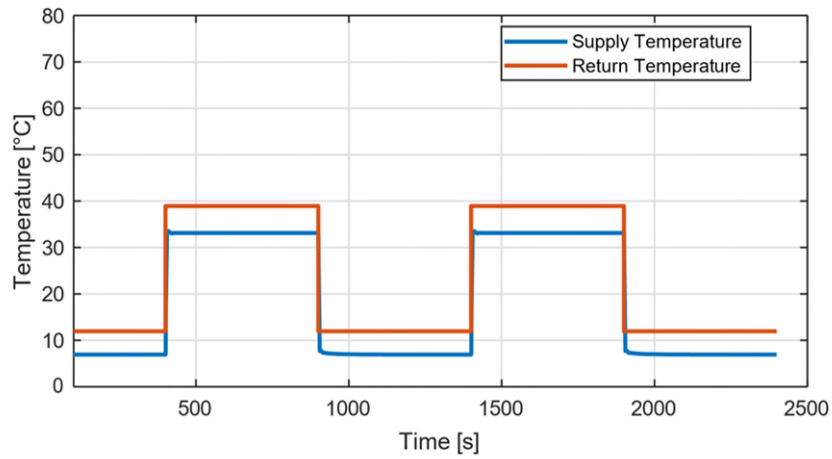


Figure 29: Evaporator temperatures in the second concept.

Figure 30 presents the refrigerant charge inside the evaporator, condenser, and receiver. The results suggest that the low-pressure receiver can allocate the charge even when a sudden change in operating mode occurs.

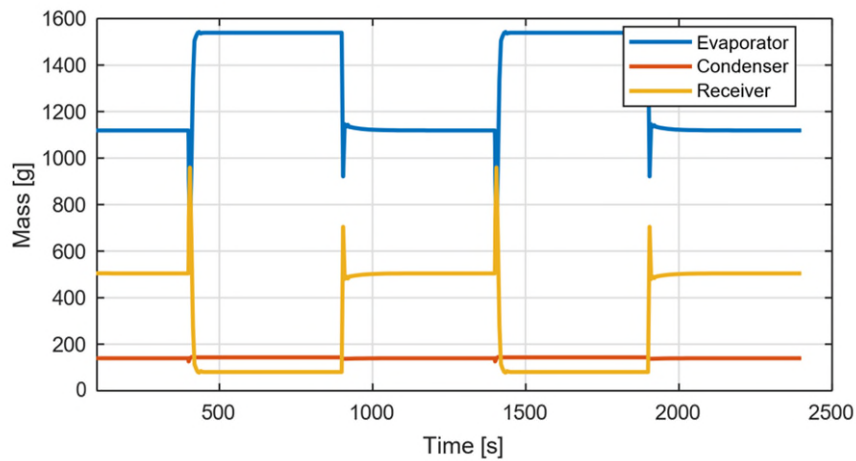


Figure 30: Refrigerant charge distribution in the second concept.

6. Research conclusions

This research is aimed at developing more energy efficient cooling and heating systems by designing a system that supplies both needs while using ammonia as a working fluid. The advantages of ammonia as a refrigerant were presented and also some of the work and studies performed by other authors to develop low charge ammonia systems.

A novel design of an ammonia chiller and heat pump unit to minimise the refrigerant charge and work with components found in the market were introduced. The possible configurations that such a system can have were investigated. It was decided that the suitable way to guarantee a low charge system would be by using a direct expansion evaporator to minimise the liquid refrigerant as much as possible. After that, three different configurations were proposed to analyse the possible COP of the unit and to define parameters such as superheating and subcooling.

After performing market research to find possible components to develop the systems, the most challenging component to find and implement is the compressor followed by the expansion valves, which should be electronic expansion valves to assure proper operation of the system.

A modelling approach was developed for the plate heat exchangers used in the system. Experimental data from an existing test rig of a compact ammonia refrigeration unit was used to validate the models. The data corresponds to two different configurations that were analysed with the models to find a set of suitable correlations of heat transfer coefficients and pressure drops that can be used to develop the proposed unit. Moreover, a suitable void fraction model was identified that could better estimate the refrigerant charge inside the evaporator and condenser.

A design of a medium capacity low charge ammonia chiller and heat pump unit was proposed using the configuration with a low-pressure receiver that was identified as the most suitable to minimise charge and facilitate control. Two concepts were proposed based on two different design conditions provided by a company interested in developing the system.

The plate heat exchanger models for condenser and evaporator with the identified correlations for heat transfer coefficient, pressure drop, and void fraction were used to perform a parameter study on the multiple geometrical parameters that affect the design of the plate heat exchangers.

The leading focus of the study was to analyse how the different geometry configurations affect the refrigerant charge and pressure drop. The accuracy of the analysis depends mainly on the accuracy of the correlations previously identified. The parameter study also allowed to identify the multiple geometries that the plate heat exchangers can have. Thus, when implementing an optimisation procedure, the boundaries of the parameters used in the optimisation can be defined appropriately based on the requirements of the designer.

A dynamic model of the chiller and heat pump units was implemented on Dymola using the thermodynamic library TIL. The components of the library were modified to include the identified correlations for heat transfer coefficient, pressure drop, and void fraction. A control structure was also defined and implemented on the dynamic models to assess the reliable operation of the system when shifting between the different modes of operation.

7. Testing of concept

7.1. Test setup

With the aim to test novel ideas of how to control the evaporator for chillers and heat pumps with very low or zero superheat, a test setup has been built. In Figure 7, the modified test setup is shown.

The PI diagram of the test setup in Figure 31 below shows the structure of the test setup. The high-pressure side is built up with condensers in series with a subcooler. The subcooler is connected in parallel with the receiver, which results in a liquid level in the subcooler during operation. The fluid level will vary depending on several parameters, i.e., the speed of the compressor as well as the selected temperatures on the warm and the cold side. Thus, the condenser will act as a partial condenser, and the subcooler can be considered as a hybrid consisting of a condenser as well as of a subcooler. The water side has been connected in series through the condenser and subcooler during all tests.

The blue boxes marked in Figure 31 show where the sensors are mounted. All the sensors are connected to the logging system. The most relevant sensors used in the measurements are listed in Table 17.

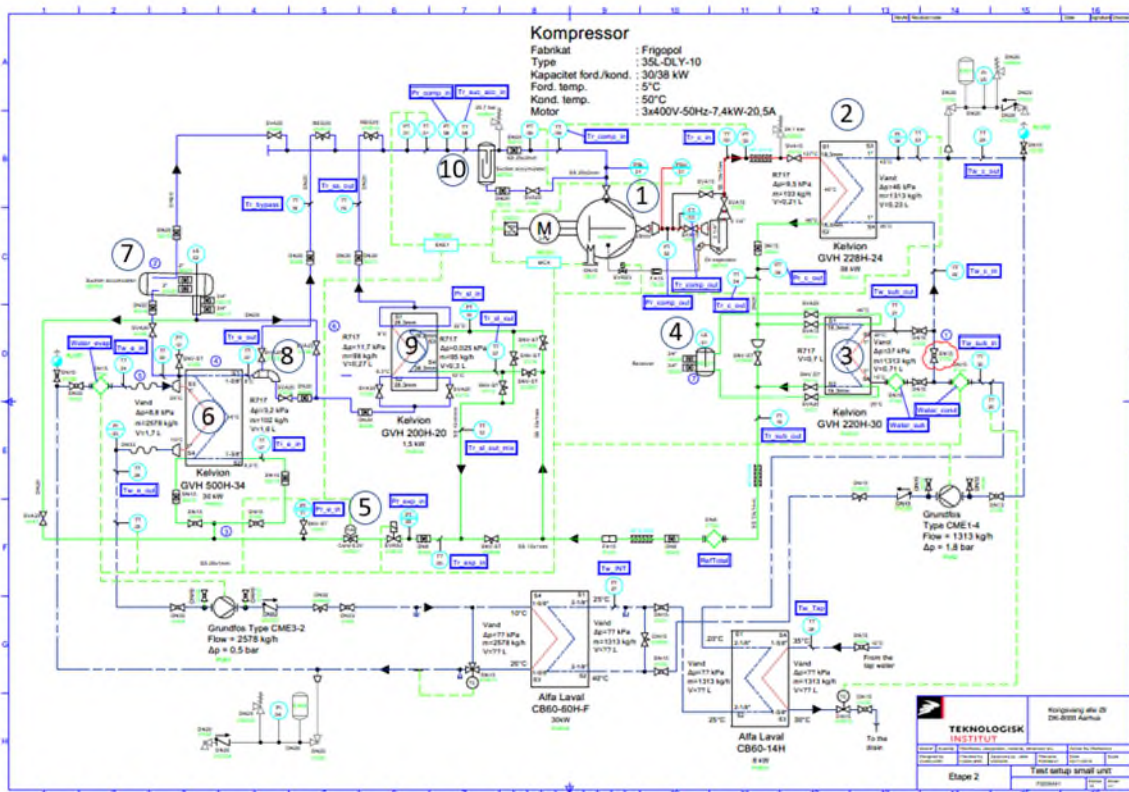


Figure 31: PI diagram of the test setup with placement of sensors for measurements (in blue boxes) 1 – Compressor, 2 – Condenser, 3 – Subcooler, 4 – Receiver, 5 – Expansion valve, 6 – Evaporator, 7 – Highly efficient liquid separator, 8 – Simple liquid separator, 9 – Suction gas heat exchanger, 10 – Suction accumulator.

The low-pressure side is shown in Figure 32. It is laid out with an evaporator, 6, which runs counter-current on the water side. The evaporator is equipped with two inlets and two outlets. Two separators, 7 and 8, are connected to the evaporator, both of which are connected in series with a suction gas heat exchanger, 9 (SGHX). The SGHX is followed by a suction accumulator, 10. From the suction accumulator, the gas is led through the compressor and from there further to the high-pressure side.

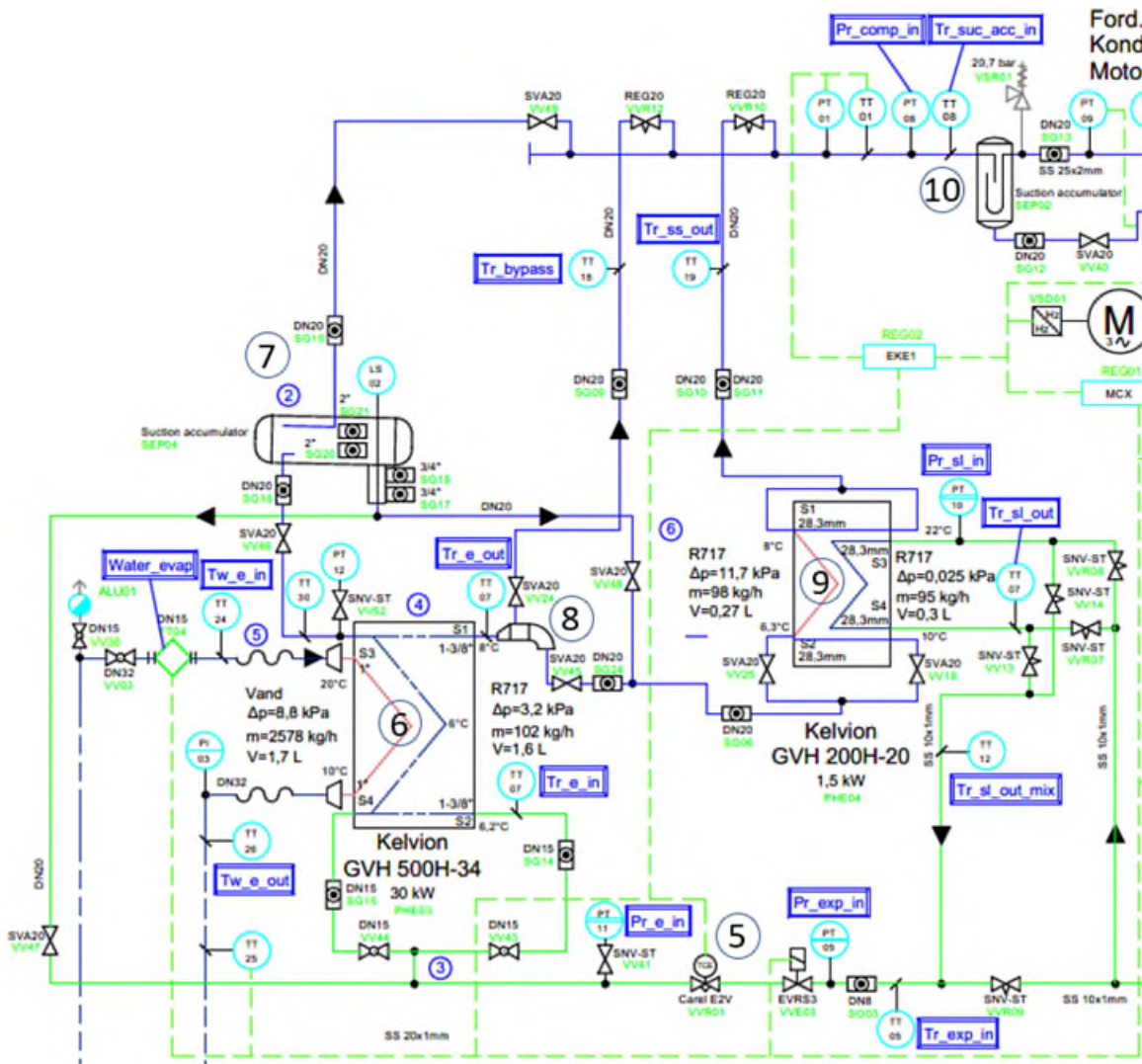


Figure 32: Zoom of left part of the PI diagram of the test setup with focus on the low-pressure part. 5 – Expansion valve, 6 – Evaporator, 7 – Highly efficient liquid separator, 8 – Simple liquid separator, 9 – Suction gas heat exchanger, 10 – Suction accumulator.

The starting point for the evaporator is that the evaporator temperature should be held close to the saturated gas temperature at the outlet, i.e., with a very low superheat and preferably with a quality of the gas just below one. This will provide a good utilization of the evaporator surface and lead to only a minimal amount of ammonia in the evaporator.

Figure 32 shows how the low-pressure side is connected in a PI diagram, and Figure 33 is a 3D representation of the same. The construction is designed to allowing several paths from the evaporator, 6, to the suction accumulator, 10. One path is through the highly efficient separator, 7. Here the dry suction gas goes through the "Dry suction separator, 7" to the suction accumulator. The separated liquid flows to the drop leg and from there to the suction gas heat exchanger to be evaporated by the heat from the liquid ammonia from the subcooler before mixing with the dry gas from the separator, 7, before entering the suction accumulator.

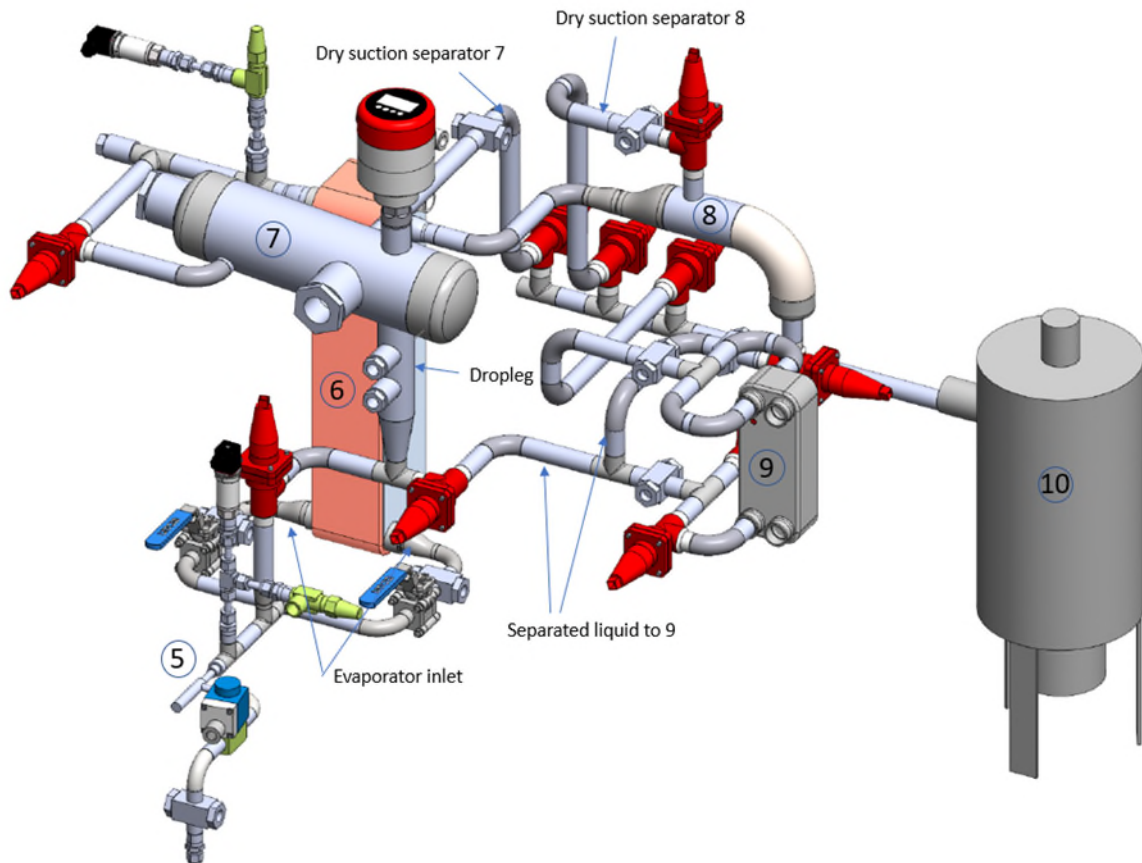


Figure 33: View of test setup. 5 – Expansion valve, 6 – Evaporator, 7 – Highly efficient liquid separator, 8 – Simple liquid separator, 9 – Suction gas heat exchanger, 10 – Suction accumulator.

An alternative route for the gas flow from the evaporator is through the simple liquid separator, 9. Here the dry gas leaves through the "Dry suction separator, 8", and the separated liquid flows from the bottom of the separator to the suction gas heat exchanger.

The evaporator is installed without a distributor, but at the inlet of the evaporator, it is possible to run with two inlets (see Figure 33). The expectation is that the distribution in this way will be improved significantly compared to a solution with only one inlet.

The path of the refrigerant to the compressor always goes via a suction accumulator, 10. The risk of ending up with liquid in the compressor is thereby minimized. The suction accumulator, 10, is important to reduce the risk of liquid to the compressor in case of an unstable control of the evaporator.

As shown in Figure 32 and Figure 33, a suction gas heat exchanger (SGHX), 9, is mounted in the refrigerant circuit. This must be able to evaporate the small liquid overflow that exits in the evaporator and additionally to generate sufficient superheating for the temperature sensor (Tr_suc.acc.in) which is used to control the expansion valve, 5, in the case where the expansion valve is superheat controlled.

In Table 17, the main sensors shown in the PI diagram are explained.

Table 17: List of selected measuring points.

Name of sensor	Placement after	Placement before	Description
T_W_e_in		Evaporator	Water in (°C)
T_W_e_out	Evaporator		Water out (°C)
T_r_succ.acc.in	SGHX	Suction accumulator	Superheat sensor for the expansion valve. (°C)
T_r_sub_out	Subcooler		Refrigerant out (°C)
T_r_sl_mix_out	SGHX		Liquid refrigerant out (°C)
T_r_exp_in		Expansion valve	Refrigerant in (°C)
T_r_e_out	Evaporator	Small separator: Test 1,2,4. Large separator: Test 3	Refrigerant out of evaporator (°C)
T_e_sat	Evaporator		Evaporation temperature. Calculated from pressure measurement (Pr_comp_in). Refrigerant (°C)
T_c_sat	Condenser		Evaporation temperature. Calculated from pressure measurement (Pr_c_out). Refrigerant (°C)
T_r_ss_out	SGHX (30 cm)		Refrigerant (°C)
T_r_bypass	Small separator		Refrigerant (°C)
Niveau liq sep			Level in large liquid separator (%)
Niveau receiver			Level in receiver (%)
EX_OD	-	-	Opening of expansion valve (%)
Ref. Total	Subcooler		Refrigerant flow (kg/h)

7.2. Description of tests

A survey and comparison of the four test setups can be seen below in Table 18. The primary variation in the tests is on the type of separator used, the type of flow in the suction gas heat exchanger, the type of control of the direct expansion, and if the subcooler has been utilized.

Table 18: Test configurations for the four tests.

Test number	1	2	3	4
Separator	Simple	Highly efficient	Highly efficient	Simple
Valve between separation drop leg and SGHX	Open	Open	Slightly open	Open
SGHX flow	Co-current	Co-current	Counter-current	Counter-current
Condensate flow	A part is bypassing the SGHX	A part is bypassing the SGHX	All condensate is passing through the SGHX	All condensate is passing through the SGHX
Evaporator	Counter-current flow and two inlets			
DX mode	Auto	Auto	Manual	Manual
Subcooler	Switched off	Switched off	Switched on	Switched on
DX sensor placement	Between the SGHX and the suction accumulator			
Compressor speed	Constant			
Temperature sensor, Tr_e_out, placement	Between outlet of evaporator and simple separator	Between outlet of evaporator and highly efficient separator	Between outlet of evaporator and highly efficient separator	Between outlet of evaporator and simple separator

7.2.1. Results from Test 1 (15/2-2022)

This test is performed to investigate the function of the simple liquid separator and to test the suction gas heat exchanger (SGHX). It was found in preliminary tests before the modification of the test setup that by running all the gas and liquid flow from the evaporator through the SGHX, the liquid ammonia in the gas stream was maldistributed in the SGHX. It was noticed that the liquid ammonia was shortcutting the SGHX through the first and last channel instead of evenly distributing along the plate pack. The liquid separator was thereby installed to separate the liquid and send it to the SGHX to be boiled off. This test is done to see how much gas that could be sent along with the liquid to the SGHX.

Following conditions are used in Test 1:

- Test with a small separator and SGHX. The test started with most of the gas bypassing the SGHX, and over time, more and more gas was forced through the SGHX.
- The SGHX is configured for co-current flow, and a part of the liquid from the condenser is bypassing the SGHX.
- The evaporator is configured for counterflow and with two refrigerant inlets.
- The evaporator is configured with direct expansion (DX) in auto mode. The superheat is static at 12 K and controlled by the superheat controller.
- The subcooler is switched off by bypassing the water around the subcooler.

- The DX sensor is placed just before the suction accumulator, but after the SGHX (T_r_succ.acc_in).
- Constant speed (rpm) of the compressor.

The measurement results are shown in Figure 36. Valve positions are seen in Figure 34 and Figure 35. The commented results from the thermographic measurements can be seen in Table 19.

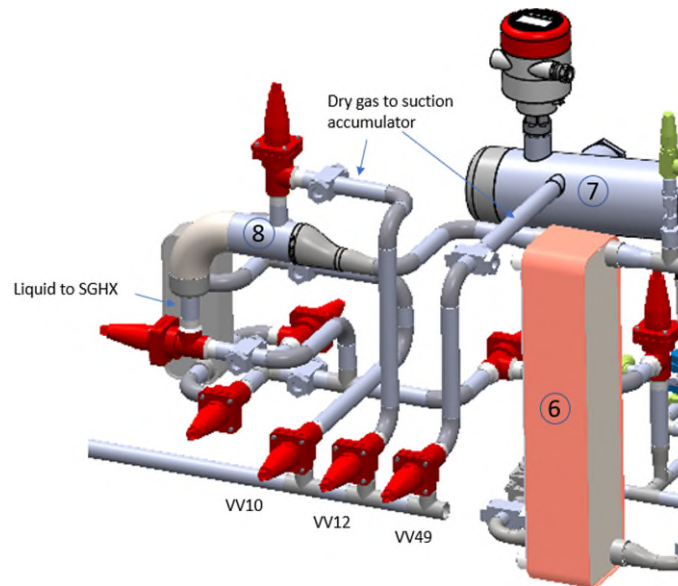


Figure 34: View of test setup. Most of the thermographic pictures are seen from this side of the test setup. 6 – Evaporator, 7 – Highly efficient liquid separator, 8 – Simple liquid separator.

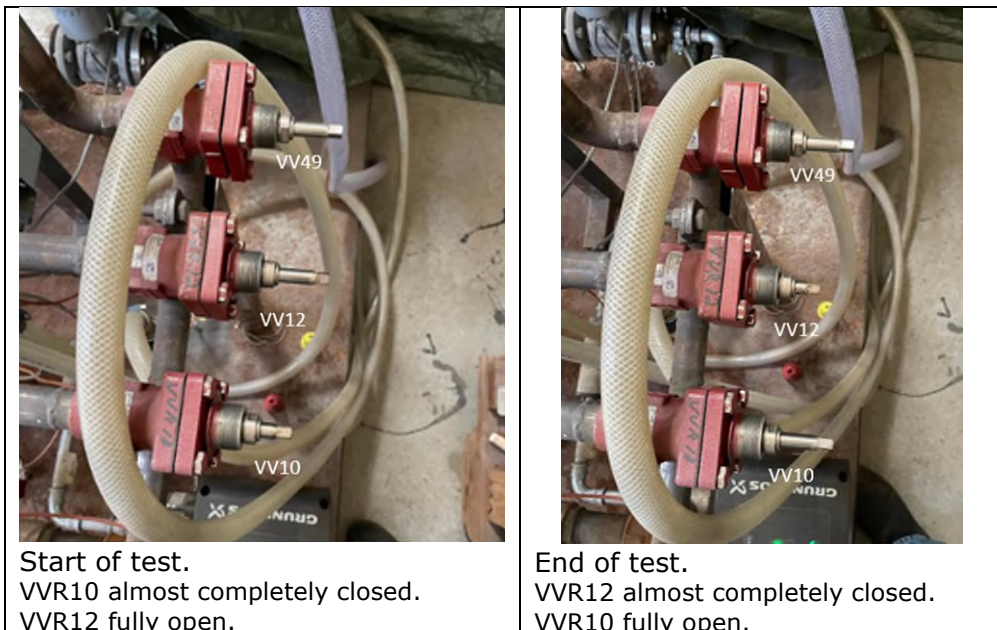


Figure 35: Valve positions at the start and at the end of the test.

The test started with almost all the refrigerant bypassing the SGHX. This was accomplished by almost closing valve VV10 in the line from the SGHX and by fully opening the valve VV12 in the dry gas line from the simple liquid separator as seen on Figure 32, left. Then, during the test, the valves were adjusted to have more and more of the refrigerant flow forced through the SGHX. At the end of the test, the valve position was according to Figure 35, right.

From Figure 36, a start of oscillations of the temperature out of evaporator ($T_{r_e_out}$) is observed, but still with a relatively constant evaporation temperature (T_{e_sat}).

Since the suction gas heat exchanger is configured to run in co-current mode, the maximum temperature that can be obtained out of the suction gas heat exchanger on the gas side (Tr_{ss_out}) is limited. It is also seen that the temperature $Tr_{sl_mix_out}$ is lower than Tr_{exp_in} , which is because a part of the condensate is bypassing the suction gas heat exchanger.

The measurements also show that in this test it is limited how much the temperature before the expansion valve (Tr_{exp_in}) changes, showing that the load from the suction gas heat exchanger is relatively small.

The temperature before the inlet to the suction accumulator ($T_{r_succ_acc_in}$), i.e., where the sensor for the expansion valve control is mounted, appears also to be relatively constant. This is partly because only a relatively small gas flow runs through the bypass, due to the valve settings during the test.

At the end of the test, where relatively much gas flows through the SGHX, it is observed that there is an incipient increase of temperature changes. This indicates that liquid is now starting to reach the suction gas heat exchanger and starts to evaporate. The expansion valve also begins to be closed more (EX_OD), and it is also clear that the mass flow to the evaporator (Ref.Total) starts to be reduced.

It has also been possible to register via the sight glass (SG) that a few drops are added to the gas that comes to the inlet of the SGHX and on the outlet towards the compressor. Therefore, the separation in the next test is switched to be done by using the large separator.

In Table 19, thermographic pictures are shown corresponding to the time marked with the blue dashed lines in Figure 36. From the first picture taken at 13:11, the outlet of the evaporator is superheated, i.e., no liquid is present. Most of the gas is flowing through valve VV12, and a small amount is going through valve VV10. The gas going through valve VV10 gets further superheated in the SGHX.

In the next picture taken at 13:19, the evaporator is slightly overflowed. Cold gas with liquid is entering the separator and some of it is going down to the SGHX and some to valve VV12. From the colors, it seems that both liquid and gas are going down to the SGHX and not just liquid. From Figure 36 it can be seen from $T_{r_e_out}$ that the pictures, except from the first, are taken when the evaporator is without superheat.

Shortly after at 13:22, the evaporator seems to be with superheat again. The evaporator seems to be swinging between flooded and superheated.

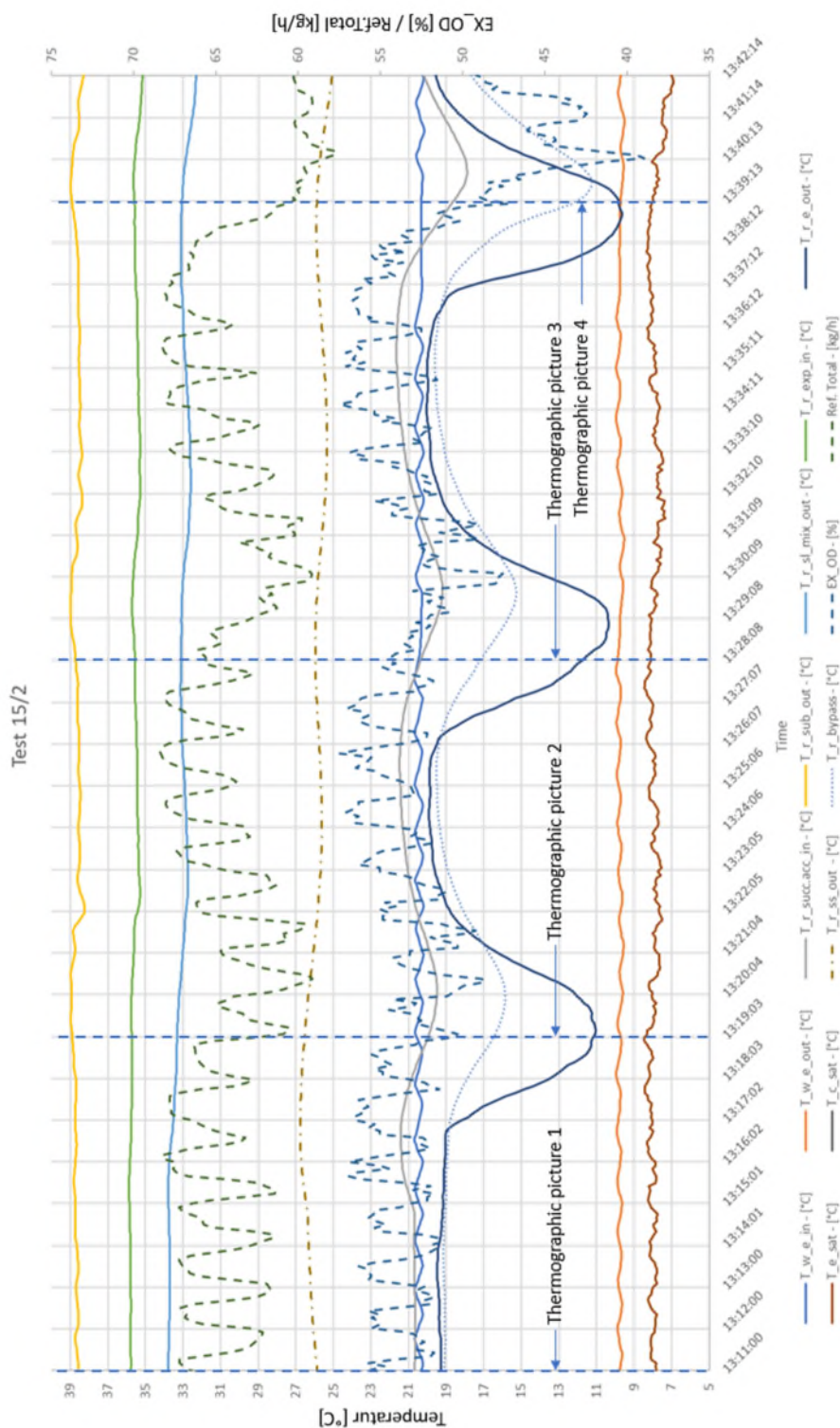
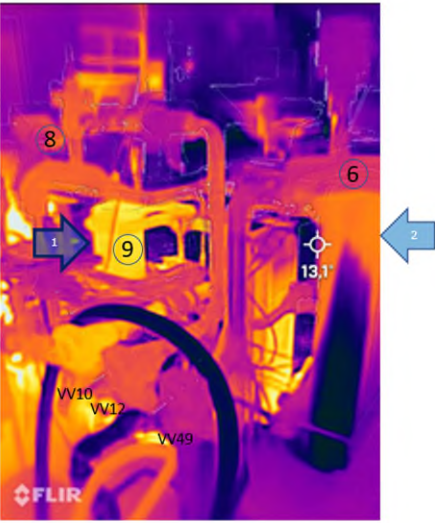
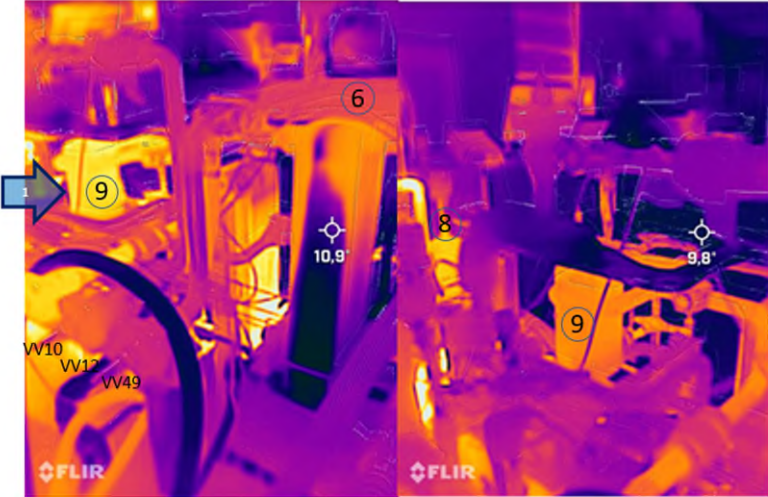

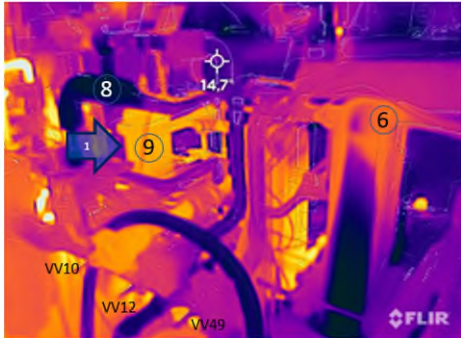


Figure 36: Measurement results from Test 1 on 15/2-2022. Explanations in Table 17.

Table 19: Thermographic measurements from Test 1.

Timestamp [h, min]		Comment
13:11 Picture 1		<p>A limited stream of ammonia gas flows through the SGHX. (Arrow 1). The evaporator outlet is superheated. (Arrow 2). The refrigerant is not perfectly distributed over the plate pack.</p>
13:19 Picture 2		<p>Flow through SGHX (Arrow 1) is increased. Liquid exiting the evaporator and entering the separator. The gas temperature out of the separator is lower than before.</p>
13:28 Picture 3		<p>Flow through the SGHX (Arrow 1) has increased even more. Evaporator is more flooded.</p>

<p>13:39 Picture 4</p>		<p>A relatively large part of ammonia from the evaporator is passed through the SGHX (Arrow 1). Evaporator is more overflowed. More liquid is escaping the separator along with gas.</p>
----------------------------	---	--

In the last picture taken at 13:39, the evaporator is more overflowed and there seems to be coming liquid together with the gas out of the separator. This indicates that the simple separator is not efficient enough to handle the amount of liquid exiting the evaporator at that stage.

There is an oscillation in the superheat with approximately 10 minutes oscillation time (see Figure 36) and a fluctuation from being superheated to overflowed. In between the drop in temperature out of the evaporator ($T_{r_e_out}$), the outlet from the evaporator is superheated with similar temperature out of evaporator ($T_{r_e_out}$) and in the dry gas passage from the separator (T_{r_bypass}). This indicates that there is no liquid in the gas exiting the evaporator. When the $T_{r_e_out}$ drops, indicating liquid in the gas from the evaporator the T_{r_bypass} also drops indicating that the SGHX gets liquid and increases the capacity. For the last flooding of the evaporator in the graph the T_{r_bypass} drops close to the saturated temperature out of the evaporator indicating that the liquid is bypassing the SGHX.

7.2.2. Results from Test 2 (15/2-2022)

This test is the same as Test 1 but where the highly efficient liquid separator is used instead of the simple one. Apart from testing the highly efficient liquid separator, the superheat settings of the expansion valve are also investigated.

The valve located in the separator drop leg is fully open. Some of the gas and liquid go through this towards the SGHX. The main part of the gas flows directly from the separator, 7, to the suction accumulator, 10, through the "Dry suction separator, 7" pipe in Figure 33. As the test progresses, the valve VV10 in Figure 38 after the SGHX is closed more and more as indicated in Figure 37 as valve position by green dashed lines and in Figure 38 as actual valve spindel position.

The static superheat is controlled by the controller to the expansion valve and is reduced in steps according to the following table. When this happens it is also drawn on the top of the graph in Figure 37.

Table 20: Superheat setpoint adjustments.

Static superheat:	12 K	12 K -> 10 K	10 K -> 8 K
Time	13:45	14:13	14:37

The measurement results for the test are shown in Figure 37. The commented results from the thermographic pictures can be seen in Table 21. The time when the thermographic pictures are taken is shown at the bottom of the graph over the measurements in Figure 37 as T1, T2 etc. and refers to the number of the picture in Table 21.

Test 2 started with both of the valves VV10 from the SGHX and VV49 from the highly efficient separator fully open. During the test, the valve VV10 was gradually closed as marked in the graph in Figure 37 and shown in Figure 38.

At time stamp 14:13, the static superheat is reduced from 12 K to 10 K. At the same time, the expansion valve begins to open for more refrigerant to enter the evaporator. The exit of the evaporator gets flooded. Shortly after, the expansion valve closes sharply again as the T_R_succ.acc_in drops rapidly and thereby the superheat drops which closes the valve again. This is due to the fact that the liquid flowing out of the separator is bypassing the SGHX without being evaporated and thereby reaches the sensor for the expansion valve with a rapid drop in superheat as a consequence.

The increased amount of ammonia that was added to the evaporator in the beginning flooded the evaporator and gave rise to a larger proportion of liquid droplets flowing to the suction gas heat exchanger. This is clearly seen by the fact that the temperature T_r_sl_mix_out suddenly drops.

A contributing factor to start oscillations in the system is that the expansion valve 5 in Figure 33 is in the process of closing because of falling superheat caused by the liquid droplets flowing through the SGHX. Shortly after when liquid from the evaporator has

accumulated in the SGHX, it gets very effective because of the liquid. This contributes to an additional subcooling of the refrigerant, which now increases the cooling performance of the refrigerant through the evaporator. The reduction in mass flow caused by closing the expansion valve will not reduce the capacity of the refrigerant flow in the same manner because of increasing subcooling. This changes the amount of liquid in the gas at the exit of the evaporator to a level much lower than otherwise. This will reduce the superheat further, and the expansion valve tries to compensate by closing more and more rapidly. At some time, the refrigerant flow to the evaporator has decreased so much that the gas gets superheated at the outlet of the evaporator again and thereby the effect of the SGHX drops and the subcooling reduces greatly. Then, the superheat for the expansion valve increases rapidly and the valve tries to compensate by opening more but the SGHX is not so effective until liquid again exits the evaporator and the cycle starts again. To compensate for this, the controller has to be more sophisticated. Another way of decoupling the influence of the SGHX is to control the expansion valve by the quality out of the evaporator.

At 14:37, the mass flow through the suction gas heat exchanger is increased, and the static superheat is reduced from 10 K to 8 K. As can be clearly seen from Figure 37, these changes amplify the oscillations.

At 15:02, the flow through the suction gas heat exchanger is completely closed. This is done by closing the valve VV10. The static superheat is still 8 K, and the system continues to oscillate, perhaps with a slight tendency to have smaller variations. This indicates that the SGHX is not the only parameter that has influence on the stability of the expansion valve.

It is clear that with both the large and the small separator there are oscillations in the system when the superheat in the regulator is reduced to around 8 K, and that the greater the flow through the suction gas heat exchanger is, the greater the tendency for oscillations in the system will be.

The reason why the suction gas heat exchanger was connected to co-current operation was to limit how much load that could be extracted from it, and the premise was also that there should be enough superheating for the regulator to work with.

To figure out if the oscillations are due to the expansion valve, the next test will be run with the expansion valve in manual mode. If it is not possible to exclude the oscillations in manual mode, it is not possible for the expansion valve to do so either.

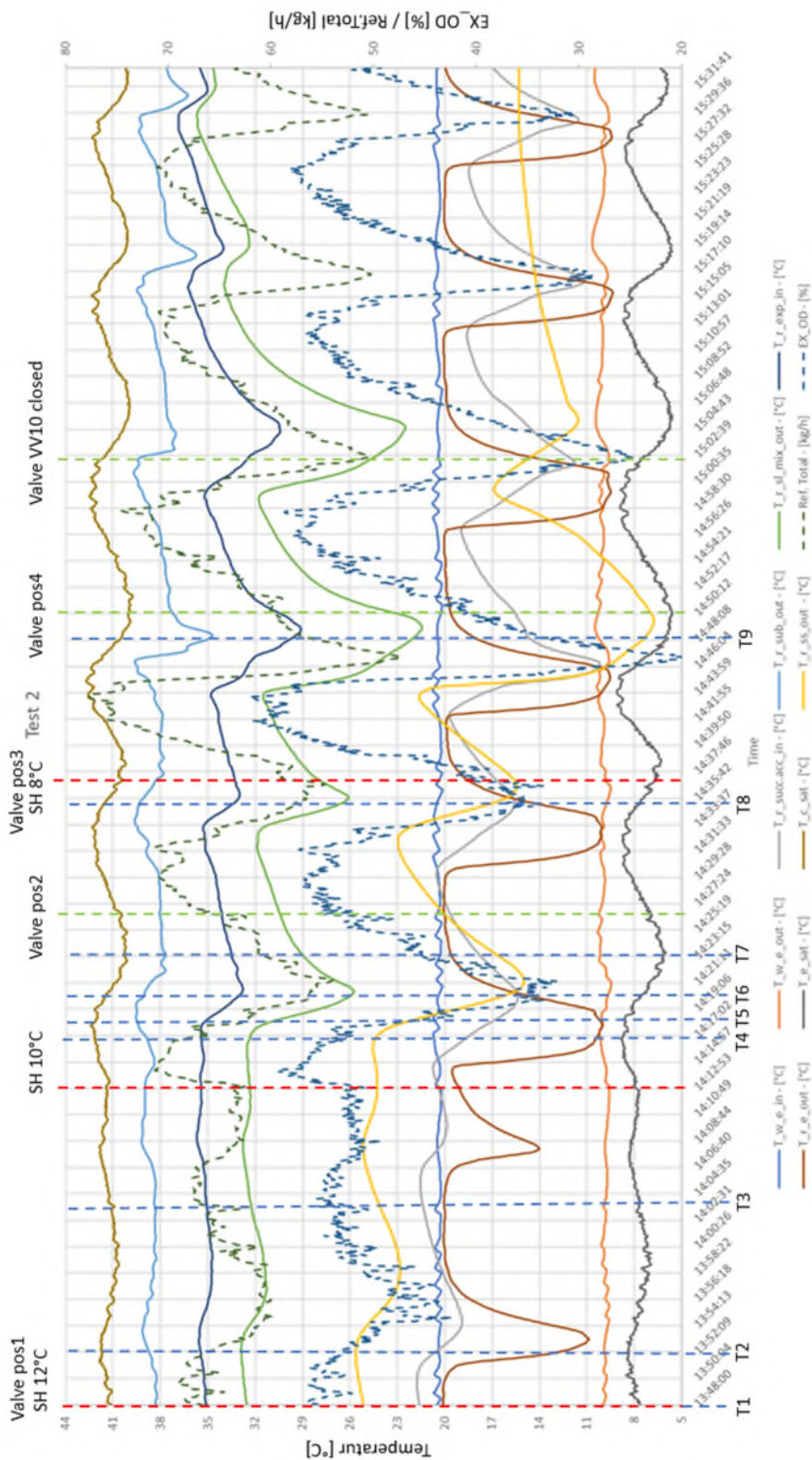


Figure 37: Measurement results from Test 2 on 15/2-2022. Explanations in Table 17.

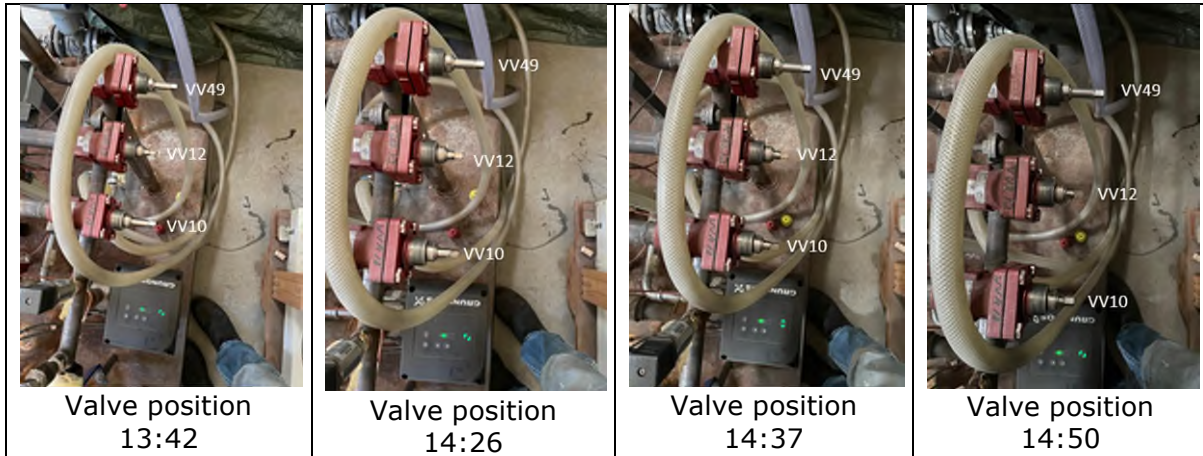


Figure 38: Valve positions in Test 2.

It is also observed that the average evaporation temperature decreases when the system starts to oscillate, and this is primarily due to insufficient supply of refrigerant to the evaporator in periods. This leads to a large superheating and thereby to a larger oscillation which results in a further reduced evaporation temperature.

The experience from the tests, until now, is that when the gas content through the SGHX becomes too large, the system ends up with oscillations. This naturally also has to do with the size of the suction gas heat exchanger itself and the temperature level at the inlet on the warm side, and whether a bypass has been made. However, if the heat exchanger becomes smaller, a larger pressure drop is generated, and this reduces the efficiency of the entire system.

It is also important to keep in mind that the temperature approach between the gas outlet temperature of the evaporator and the water entering the evaporator of the two different separators for the two tests is not completely comparable, since the pressure drops across the separators, and the pipe sections are different.

Of course, the values of the PID settings in the controller for the expansion valve also influence the results obtained. However, these have been kept constant during all the tests. These could probably have been fine-tuned during the tests and could thus have reduced the oscillations and gained more stable conditions in some of the cases.

In Table 21, the thermographic pictures from the test are presented. The time when the picture was taken is marked into the graph in Figure 37 with T1, T2, and so on, where the number refers to the numbers in Table 21. The following pictures show the angles for the thermographic pictures in the table.

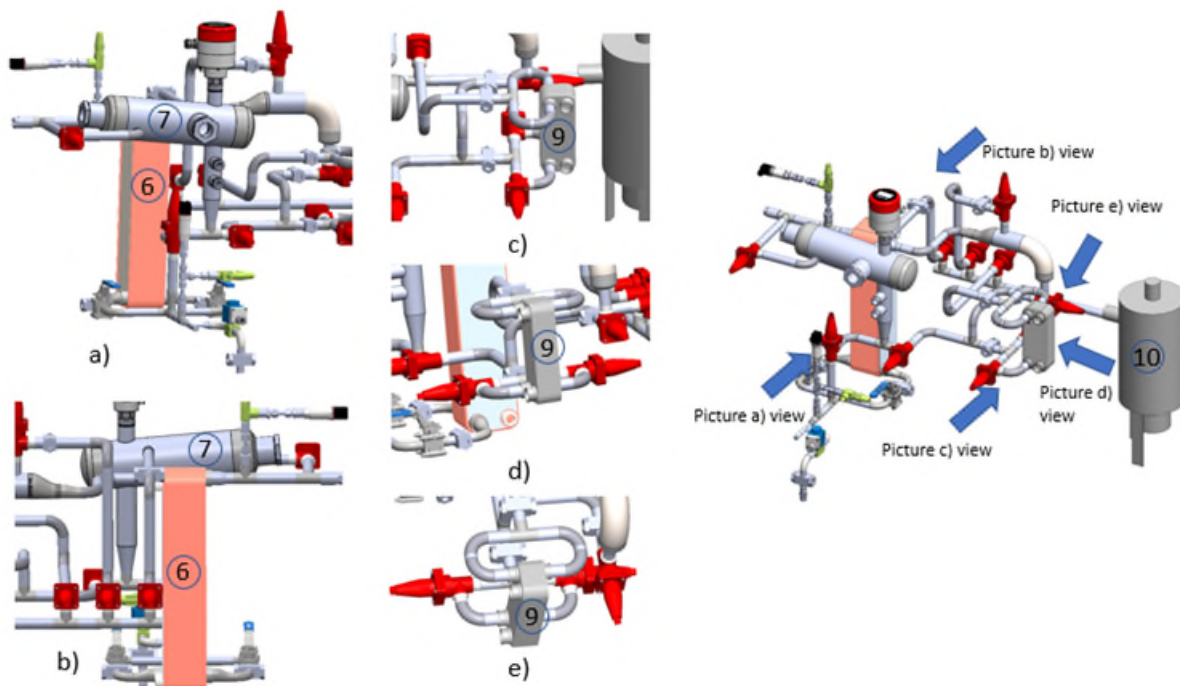

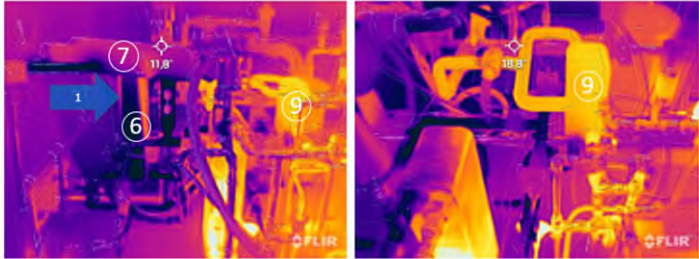
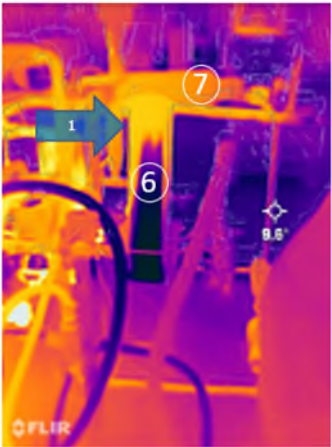
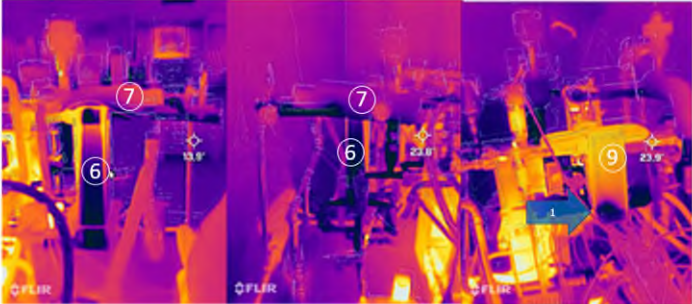

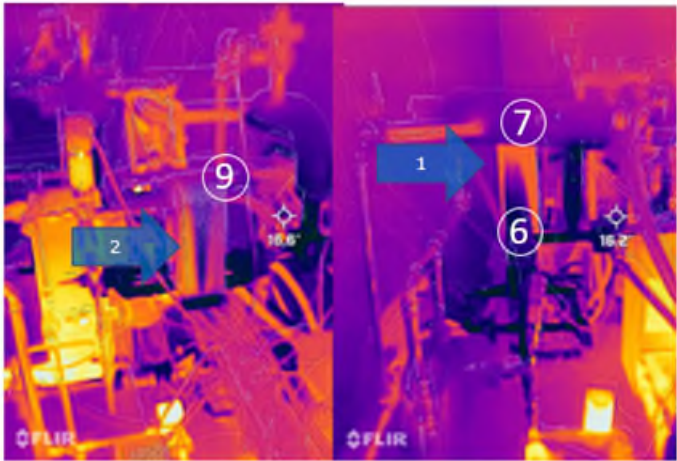

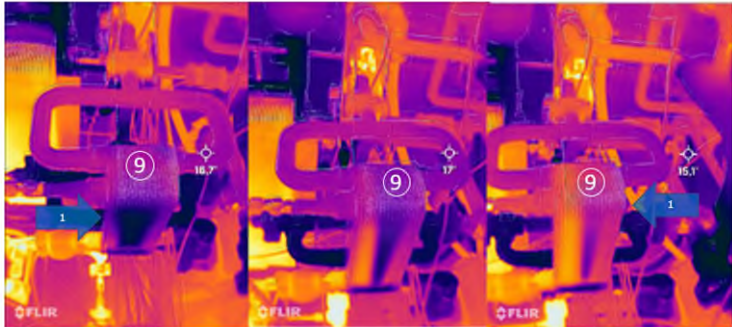


Figure 39: The view of the thermographic pictures referenced in Table 21. a) shown from the highly efficient separator side, b) shown from the other side compared to picture a), c) SGHX side view, d) SGHX back view, e) SGHX top view.

Table 21: Thermographic pictures from Test 2.

Timestamp [h,min]		Comment
13:48 T1		The gas out of the evaporator is superheated (Arrow 1). The valve after the SGHX is fully open. The same applies to the valve between the separator and the suction accumulator. Refers to Figure 38a.
13:52 T2		Now liquid also flows out of the evaporator (Arrow 1). Refers to Figure 38a and c.

<p>14:03 T3</p>		<p>Here, the DX valve has closed a bit and reduced the mass flow. Superheated (Arrow 1). Refers to Figure 38b.</p>
<p>14:16 T4</p>		<p>Superheat has been reduced from 12 to 10 K, to which the valve has responded. It is also clear that liquid has started to run up through the SGHX. (Arrow 1). Refers to Figure 38b, a and d.</p>
<p>14:18 T5</p>		<p>Liquid has climbed a little higher up in the SGHX. (Arrow 1). Refers to Figure 38d and a.</p>

<p>14:20 T6</p>		<p>The picture shows that the evaporator has started to be superheated at the outlet (Arrow 1), and the SGHX is in the process of boiling the last liquid off. (Arrow 2). Refers to Figure 38d and a.</p>
<p>14:23 T7</p>		<p>It can be clearly seen that the evaporator is fully overheated (Arrow 1). Refers to Figure 38b.</p>
<p>14:35 T8</p>		<p>Here is seen the same patterns as on the SGHX at the time stamp 14:20 (Arrow 1). These three photos were taken within a minute. The left is the first. Refers to Figure 38e.</p>

<p>14:48 T9</p>		<p>Static superheat has been reduced from 10 to 8 K. At 14:44, liquid droplets were observed in the sight glass (SG) mounted at the outlet of the SGHX (Arrow 1). No droplets at the SG at the bottom of the suction accumulator. It appears that there may be liquid entering the suction gas accumulator (Arrow 2).</p>
---------------------	--	---

7.2.3. Results from Test 3 (22/2-2022)

The purpose of this test is to see how the system performs when the control of the expansion valve is switched to manual mode. At the same time, the gas flow from the evaporator to the SGHX is limited by slightly opening the valve in the drain line. In addition, the subcooler is working to limit the available heat load on the SGHX. In this test, the highly efficient liquid separator is used as for Test 2.

The test conditions have been changed compared to Test 2 in the following way:

- The test is performed with the highly efficient separator.
- The control valve on the dry gas line from the separator and leading to the suction accumulator is fully open.
- The valve located between the drop leg and the SGHX is slightly open, resulting in that only liquid runs through it towards the SGHX.
- The SGHX is configured in counter-current flow fashion. All the condensate flows through the SGHX.
- The evaporator is configured for control of the expansion valve in manual mode, i.e., fixed opening degree adjusted manually.
- In this test, the cooling water of the subcooler flows through the subcooler and thereby the subcooler is in operation.
- Temperature sensor Tr_e_out has been moved to the pipe on the outlet of the evaporator which runs from the evaporator to the highly efficient separator.

The measurement results are shown in Figure 40. The commented results from the thermographic measurements can be seen in Table 22.

At time stamp 11:11, manual control of the expansion valve has been switched on. The degree of opening is indicated by EX_OD.

As a result of the expansion valve being opened more, the superheat in the evaporator is reduced. But since the gas does not flow through the SGHX, there is no change in the temperature in front of the expansion valve, T_r_exp_in. It can also be seen that the temperature T_r_succ.acc_in follows the temperature T_r_e_out. The sensor measuring T_r_succ.acc_in is mounted just in front of the suction accumulator, which leads directly to the compressor.

T_r_ss_out is the temperature just after the SGHX. This temperature is only affected when liquid begins to flow into the SGHX, which starts to happen after time stamp 11:45.

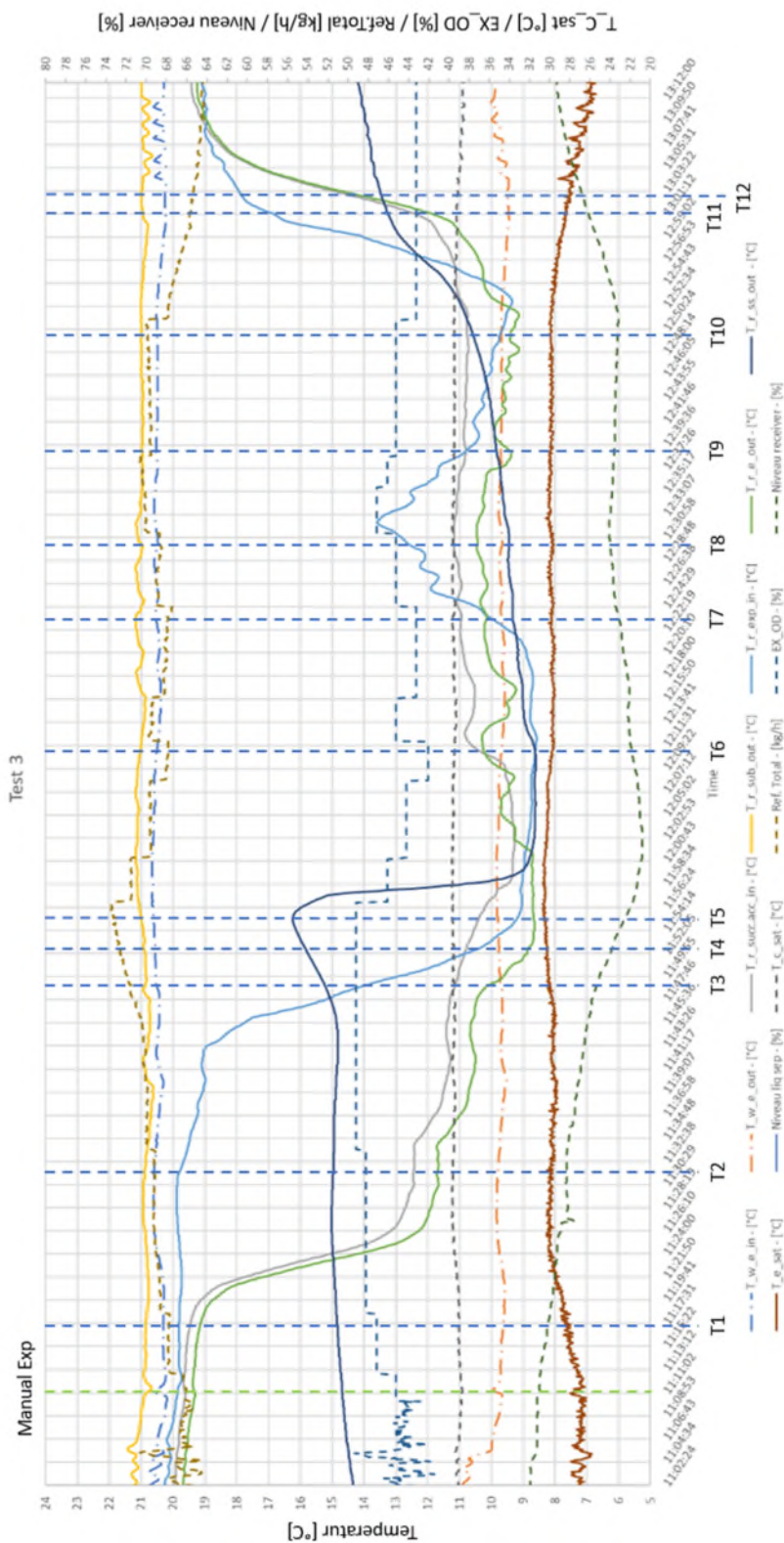


Figure 40: Measurement results from Test 3 on 22/2-2022. Explanations in Table 17.

In the time interval from 11:17 to 11:56, the opening of the expansion valve is nearly unchanged. To begin with, the temperature measured at the outlet of the evaporator, Tr_{e_out} , drops quite rapidly, after which it slowly flattens out. But after time stamp 11:43, it can be registered that the temperature Tr_{exp_in} drops quickly, which is a result of liquid running into the SGHX. At 11:52, the temperature measurement at the outlet of the evaporator also shows that there is no superheating, which also means that liquid has flowed into the SGHX for some time. This is also the time where the highest evaporator temperature is observed.

The next change is stepping down in the opening of the expansion valve in order to limit the amount of liquid coming out of the evaporator.

The goal is to have a gas quality close to 1 at the outlet of the evaporator. The optimum heat transfer coefficient on the refrigerant side is usually achieved at an outlet quality between 0.85 and 0.7, but that is not the primary goal. It can clearly be seen that after the time stamp 11:26, the evaporation temperature does not increase very much, but it peaks at the time 11:56.

The next step is to try to shed light on whether the valve can be regulated manually to achieve that only a small quantity of liquid comes out of the evaporator – enough to gain a sufficient high evaporation temperature, but not the maximum achievable.

Around 11:45, the temperature Tr_{ss_out} starts to increase. It is measured at the outlet 30 cm from the suction gas heat exchanger. It increases because superheated gas (evaporated liquid) now slowly starts to flow through the SGHX. At 11:56, the temperature drops suddenly. This is because the boiling liquid has moved well up in the suction gas heat exchanger and since the expansion valve, at the same time, is closed a bit.

Around 12:11, the temperature $T_{r_succ.acc_in}$ increases, which indicates that the boiling front has started to pull backwards in the SGHX again.

Hereafter, the expansion valve is manually adjusted in order to achieve a relatively constant temperature measured just before the suction accumulator ($T_{r_succ.acc_in}$).

The experiment is completed by gradually closing the expansion valve until the starting point of the test is obtained again.

It seems that it is possible to control the expansion valve manually, so the evaporator is slightly flooded, and separated liquid is flowing to the SGHX. The obtained superheat before the suction accumulator is low or around 3 K. The temperature of the gas out of the SGHX steadily rises from 12:11 to 12:50 indicating that the liquid is being boiled off in the SGHX. At 12:50, the valve is closed 1.5 % and this increases the temperature out of the evaporator indicating a superheated evaporator. This indicates that it is hard to use the superheat signal before the suction accumulator to control the valve because of the large fluctuations in the superheat signal when the SGHX kicks in and out.

When the evaporator runs with superheat, the T_{e_sat} drops again reducing the efficiency of the system. The measurements show how important it is to run the evaporator slightly flooded, but the degree of flooding is less important. The T_{e_sat} is around 8.3 °C when the evaporator is more flooded and drops to 8.0 °C when it is on the limit to be dry. The conclusion is that the evaporator should run just slightly flooded. This makes the control of the expansion valve by using the superheat after the SGHX hard to accomplish because of the large fluctuation in the capacity of the SGHX around the dry/flooded point. To solve this issue, the control of the expansion valve should be decoupled from the SGHX. This can be done by measuring the dryness of the gas leaving the evaporator and use it as a control for the expansion valve. Then the only function of the SGHX is to boil off the small amount of liquid exiting the evaporator. The system gains in running with a slightly flooded evaporator are measured to be a 1 K higher saturated suction temperature. This is a rather small improvement and is due to the oversized evaporator in the test setup. For a normal sized evaporator, the benefit would be higher.

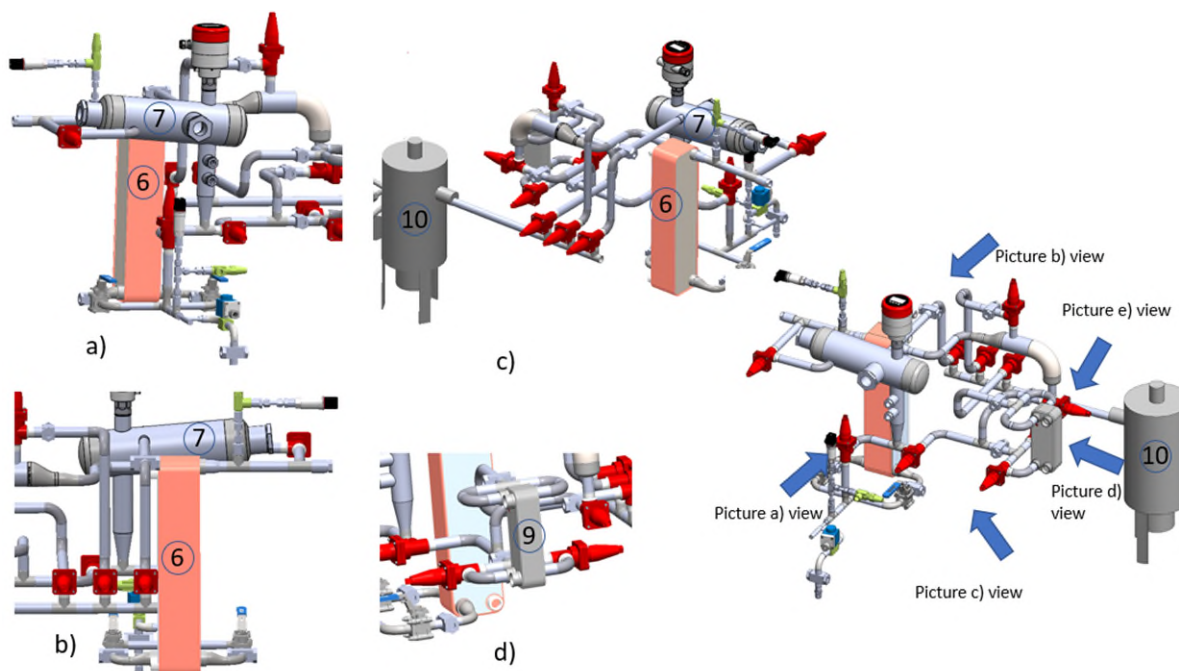
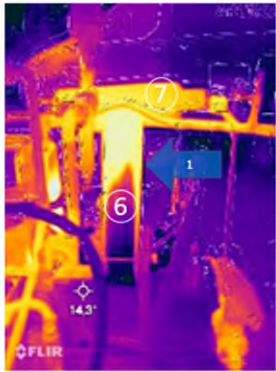

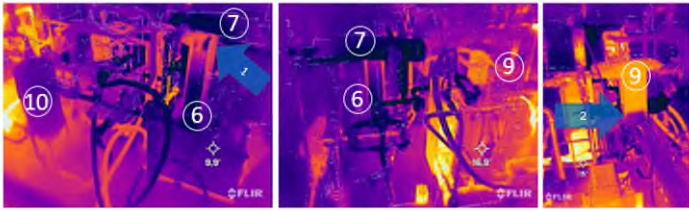

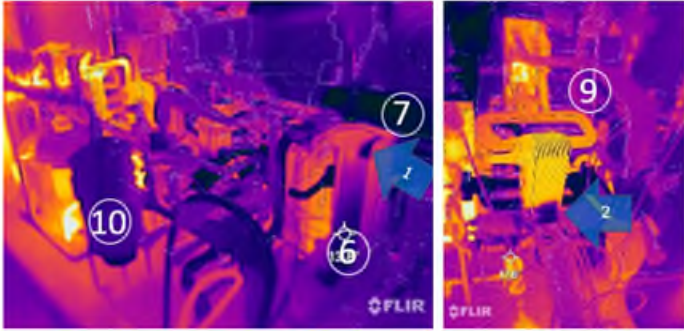
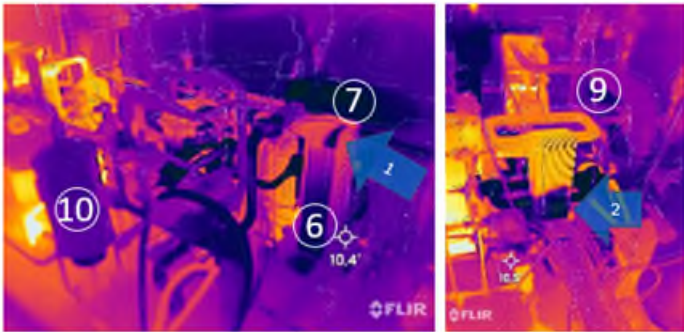
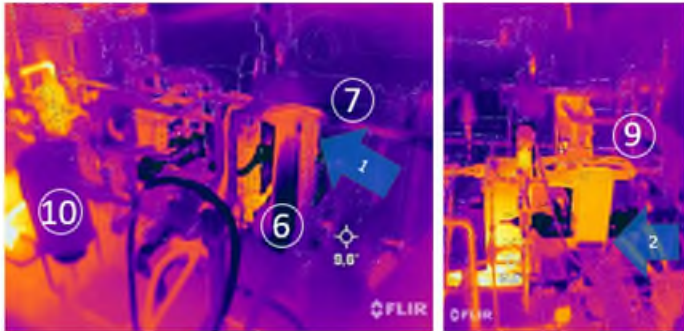
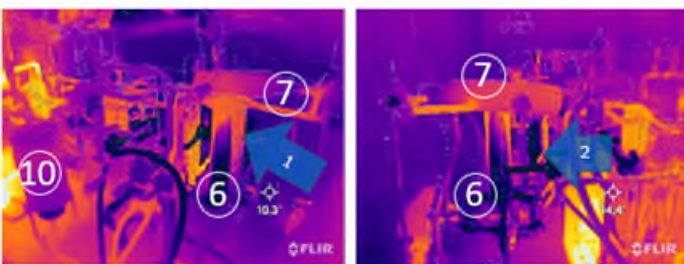


Figure 41: The view of the thermographic pictures referenced in Table 22. a) shown from the highly efficient separator side, b) shown from the other side compared to picture a), c) seen from above, d) SGHX back view.

Table 22: Thermographic pictures from Test 3.

Time-stamp [h,min]		Comment
11:17 T1		<p>Superheat is about 11 K. Here, there a large area of the evaporator is used (Arrow 1) to generate the 11 K of superheat. Refers to Figure 41b.</p>
11:31 T2		<p>Small amount of liquid exiting the evaporator (Arrow 1) and entering the separator. The bottom of the separator (Arrow 2) is cooled by liquid droplets. No liquid level is measured in the separator. Refers to Figure 41c and a.</p>
11:49 T3		<p>Increased liquid out of the evaporator (Arrow 1). Liquid is boiling in the suction gas heat exchanger (Arrow 2). Refers to Figure 41c, a and d.</p>
11:52 T4		<p>More liquid is coming out of the evaporator (Arrow 1), and more boiling liquid in the suction gas heat exchanger (Arrow 2). Refers to Figure 41c and d.</p>

<p>11:55 T5</p>		<p>Increasing amount of liquid is coming out of the evaporator (Arrow 1). The picture shows that some liquid is coming out of the suction gas heat exchanger. However, no liquid was observed in the suction gas accumulator, and the pipes exiting from the SGHX seem to be warm (Arrow 2). Refers to Figure 41c and d.</p>
<p>12:11 T6</p>		<p>Liquid exiting the evaporator (Arrow 1) and also the SGHX. This picture and the following pictures, T7 to T11 below, show how the liquid level in the suction gas heat exchanger (Arrow 2) moves up and down. Refers to Figure 41c and d.</p>
<p>12:23 T7</p>		<p>The liquid exiting the evaporator is boiled off the SGHX. The left outlet pipe from the SGHX is cold indicating liquid is bypassing the SGHX in this end. Refers to Figure 41c and d.</p>
<p>12:30 T8</p>		<p>Slightly overflowed evaporator and low liquid level in the SGHX. Seems to be no liquid short cut through the SGHX. Refers to Figure 41c and d.</p>

<p>12:39 T9</p>		<p>Slightly overflowed evaporator and rising liquid level in the SGHX. Seems to be no liquid short cut through the SGHX. Refers to Figure 41c and d.</p>
<p>12:50 T10</p>		<p>Slightly overflowed evaporator and rising liquid level in the SGHX. Seems to be no liquid short cut through the SGHX. Refers to Figure 41c and d.</p>
<p>13:01 T11</p>		<p>Slightly overflowed evaporator (Arrow 1) and low liquid level in the SGHX. Seems to be no liquid short cut through the SGHX. Refers to Figure 41c and d.</p>
<p>13:03 T12</p>		<p>There is no liquid in the drop leg from the separator. The reason why the drop leg (Arrow 1) is very cold is because gas from the evaporator is now bypassing the SGHX on the way to the suction accumulator. Refers to Figure 41c and a.</p>

As can be seen from the thermographic pictures, the SGHX is working fine in T8 to T11. Here, the evaporator is slightly flooded with optimum saturated suction temperatures. The conclusion is that this can be done but needs another type of control for the expansion valve.

7.2.4. Results from Test 4 (4/3-2022)

In this test, the mass flow of water is increased in order to achieve a smaller temperature drop across the evaporator. One of the reasons for this is to get a better impression of the influence of the size of superheat on the evaporation temperature. It now also becomes clear that a result of an increasing evaporation temperature is an increased cooling load.

The first test, Test 1, also used the small separator in series with the SGHX. The test was done without the use of a subcooler and with a constant static superheat. More and more gas was forced through the SGHX during this test. The superheat began to fluctuate after some time, as the gas flow through it had reached a certain magnitude, and the effect was greatly amplified when liquid began to enter together with the gas as the capacity of the SGHX was increased drastically. A problem with this configuration was probably that the droplets at some point reached too high a speed so they did not have time to evaporate and then exit the SGHX in liquid form which was confusing the temperature sensor for the superheat control. Another issue is that too high a velocity of gas containing liquid droplets will give a poor distribution across the plate pack and a maldistribution of the liquid occurs. In this case, most of the liquid enters the first and last channel and bypasses the SGHX without being evaporated.

The test conditions have been changed compared to Test 3 in the following way:

- The test is done with the small separator and the SGHX. A small opening is used on the valve which is located between the small separator and the suction gas accumulator. Thus, it is not the whole mass flow of gas that is running through the SGHX.
- The SGHX is configured for counter-current flow.
- The expansion control is configured in manual mode. The degree of opening of the expansion valve is increased in small steps resulting, at last, in a liquid flow out of the evaporator.
- In this test, the subcooler is operational.
- The temperature sensor Tr_e_out has been moved to the pipe on the outlet of the evaporator which runs from the evaporator to the small separator.

The measurement results are shown in Figure 42. The commented results from the thermographic measurements can be seen in Table 23.

In Test 4, the subcooler is in operation, which is a normal configuration for a heat pump. The test is performed with the expansion valve in manual mode. The degree of opening the valve after the SGHX is also reduced to limit the gas flow from this part.

After increasing the opening degree of the expansion valve in several steps, the superheat begins to decrease at the time stamp 13:33. The reduction in superheat results in an increasing evaporation temperature until the outlet temperature of the

water becomes the limiting factor. The increase in evaporation temperature from superheated gas from the evaporator and until slightly flooded is from about 6.5 °C to 10.8 °C. This is an increase of 4.3 K which would represent an around 17 % more efficient system.

The fact that the temperature sensor mounted in connection with the bypass, T_{r_bypass} , does not follow the temperature, $T_{r_e_out}$, at the outlet of the evaporator could be due to a mixture of liquid and superheated gas coming out of the evaporator. The temperature measured in the bypass is dominated by the superheated gas, while the temperature sensor at the outlet of the evaporator also senses the influence of the liquid droplets. At time stamp 13:49, the two temperature sensors measure more or less the same temperature. No liquid has been seen in the SG mounted in the suction accumulator.

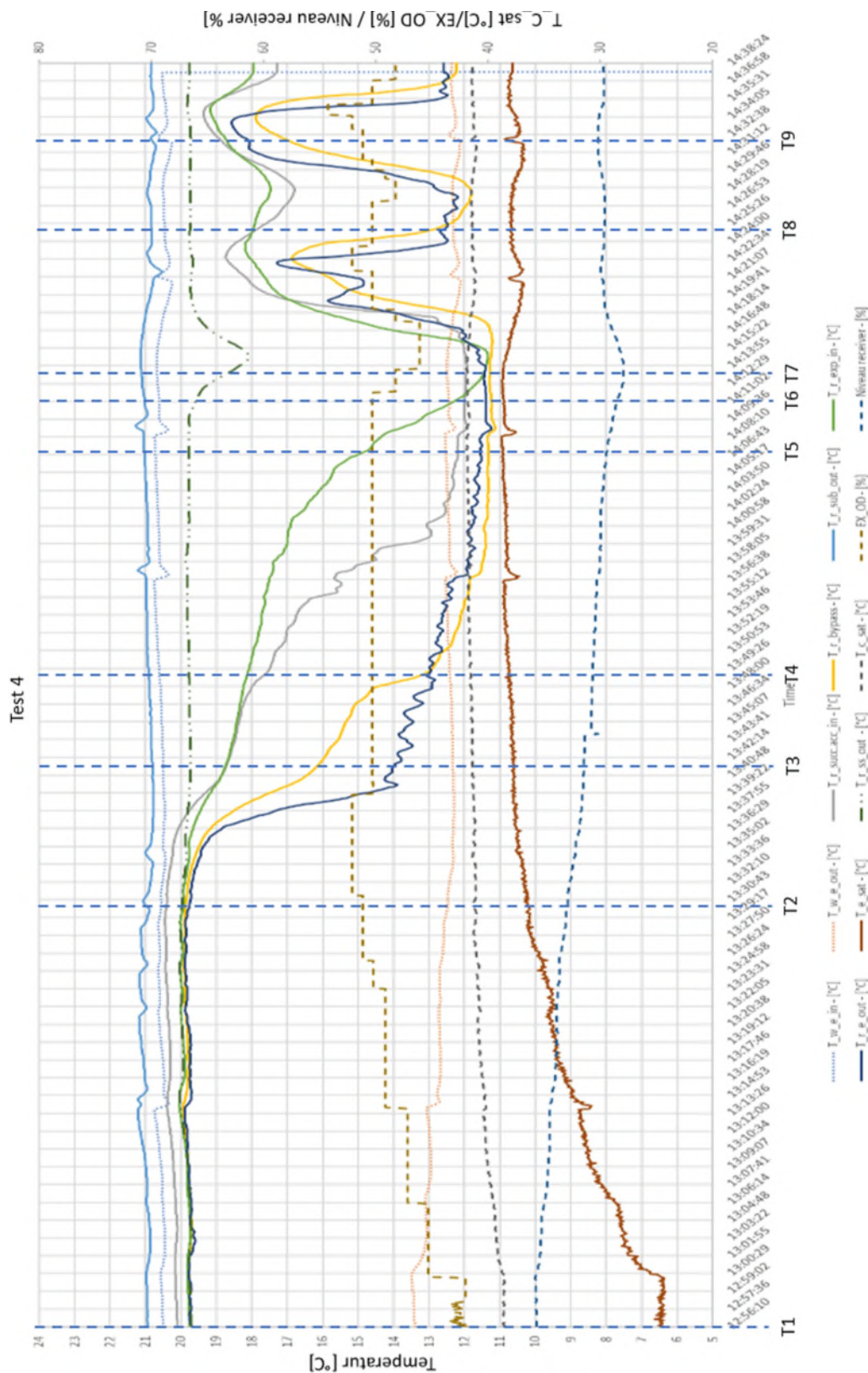


Figure 42: Measurement results from Test 4 on 4/3-2022. Explanations in Table 17.

The temperature ($T_{r_ss_out}$) out of the SGHX on the low-pressure side is relatively constant. Unlike Test 3, where gas only flowed through when there was liquid evaporating, there is, in this Test 4, always gas through the SGHX.

The temperature measured just before the suction gas accumulator, $Tr_suc_acc_in$, is a mixture of $T_{r_ss_out}$ from the SGHX and T_{r_bypass} that comes directly from the small separator. This mixed temperature drops more slowly than the $T_{r_ss_out}$.

From time stamp 13:58, there is more or less saturated gas out of the evaporator together with small liquid droplets, and at 14:03, liquid was visible in the SG mounted at the bottom of the suction accumulator. At 14:04, the SG was more or less completely covered with liquid.

After the liquid enters the suction accumulator, the expansion valve is closed around 5 % in two steps. This gives a superheated gas coming from the evaporator. Then the valve is opened. First the previous 5 % in two steps. As this opening degree does not reduce the superheat that continues to rise, the valve is closed additionally 2.5 %. Here, the superheat reversed, and the evaporator gets flooded. This shows how difficult it is to control the evaporator on the limit between dry and flooded.

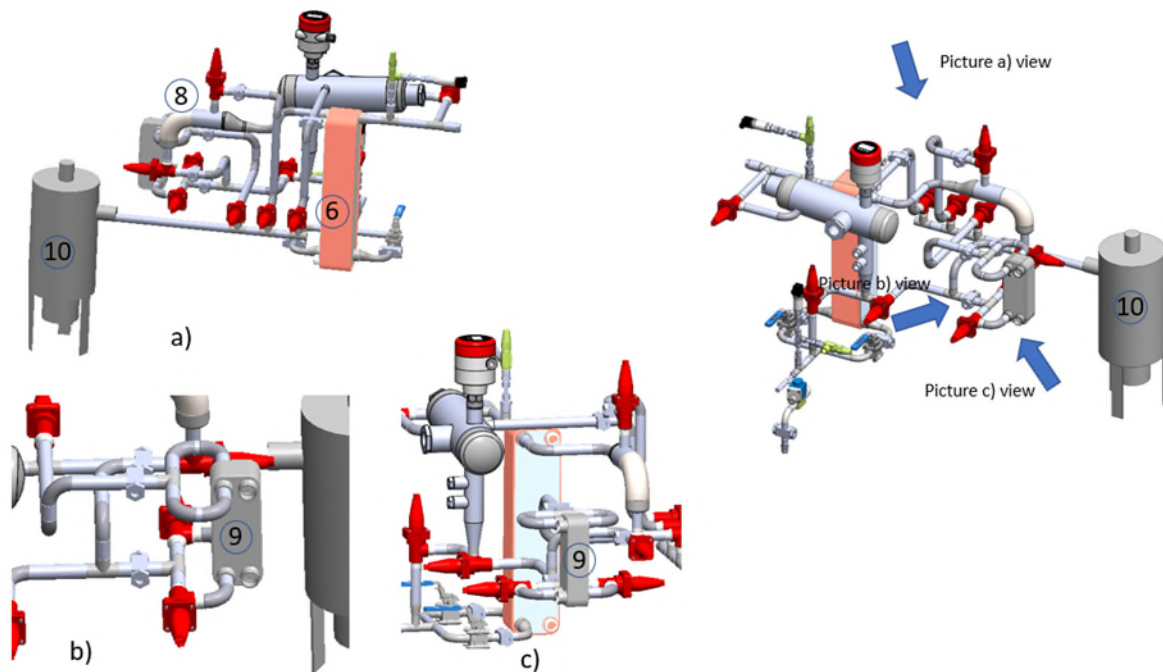
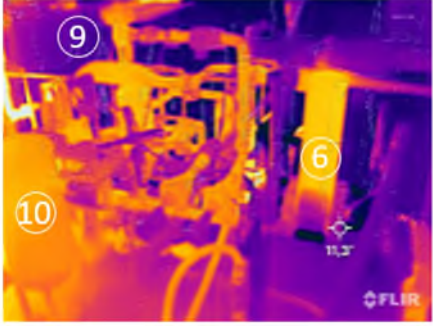
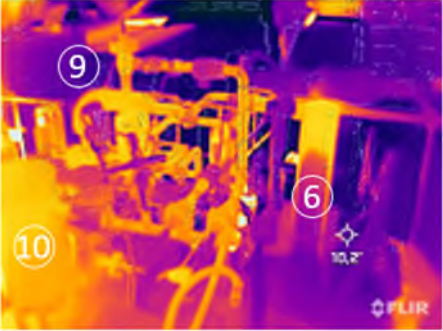
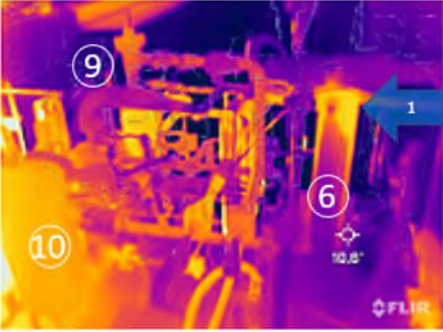
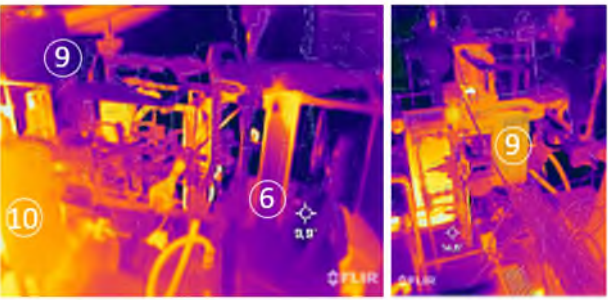
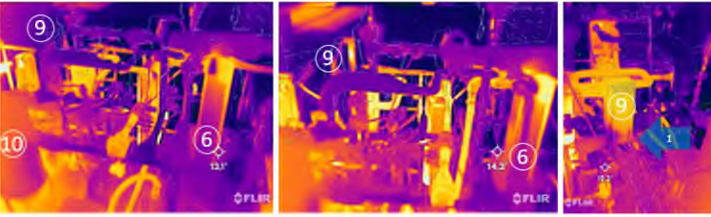

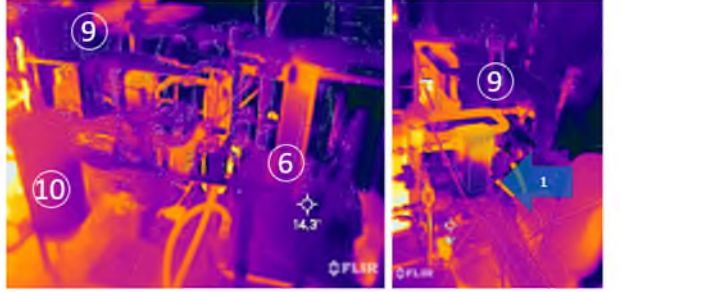
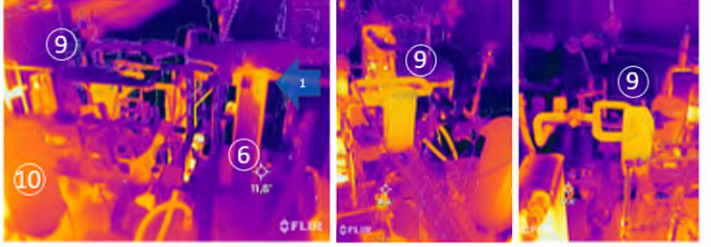



Figure 43: The view of the thermographic pictures referenced in Table 23. a) shown from the evaporator side, b) SGHX side view, c) SGHX back view.

Table 23: Thermographic pictures from Test 4.

Time stamp [h,min]		Comment
12:56 T1		<p>Superheat is 13 K. Picture taken while the expansion valve was in auto mode. Refers to Figure 43a.</p>
13:30 T2		<p>Expansion valve in manual mode. This is the latest state with gas temperature out of the evaporator close to the inlet water temperature. Refers to Figure 43a.</p>
13:41 T3		<p>Now the minimum temperature in the heat exchanger must move to the outlet seen from the water side. It is seen that the evaporator is slightly flooded (Arrow 1). Refers to Figure 43a.</p>
13:49 T4		<p>After this time stamp, only very modest temperature rise of the evaporation temperature occurs. Refers to Figure 43a and c.</p>

<p>14:07 T5</p>		<p>The temperature at the sensor located before the suction accumulator T_r_Succ_acc_in has now dropped significantly. There is boiling liquid inside the bottom of the SGHX (Arrow 1). Refers to Figure 43a, a and c.</p>
<p>14:11 T6</p>		<p>Here, the conditions are close to have achieved the largest subcooling of the condensate via the SGHX. The SG mounted at the bottom of the suction accumulator is empty despite a little dark shade is seen on the outside of the accumulator. Refers to Figure 43a, b and c.</p>
<p>14:13 T7</p>		<p>Here, the highest level of boiling liquid in the SGHX is observed (Arrow 1). Refers to Figure 43a and b.</p>
<p>14:25 T8</p>		<p>Here, the temperatures during the next dive in superheating can be observed (Arrow 1). Refers to Figure 43a, c and b.</p>
<p>14:32 T9</p>		<p>Here, an overheating of the small separator (Arrow 1) is shown. Refers to Figure 43a.</p>

The overall conclusion of the manual test with the small separator is that it can run in manual mode, but it is hard to control since small changes around dry and flooded conditions have a large influence on the superheat. It would be beneficial to decouple the SGHX from influencing the control signal to the expansions valve.

7.2.5. Results from Test 5

In this test, it was investigated if the control of the evaporator would be possible if the control of the expansion valve was decoupled from the SGHX. A new patented sensor under development from Danfoss to control the dryness in a pipe from evaporators was tested. The sensor is called "Heated sensor" (see Figure 44). It works by using a heating element in an aluminium housing and gives the sensor constant power and then measures the temperature in the aluminium housing.

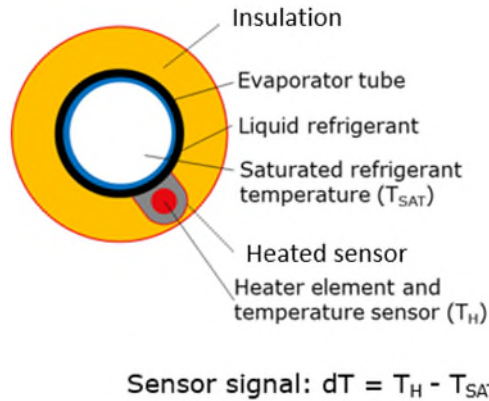


Figure 44: The heated sensor clamped on a pipe.

The measured temperature is related to the quality of the two-phase flow inside the pipe.

This test was performed on the test setup before modifications were made, i.e., the liquid separators were not installed, and the exit of the evaporator went directly to the SGHX.



Figure 45: Heated sensor test setup. 6) Evaporator, 9) SGHX, 10) Suction accumulator.

Figure 45 shows the test setup. The flow from the evaporator, 6, flows in direction of the white arrow to the SGHX, 9. The SGHX has two inlets and two outlets.

Figure 46 shows the PI diagram of the low-pressure side.

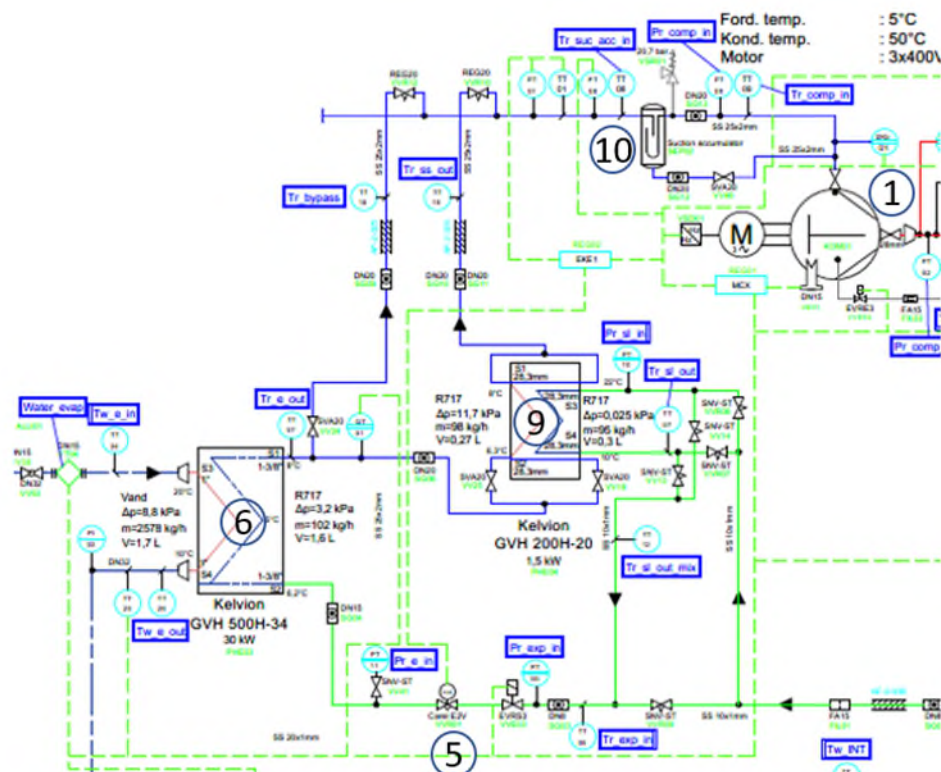


Figure 46: PI diagram of the test setup with placement of sensors for measurements (in blue boxes) 1 – Compressor, 5 – Expansion valve, 6 – Evaporator, 9 – Suction gas heat exchanger, 10 – Suction accumulator.

An adjustable voltage supply with a maximum voltage of 24.4 V was connected to the heated sensor and the sensor connected to the expansion valve controller. The fictive superheat, which is the temperature on the heating element in the sensor minus the saturated suction temperature after the evaporator, was set to 30 K. The voltage on the sensor was adjusted to 23.8 V. By changing the voltage to the sensor, the power on the heating element is adjusted. The test was run with the subcooler in operation.

Figure 47 shows the thermographic pictures taken of the evaporator and the SGHX during different compressor speed. The pictures show that for a low compressor speed of 25 Hz, liquid is exiting the SGHX. Here, the voltage should have been lowered to ensure dry gas out of the SGHX. For a compressor speed of 30 Hz, liquid exits the SGHX because of maldistribution in the SGHX where liquid flows up through the first and last channels. Here, the voltage would be fine if the maldistribution was not present. For a compressor speed of 35 Hz and above, the voltage is fine to keep the evaporator flooded and secure dry gas out of the SGHX. This shows that the sensor must be able to

compensate the power to the heating element according to the load. This type of control is being developed at Danfoss.

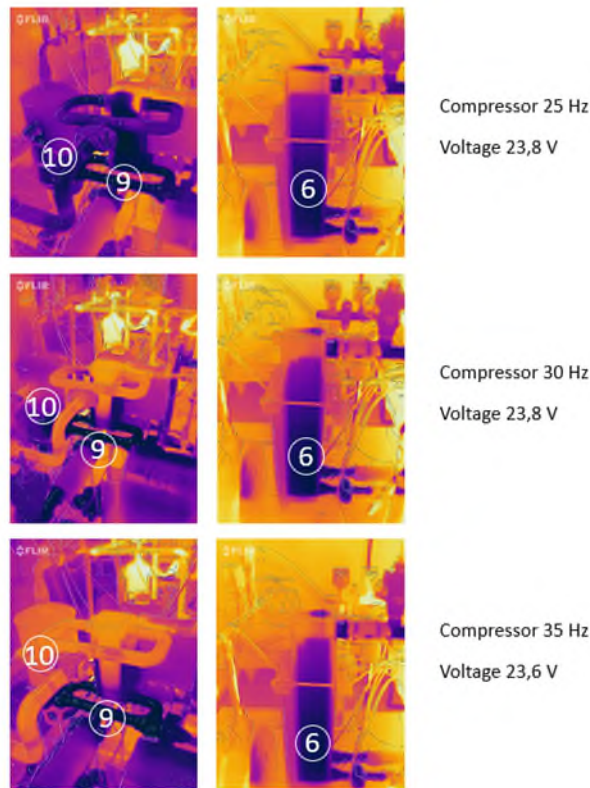


Figure 47: Thermographic pictures of the control with different voltage on the heated sensor and compressor speed.

When looking at the thermographic pictures in Figure 47 and at the measurements in Figure 48, the evaporator is flooded all the time, as the superheat out of the evaporator, $dT_{Evap_SH_corr}$, is close to 0 K. For 25 and 30 Hz on the compressor, the SGHX is bypassing liquid keeping the SGHX flooded. Here, the voltage should have been adjusted to keep the quality out of the evaporator. For a compressor speed of 35 and 40 Hz, the evaporator is flooded, and the gas into the suction accumulator is superheated. When looking at the refrigerant flow, it evens out after changes in compressor speed indicating that the expansion valve is controlling the flow. The overall conclusion is that with the heated sensor it is possible to control the evaporator if the power reference of the sensor is adjusted without oscillation in the superheat. Here, the influence of the SGHX has been minimized, and the coupling between the control of the expansion valve and the capacity of the SGHX is detached.

Refrigerant temperature suction side

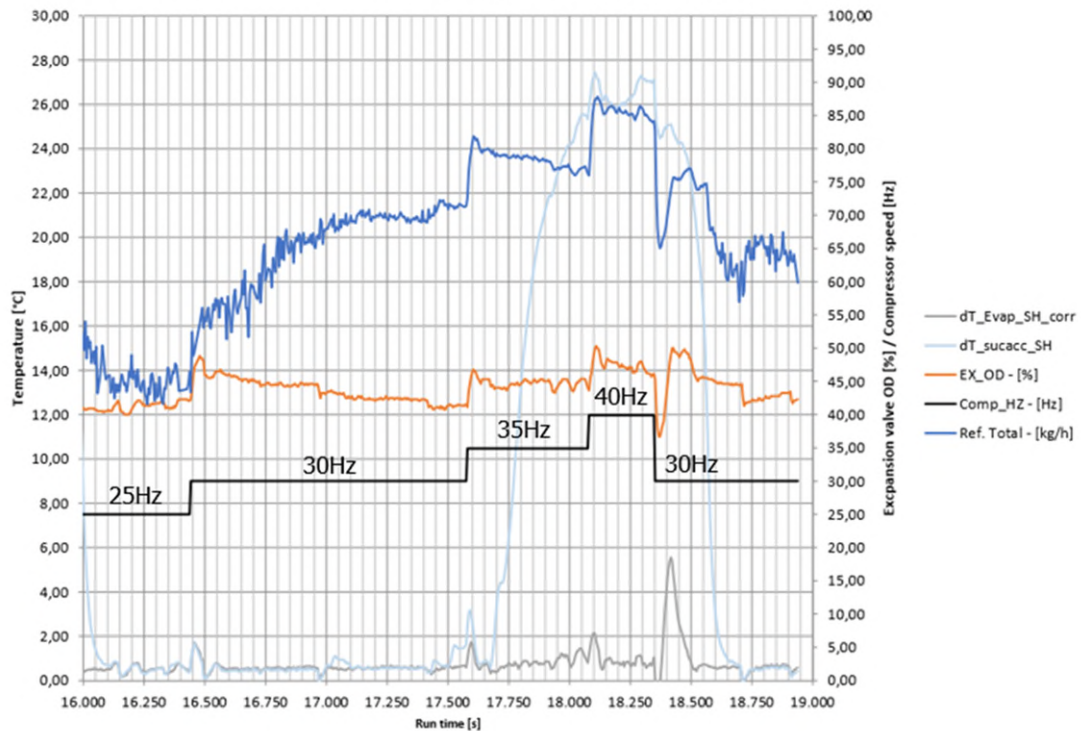


Figure 48: Measurements with heated sensor. dT_Evap_SH_Corr is the superheat out of the evaporator, dT_sucacc_SH is the superheat before the suction accumulator, EX_OD expansion valve opening degree, Comp_HZ the compressor speed and Ref.Total the refrigerant mass flow.

7.3. Conclusions

The *efficiency of the small separator* is expected to be improved by incorporation of relatively small modifications. In the present configuration, a part of the fluid in the gas fluid mixture will not be separated. By introducing a separator where the flow is forced to make a sufficient large number of bends, the amount of separated fluid will be increased. For each change in direction of the flow, there will be an increase of the separation of the fluid.

In the *suction gas heat exchanger (SGHX)*, the gas flow should be minimized. With a large gas flow, the gas speed is high which will result in a shortcut of the liquid where the liquid is not evaporated and will end up entering the expansion valve control sensor. A too high speed will also increase the liquid maldistribution in the SGHX which increases the problem. If there is only liquid flow to the SGHX, the pressure drop will also be at a minimum.

The *expansion valve* has been controlled manually in many of the tests. In those cases where the control was shifted to auto mode control, the temperatures began to fluctuate. This is due to the slow response of changes in the control parameters as, e.g., the expansion valve opening. One solution to this problem might be a "feed forward" type of control which measures other places in the system. Examples might be measurements of the inlet temperatures and the flow. This complicates the solution and leads to a more expensive solution.

Another factor is the *compactness of the system*. Long pipes will lead to a long time period (dead time) before the sensors notice changes. Therefore, a reduction of the length of the pipes will be an important factor for a fast response obtained by the control system.

Also, the application of a SGHX will increase the tendency for instability of the system. This is also an argument for application of an advanced control system.

Decoupling of the influence of the SGHX on the expansion valve seems to be the most sensible solution to control the evaporator in a slightly flooded mode. This can be accomplished with a new patented solution that is under development from Danfoss which measures the quality of the gas out of the evaporator. In this way, the expansion valve control gets stable.

The *distribution in the evaporator* is also a factor with influence on the stability. A distributor has not been used for the evaporator. Instead, two inlets have been used to reduce the maldistribution. The problem with the maldistribution is that the liquid tends to bypass the SGHX in the first and last channels if the gas speed is too high. By using a liquid separator, the flow through the SGHX could be minimized so it just boils off liquid. When using quality control without the separator, care should be taken in designing the SGHX so the liquid distribution over the plate pack is ensured. This could be accomplished with distributors in the inlet of the SGHX.

One observation is that there easily comes to much liquid out of the evaporator. If liquid is leaving the evaporator, there will not be any possible additional increase of the efficiency by increasing the liquid flow further. The measurement showed that the largest increase in efficiency was obtained by a slight overfeeding of the evaporator. After that, an increase in overfeed only resulted in small efficiency improvements. Therefore, the best way to increase the efficiency is to control the liquid flow out of the evaporator as slightly flooded with assistance of a quality control sensor.

8. References

- Andersson, J., Gillis, J., Rawlings, G., & Diehl, M. (2019). CasADi – A software framework for nonlinear optimization and optimal control. *Mathematical Programming Computation*, 11(1), 1–36.
- Arman, B., & Rabas, T. J. (1995). Condensation analysis for plate-frame heat exchangers.
- Aute, V., Martin, C., & Radermacher, R. (2015). AHRI Project 8013 : A Study of Methods to Represent Compressor Performance Data over an Operating Envelope Based on a Finite Set of Test Data. *Air-Conditioning, Heating, and Refrigeration Institute*.
- BITZER. (2021). Bitzer Software.
- Dempsey, M. (2006). Dymola for Multi-Engineering Modelling and Simulation. *2006 IEEE Vehicle Power and Propulsion Conference*, 1–6. <https://doi.org/10.1109/VPPC.2006.364294>
- European Committee for Standardization. (2018). *EN 14511 Air conditioners, liquid chilling packages and heat pumps for space heating and cooling and process chillers, with electrically driven compressors* (tech. rep.).
- Longo, G. A., & Gasparella, A. (2007). Refrigerant R134a vaporisation heat transfer and pressure drop inside a small brazed plate heat exchanger. *International Journal of Refrigeration*, 30(5). <https://doi.org/10.1016/j.ijrefrig.2006.11.011>
- MATLAB. (2021). MATLAB version 9.10.0.1710957 (R2021a).
- Modelica, A. (2022). *Modelica – A Unified Object-Oriented Language for Systems Modeling* (tech. rep.). Modelica Association. Linköping. <https://specification.modelica.org/master/>
- Richter, C. C. (2008). Proposal of New Object-Oriented Equation-Based Model Libraries for Thermodynamic Systems. PhD Thesis. *PhD Thesis*.
- Shen, B., Braun, J. E., & Groll, E. A. (2006). A method for tuning refrigerant charge in modeling off-design performance of unitary equipment (RP-1173). *HVAC and R Research*, 12(3). <https://doi.org/10.1080/10789669.2006.10391188>
- SWEP. (2021). DThermX.
- Wächter, A. (2002). *An Interior Point Algorithm for Large-Scale Nonlinear Optimization with Applications in Process Engineering* (Doctoral dissertation). Carnegie Mellon University. Pittsburgh.
- Zhang, J., Kærn, M. R., Ommen, T., Elmegaard, B., & Haglind, F. (2019). Condensation heat transfer and pressure drop characteristics of R134a, R1234ze(E), R245fa and R1233zd(E) in a plate heat exchanger. *International Journal of Heat and Mass Transfer*, 128. <https://doi.org/10.1016/j.ijheatmasstransfer.2018.08.124>
- Ciconkov, Risto (2009). New Technologies in Ammonia Refrigerating and Air-Conditioning Systems. *Heat Transfer Engineering, Vol 30, no. 4*.
- Tomooka, Mark (2011). Application of Micro-Channel Heat Exchangers to Compact Ammonia Systems. *33rd Annual Meeting, International Institute of Ammonia Refrigeration, March 27-30*.
- Hansen, Svend, Lund, Søren (199). Indførelse af ammoniak i mindre køleanlæg. *Teknologisk Institut, Energydivisionen, Køle- og varmepumpeteknik, Desember*.

- Bjørn, Palm (2007). Ammonia in low-capacity refrigeration and heat pump systems. *International Journal of Refrigeration* 31 (2008) 709-715.
- Hrnjak, Pega (2007). Microchannel heat exchangers for charge minimization in air-cooled ammonia condensers and chillers. *International Journal of Refrigeration* 31 (2008) 658-668.
- Zimmermann, Lars (2007). Low-Cost, Energy-savings, Flooded-evaporator-Technology. *International Congress of Refrigeration 2007, Beijing*.
- Minds, Gunnar (1995). Udvikling af små ammoniakkeøleanlæg. *Dansk Teknologisk Institut*.
- Madsen, Claus (2018). Udvikling af energieffektivt hybridfordampersystem. *Dansk Teknologisk Institut*.
- Monfared , Behzad Abolhassani (2010). Design and construction of a small ammonia heat pump. *Master of science thesis - KTH School of industrial engineering and management*.
- Hansen, Svenn Ole Kjøller (2018). HB Products delrapport fase 4 - Laboratorietest ved dynamiske forhold. *Dansk Teknologisk Institut*.
- Hansen, Torben M. (2001). HFC-frie mælkekøleanlæg. *Dansk Teknologisk Institut*.
- Graham, D.M., Kopke, H. R., Wilson, M. J., Yashar, D. A., Chato ,J. C. and Newell, T. A. (1999). An Investigation of Voil Fraction in the Stratified/Annular Flow Regions in Smooth, Horizontal Tubes. Air Conditioning and Refrigeration Center, University of Illinois, Mechanical & Industrial Engineering Dept., 1206 West Green Street, Urbana, IL 61801.
- Zajacs, Aleksandrs, Lalovs, Arthurs, Borodinecs, Anatolijs, Bodanovics, Raimonds, (2017). *Small ammonia heat pump for space and hot tap water heating. Energy Procedia* 122 (2017) 74-79.
- Luckmann, Ejnar (2018). *Selecting the right evaporator injection algorithm makes the world of difference. Technical articles, Danfoss*.
- Nielsen, Stefan, Christensen, Stefan Wuust, Thorsen, Richard S., Elmegaard, Brian (2018). *Comparision of heat pump design and performance for modern refrigerants. 13th IIR Gustav Lorentzen Conference on Natural Refrigerants, Valencia, Spain, 2018*.
- Amalfi, Raffaele L., Vakili , Farzad, Thome , John R. (2015). *Flow boiing and frictional pressure gradients in plate heat exchangers-Part 1. International Journal of Refrigeration* 61 (2016) 166-184.
- Amalfi, Raffaele L., Vakili , Farzad, Thome , John R. (2015). *Flow boiing and frictional pressure gradients in plate heat exchangers-Part 2. International Journal of Refrigeration* 61 (2016) 185-203.
- AlbertoDopazo, J., Fernandez-Seara, Jose (2011). *Experimental evaluation of an ejector as liquid re-circulator in an overfeed NH3 system with a plate evaporator. International Journal of Refrigeration* 34 (2011) page 1675-1683.
- Clarence, Flemming Larsen (2017). *Cooling System and a Method for Separation of Oil. European Patent Specification*.
- Koster, G. J., (1984-1985). *Energy Savings in Ammonia Refrigeration Plant by Using Oil Scrubbers. The Institut of Refrigeration*.
- Xu, Jiu, Hrnjak, Pega (2019). *Coalescing oil separator for compressors. International Journal of Refrigeration* 106 (2019) page 41-53.

Kim, Hak Soo, Kang, Gu Hwang, Yoon, Pil Hyun, Sa, Yong Cheol, Chung, Baik Young, Kim, Min Soo (2016). *Flow characteristics of refrigerant and oil mixtures in an oil separator. International Journal of Refrigeration 70 (2016) page 206-218.*

Zimmermann, Augusto Jose Pereira, Hrnjak, Predrag S. (2014). *Source identification and in situ quantification of oil-refrigerant mist generation by discharge valve opening process. 22nd International Compressor Engineering conference at Purdue, July 14-17, 2014.*

Frank, Michael, Kamenicky, Robin, Drikakis, Dimitris, Thomas, Lee, Ledin, Hans, and Wood, Terry (2019). *Multiphase Flow Effects in a Horizontal Oil and Gas Separator. Energies 2019, 12 2116.*

Zimmermann, Augusto Jose Pereira, Hrnjak, Predrag S. (2014). *Visualization of the Opening Process of a Discharge Reed Valve in the Presence of Oil. 22nd International Compressor Engineering conference at Purdue, July 14-17, 2014.*

Feja, S., Hanzelmann, C., Zuber, S. (2018). *PT and viscosity measurements of high-temperature ammonia heat pump lubricants. International Journal of Refrigeration 88 (2018) 221-228.*

Fuentes, Valentin Salgo (2019). *Medium capacity low charge ammonia chiller and heat pump. 13th IEA Heat Pump Conference, May 1-14, 2020 Jeju, Korea.*

Amalfi, Raffaele L., Vakili, Farzad, Thome, John R. (2015). *Flow boiling and frictional pressure gradients in plate heat exchangers-Part 1. International Journal of Refrigeration 61 (2016) 166-184.*

Amalfi, Raffaele L., Vakili, Farzad, Thome, John R. (2015). *Flow boiling and frictional pressure gradients in plate heat exchangers-Part 2. International Journal of Refrigeration 61 (2016) 185-203.*

LI, Zhaohua, Liang, Kun, Jiang, Hanying, Dadd, Mike (2019). *Modelling of a Novel Oil-free Linear Compressor for Small Ammonia Refrigerator. 8th IIR Conference: Ammonia and CO2 Refrigeration Technologies, Ohrid, 2019.*

Svingal, Juraj (2019). *Extreme low charge units with ammonia blend R723 applications in practice. 8th IIR Conference: Ammonia and CO2 Refrigeration Technologies, Ohrid, 2019.*

Appendix 1 – List of dissemination activities

Publications

Paper I

Salgado Fuentes, V., Boccia, R., Markussen, W. B., Rothuizen, E. D., Kristófersson, J., Madsen, C. Elmegaard, B., "Comparison of correlations for modelling heat exchanger performance in a compact ammonia refrigeration unit", Proceedings of the 14th IIR-Gustav Lorentzen Conference on Natural Refrigerants, 2020. International Institute of Refrigeration, p. 610-615 1128.

Paper II

Salgado Fuentes, V., Markussen, W. B., Rothuizen, E. D., Kristófersson, J., Madsen, C. Elmegaard, B., "Medium capacity low charge ammonia chiller and heat pump", Proceedings of the 13th IEA Heat Pump Conference. Heat Pumping Technologies, 2021.

Paper III

Salgado Fuentes, V., Boccia, R., Markussen, W. B., Rothuizen, E. D., Kristófersson, J., Madsen, C. Elmegaard, B., "Modelling heat exchanger performance and refrigerant charge distribution in compact ammonia refrigeration units", Submitted to the International Journal of Refrigeration.

PHD Thesis

Design, modelling and simulation of compact ammonia chiller and heat pump units. PhD Thesis. February 2022 By Valentin Salgado Fuentes. Published by: DTU, Department of Mechanical Engineering, Nils Koppels Allé, Building 403, 2800 Kgs. Lyngby, Denmark. www.mek.dtu.dk ISBN: [9788774756750] (electronic version) ISBN: [9788774756750] (printed version).

Conferences

8th IIR Conference: Ammonia and CO2 Refrigeration Technologies, Ohrid, 2019

14th IIR-Gustav Lorentzen Conference on Natural Refrigerants, 2020

13th IEA Heat Pump Conference. Heat Pumping Technologies,

2021 Køle og Varmepumpeforum 04-10-2021